CONTROLLER DESIGN AND SIMULATION FOR A HELICOPTER DURING TARGET ENGAGEMENT

A THESIS SUBMITTED TO
THE GRADUATE SCHOOL OF NATURAL AND APPLIED SCIENCES
OF
MIDDLE EAST TECHNICAL UNIVERSITY

BY

SEVİL AVCIOĞLU

IN PARTIAL FULFILLMENT OF THE REQUIREMENTS
FOR
THE DEGREE OF MASTER OF SCIENCE
IN
AEROSPACE ENGINEERING

OCTOBER 2011

Approval of the thesis:

CONTROLLER DESIGN AND SIMULATION FOR A HELICOPTER DURING TARGET ENGAGEMENT

submitted by **SEVİL AVCIOĞLU** in partial fulfillment of the requirements for the degree **of Master of Science in Aerospace Engineering Department, Middle East Technical University** by,

Prof. Dr. Canan Özgen
Dean, Graduate School of **Natural and Applied Sciences** _____

Prof. Dr. Ozan Tekinalp
Head of Department, **Aerospace Engineering** _____

Assist. Prof. Dr. İlkay Yavrucuk
Supervisor, **Aerospace Engineering Dept., METU** _____

Examining Committee Members:

Prof. Dr. Ozan Tekinalp
Aerospace Engineering Dept., METU _____

Assist. Prof. Dr. İlkay Yavrucuk
Aerospace Engineering Dept., METU _____

Assoc. Prof Dr. Tayfun Çimen
Sr. Systems & Control Engineer, ROKETSAN _____

Assist. Prof. Dr. Ali Türker Kutay
Aerospace Engineering Dept., METU _____

Dr. Osman Merttopçuoğlu
Sr. Guidance & Control Engineer, ROKETSAN _____

Date: _____

I hereby declare that all information in this document has been obtained and presented in accordance with academic rules and ethical conduct. I also declare that, as required by these rules and conduct, I have fully cited and referenced all material and results that are not original to this work.

Name, Last Name: SEVİL AVCIOĞLU

Signature :

ABSTRACT

CONTROLLER DESIGN AND SIMULATION FOR A HELICOPTER DURING TARGET ENGAGEMENT

Avcıoğlu, Sevil

M.S, Department of Aerospace Engineering

Supervisor: Assist. Prof. Dr. İlkay Yavrucuk

October 2011, 105 pages

The aim of this thesis is to design a controller for an unmanned helicopter to perform target engagement. This mission is briefly defined as; the helicopter flies to a firing point under the commands of a trajectory controller, and then it is aligned to the target with attitude control. After weapon firing, the helicopter initiates a return maneuver under again the commands of the trajectory controller. This mission where the continuous systems and discrete guidance decisions are to be executed in coherence can be studied as a hybrid control problem. One hybrid control approach which is used in this study is the representation based on two motion primitives: trim trajectories and maneuvers. To obtain the desired trim trajectories and the maneuvers, a dynamic inversion based controller is developed. The controller has two loops: the inner loop which controls the helicopter attitudes and the outer loop which controls the helicopter trajectory. A guidance algorithm is developed which enables the controller to switch from the inner loop to the outer loop or vice versa. Simulations are generated to test the controller performance.

Keywords: helicopter, dynamic inversion, controller, target alignment

ÖZ

HEDEF TEVCİHİNE YÖNELİK HELİKOPTER KONTROLCÜ TASARIMI VE UÇUŞ BENZETİMİ

Avcıoğlu, Sevil

Yüksek Lisans, Havacılık ve Uzay Mühendisliği Bölümü

Tez Yöneticisi: Yrd. Doç. Dr. İlkay Yavrucuk

Ekim 2011, 105 sayfa

Bu tezin amacı, helikopterler için hedef tevcihine yönelik bir kontrolcü tasarlamaktır. Hedef tevcihi; yörünge kontrolcüsü ile atış noktasına uçuş, yönelim kontrolcüsü ile hedef hizalama, atış ve yine yörünge kontrolcüsü ile görev bölgesinden kaçış olarak tanımlanabilir. Sürekli zamanlı sistemlerin ayrık zamanlı güdüm komutları ile çalıştırıldığı bu problem tipik bir hibrid control problemidir. Bilinen bir hibrid control yöntemi olarak; bu tezde kullanılan yöntem hareketin trim yörüngeleri ve manevralar üzerine kurgulanması esasına dayanmaktadır. İstenen trim yörüngeleri ve manevraların oluşturulabilmesi için dinamik tersleme yöntemi esas alınarak bir kpontrolcü geliştirilmiştir. Kontrolcü iki döngüden oluşmaktadır. Iç döngüde helicopter yönelim açıları, dış döngüde ise helicopter yörüngesi kontrol edilmektedir. Iç döngü ile dış döngü arasındaki geçişi modellemek için bir güdüm algoritması oluşturulmuştur. Geliştirilen kontrolcünün performansını test etmek amacı ile simulasyonlar oluşturulmuştur.

Anahtar Kelimeler: helikopter, dinamik tersleme, kontrolcü, nişan alma / tevcih

ACKNOWLEDGMENTS

I want to express my gratitude to Assist. Prof. Dr. İlkay Yavrucuk for his supervision throughout this thesis. I would like to thank Turkish Army Pilot Gökhan Korkmaztürk for sharing his experience and knowledge on Cobra helicopter tactical usage.I also want to express my thanks to Onur Tarımcı, F. Demet Ülker and Tolga Avcıoğlu for their help throughout the thesis.

TABLE OF CONTENTS

LIST OF TABLES

TABLES

LIST OF FIGURES

FIGURES

LIST OF ABBREVIATIONS

A, B : full stability and control matrices

A_1 : stability matrix containing the effects of rotational states on themselves

A_2 : stability matrix containing the effects of translational states on Rotational states

a_B : helicopter actual acceleration vector in Body-Fixed Reference Frame

a_D : desired acceleration

Alt : altitude in Earth-Fixed Reference Frame

a_x, a_y, a_z : actual acceleration components in Earth-Fixed Reference Frame

B_1 : the control matrix containing the effect of controls on rotational states

F_x, F_y, F_z : aerodynamic and propulsive forces in Body-Fixed Reference Frame

g : specific gravity force

L_{EB} : transformation matrix from Body-Fixed Reference Frame to Earth-Fixed Reference Frame

L, M, N : body moments

m : helicopter mass

R : radius of curvature

p, q, r : body angular velocities (roll rate, pitch rate, yaw rate)

t : time

u : full control vector

u_1 : the control vector containing the longitudinal, lateral and pedal

controls

u, v, w : body translational velocities (forward velocity, side velocity, vertical velocity)

u_e, v_e, w_e : body translational velocities (equilibrium values)

$U_{X_n}, U_{X_e}, U_{Alt}$: outer loop PD controller outputs

X_n, X_e, X_d : positions on Earth-Fixed Reference Frame (north, east, down)

X, Y, Z : body forces

x : full state matrix

x_1 : the state vector containing rotational states (p, q, r)

x_2 : the state vector containing translational states and collective control (u, v, w, δ_c)

V_n : velocity component in north direction

V : helicopter forward velocity

ϕ, θ, ψ : Euler angles (roll, pitch, yaw)

ϕ_e, θ_e, ψ_e : Euler angles (equilibrium values)

δ_a : control input (lateral control)

δ_b : control input (longitudinal control)

δ_c : control input (collective control)

δ_p : control input (pedal control)

ω_n : natural frequency

ξ : damping ratio

γ : flight path angle

Subscripts and Superscripts

$()_D$: desired

$()_C$: commanded

$()_{trim}$: trim condition

$\dot{()}_C$: first derivative with respect to time

$\ddot{()}_C$: second derivative with respect to time

Acronyms

FFAR : Folding-Fin Aircraft Rocket

ISR : Intelligence, Surveillance and Reconnaissance

NOTS : Naval Ordnance Test Station

PI : Proportional-Integral

PD : Proportional-Derivative

UCAR : The Unmanned Combat Armed Rotorcraft

CHAPTER 1

INTRODUCTION

Unmanned helicopter technology is increasingly advancing in the past few years. With improved and cost effective computational power of flight computers, superior sensor technologies unmanned helicopters are becoming attractive to both civil and military applications. Especially the ability to approach target area without the risk of pilot loss consequently makes these vehicles desirable in military applications. However, the effective use of an unmanned helicopter in a battlefield is a complex problem. For example, target engagement is one of them. Usually it is required that the helicopter is switched from trajectory control to attitude control and back. In this case, trajectory control, attitude control and discrete guidance decisions are to be executed in coherence and the stability must be guaranteed when switching occurs.

Problems in which continuous systems are manipulated by discrete system dynamics are known as hybrid control problems [1, 2]. Here, two or more continues systems are switched in a discrete fashion, where stability is still guaranteed. One approach is the representation based on motion primitives [1, 3, 4, 5]. Here, two types of motion primitives are defined: trim conditions and maneuvers. Trim conditions are defined as the equilibrium points of the system and maneuvers are described as the finite time transitions between two trim conditions [1, 3, 4] and the stabilization is guaranteed by switching the system only at the trim conditions [1].

In this thesis a controller is also developed to obtain the desired trim trajectories and the maneuvers to perform the mission; target engagement. Dynamic inversion based controllers [7] are used for this work. In Refs. [6-10] a time scale separated two loop approach is used, called the inner loop and the outer loop. Attitude control

and stability augmentation are performed by the inner loop. Trajectory control is achieved with the outer loop [6].

This thesis is focused on the controller design of an unmanned helicopter to perform the mission; target engagement. The controller method is chosen as dynamic inversion based controller. The hybrid control architecture is based on setting the motion primitives as trim trajectories and maneuvers and the controller switching actions are performed at trim conditions.

In this thesis, the trajectory and the attitude control is designed for an unmanned attack helicopter similar to the AH-1G helicopter. Models for unguided 2.75" rockets are considered as a weapon type in the mission scenarios. Detail information about the AH-1G helicopter and unguided 2.75" rockets (MK 66) are given in APPENDIX A.

1.1 Literature Survey

It is sensible if the hybrid controllers are based only on trim trajectories [5, 11]. Consequently, the controllers are expected to be switched in a "slow" manner [5]. However, some missions may require aggressive maneuvers which results in the systems moving "far" from trim trajectories. In the past few years, several studies are performed to be earned aggressive maneuvering capabilities to unmanned helicopters. In [5], hierarchical control architecture is presented for aggressive maneuvering of autonomous helicopters. This architecture is based on the trajectory primitives: trim trajectories and maneuvers. An example application study is performed for an unmanned helicopter to make maneuvers from hover condition in [5]. Related to this work, maneuver automation method is introduced in [1]. In this work, the issue of motion planning for agile autonomous vehicles is analyzed. Problem is studied in the obstacle-free environment and in the dynamic environment. Also the robust maneuver automation is analyzed in [1]. Later, this method is enhanced with bringing the robust guidance method for autonomous vehicles [3]. Then this approach is applied to X-Cell 60 miniature helicopter and an example result is given to show the performance improvement achieved with the

robust policy [3]. Further studies are performed to execute completely automatic aerobatic maneuvers on the same helicopter, X-Cell 60. The control logic described here consists of trim trajectory controllers which are used before and after maneuvers and the maneuvers modeled by studying the human pilot strategies [12]. The flight test and the simulation results of X-Cell 60 miniature helicopter under some aerobatic maneuvers are published in [13] in 2002.

Besides these studies, several papers are found in literature about dynamic inversion based controller method which is selected in this thesis as an unmanned helicopter trajectory and attitude controller. The earlier studies about the theory of dynamic inversion have been aroused in 1980's. This method is mainly applied to nonlinear systems such as the helicopters [6, 16-20] or the fixed wing aircrafts at nonlinear flight regimes [14-15].

In [16], by commanding some moderate and aggressive maneuvers, the performance of the trajectory controller which is based on dynamic inversion method is tested. The nonlinear simulation model of the Yamaha R-50 helicopter is used here as a helicopter model. Later, a dynamic inversion based controller is designed for the non-linear AH-1S helicopter model and the controller performance is tested in simulation environment by commanding several challenging maneuvers under turbulence [6].

Several adaptive methods are applied to the dynamic inversion based controller to compensate the inversion errors which arises from the approximations used to find the inverted model [6, 9, 19]. The common adaptive methods are linear sigma-pi neural network architecture [9] and single hidden layer neural network architecture [6].

The experience on arming unmanned helicopters is not well developed. There are some ongoing projects about this subject. One of them is UCAR (The Unmanned Combat Armed Rotorcraft) program started in 2002. This program carried out to develop an unmanned combat helicopter armed with the weapons [21-22]. The basic utilities of UCAR program are survivability, autonomous operations, command

and control, and weapon firing. Another program is MQ-8B Fire Scout (Figure 1) developed by Northrop Grumman Corporation as a Vertical Takeoff Unmanned Air Vehicle. With electro-optical / infrared sensors and a laser designator installed on it Fire Scout can perform multiple roles like detecting targets, tracking and designating them accurately and providing targeting data [23]. The other unmanned combat helicopter is Fire-X (Figure 2). This vehicle is being developed by Northrop Grumman Corporation and Bell Helicopter. Fire-X will carry battlefield ISR (intelligence, surveillance and reconnaissance) sensors. First flight test of Fire-X was a hover test to validate safe and reliable autonomous flight [24].

Figure 1 Fire Scout 2.75” Rocket Firing Test View [23]

Figure 2 Fire-X View [24]

1.2 Thesis Structure

In Chapter 1 the purpose and the scope of the study are described and relevant previous studies are explained. In Chapter 2 the problem definition is given and the reference frames are defined. In Chapter 3 the AH-1G helicopter stability is analyzed for different forward velocity conditions. In Chapter 4 controller architecture is given. Dynamic inversion based controller, guidance algorithm and

controller switching logic are explained here. In Chapter 5 the simulations are performed for different firing conditions and the results are discussed. In Chapter 6 the studies are summarized as a conclusion and the ideas are given for future works.

CHAPTER 2

PROBLEM DEFINITION AND PRELIMINARIES

2.1 Problem Definition

This study is focused on controller design and simulation of an unmanned helicopter during target engagement. The mission is briefly defined as; the helicopter flies to a firing point under the commands of a trajectory controller, and then it is aligned to the target with attitude control. After satisfying the firing conditions, weapon firing is performed, and then the helicopter initiates a return maneuver under again the commands of the trajectory controller. Concept drawing of the target engagement is given in Figure 3.

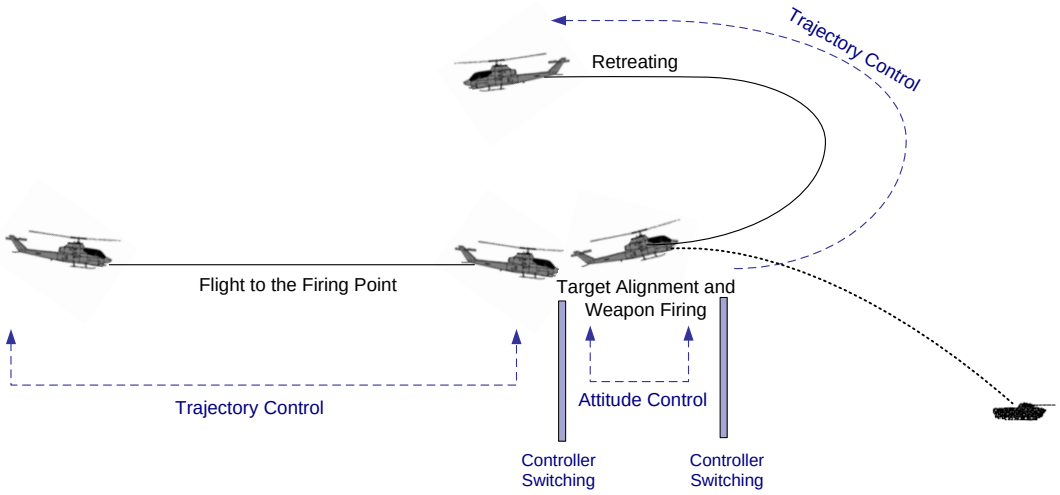

Figure 3 Target Engagement Concept

The hybrid control strategy given in [26] is tailored to target engagement in this study as following;

Task 1) Trajectory Tracking: Helicopter flights to the firing point with trajectory controller and it is trimmed before Task 2.

Task 2) Maneuver Execution Start: Switching from trajectory controller to attitude controller is performed at trim condition. Target alignment is executed with attitude controller.

Task 3) Maneuver Execution End: After target alignment and weapon firing the helicopter attitude is commanded to back to the conditions (trimming conditions) at the end of Task 1.

Task 4) Trajectory Tracking: Switching from attitude controller to trajectory controller is performed at trim condition. Helicopter retreats with trajectory controller to complete the mission.

The details about trajectory and the attitude control design which is based on dynamic inversion method and the guidance algorithm which constitutes the controller switching logic with some guidance commands are given in Chapter 4.

In this study, the Cobra helicopter tactical usage is taken as a reference. According to this, the guidance commands are established by considering three main topics: helicopter attack patterns, weapon firing types and the target alignment details.

2.1.1 Attack Patterns

The most common attack patterns are “Racetrack Pattern” [27] and “Cloverleaf Pattern” [27] for the Cobra helicopter. The concept drawing of these patterns are given in Figure 4 and Figure 5 respectively.

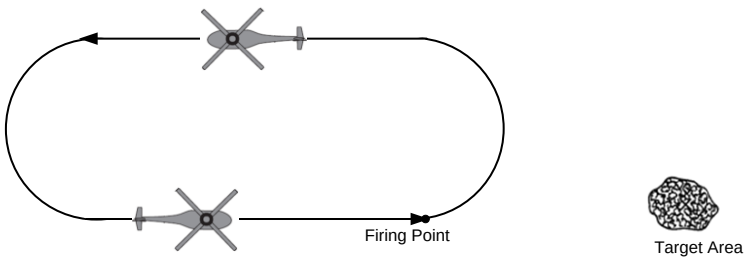

Figure 4 Racetrack Pattern (Top View) [27]

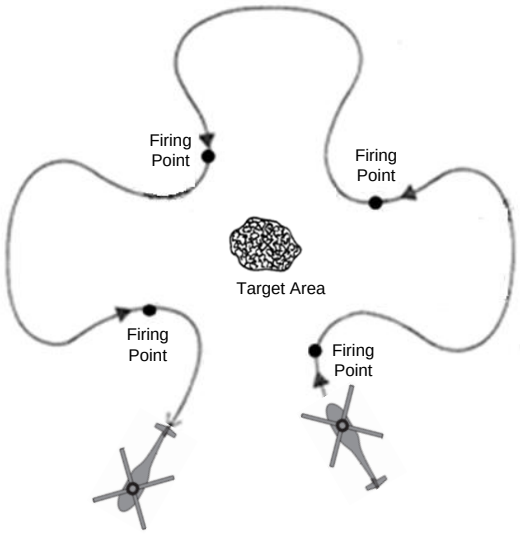

Figure 5 Cloverleaf Pattern (Top View) [27]

The attack pattern is selected as a u-turn maneuver which is the common point in Racetrack and Cloverleaf patterns. The concept of u-turn maneuver is shown in Figure 6.

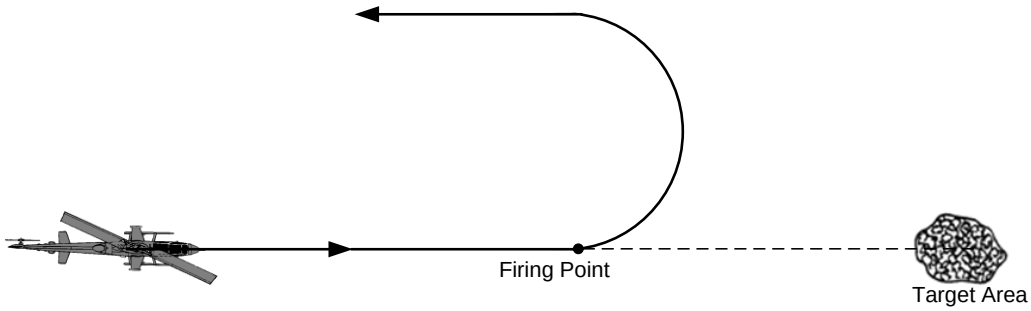

Figure 6 Attack Pattern for Test Cases (u-turn maneuver)

2.1.2 Firing Types

There are three common firing types for Cobra helicopter: hover fire, running fire and diving fire [28].

The possible helicopter forward velocity range at firing instant is 0-40 knot for hover fire and 40-120 knot for both running and diving fire. The relative altitude[1] range is 10 – 300 ft for hover fire, 50 – 1000 ft for running fire. However, firing is practicable from relatively high altitudes for diving fire. The concept drawings of these firing types are given in Figure 7-Figure 10.

Figure 7 Attack Pattern for Hover Fire (Top View)

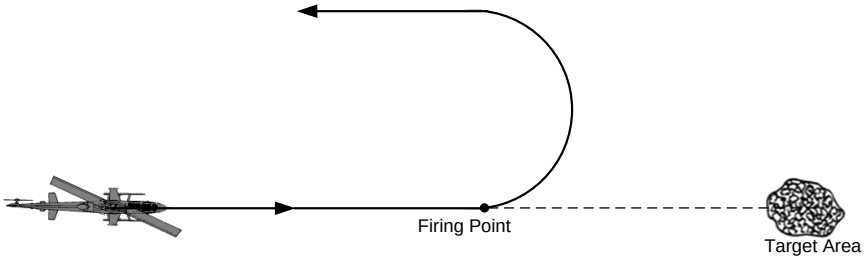

Figure 8 Attack Pattern for Running Fire (Top View)

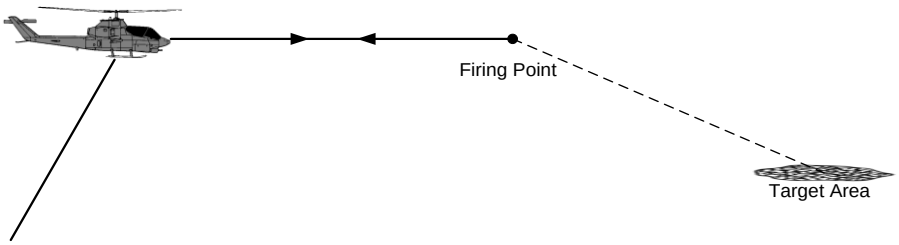

Figure 9 Attack Pattern for Hover Fire and Running Fire (Side View)

[1]Relative Altitude : Vertical distance between helicopter and the target at firing instant

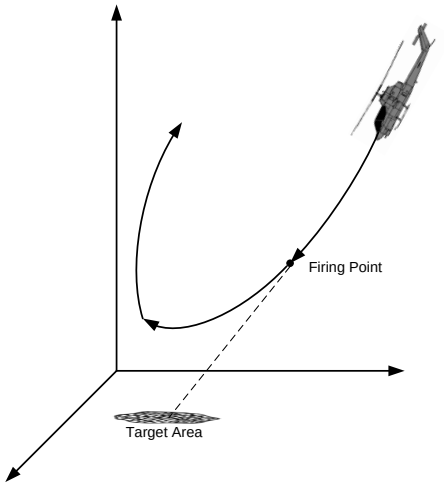

Figure 10 Attack Pattern for Diving Fire

2.1.3 Target Alignment

Target alignment is defined as an adjustment of helicopter attitude according to the weapon ballistic trajectories (detail explanation about weapon ballistic trajectories is given in APPENDIX B). Helicopter pitch attitude mainly affects the target range. Concept representation of the helicopter pitch attitude on rocket ballistic range is given in Figure 11. Also, the helicopter heading fundamentally determines the firing direction. However, the helicopter roll angle has not a significant importance on the rocket ballistic trajectory but it may be required to set it to the certain values for safe separation.

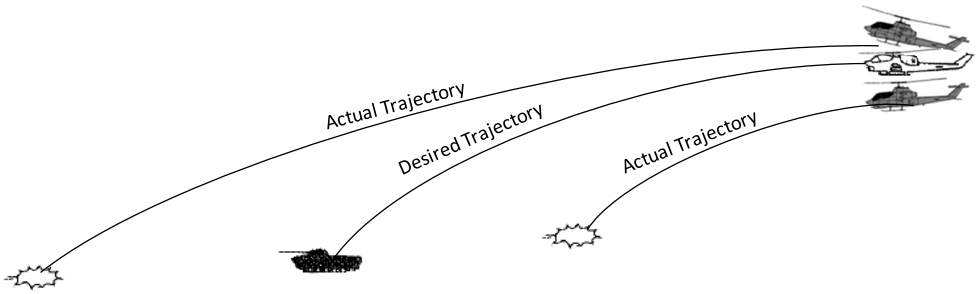

Figure 11 Pitch Attitude Error Effect on Target Range

The required helicopter attitudes for the mission scenarios whose simulation results are discussed in Chapter 5 are determined from [27]. It must be noticed that the resulting trajectory after rocket separation is not the subject of this thesis.

2.2 Preliminaries

2.2.1 Reference Frames

There are two reference frames used in this study. These are Earth-Fixed Reference Frame, F_E and Body-Fixed Reference Frame, F_B. It is assumed that the earth is non-rotating and flat.

2.2.1.1 Earth-Fixed Reference Frame, F_E

The Earth-Fixed Reference Frame at a fixed point on earth.

- the x_E axis is positive to the north
- the y_E axis is positive to the east
- the z_E axis is positive to down to form a right handed orthogonal axis system and coincides with the gravity vector.

2.2.1.2 Body-Fixed Reference Frame, F_B

The Body-Fixed Reference Frame is fixed to the center of gravity of the aircraft and it moves and rotates with the aircraft.

- the x_B axis is positive in the forward direction of the aircraft
- the y_B axis is positive to the right of the forward direction of the aircraft
- the z_B axis is positive to down to form a right handed orthogonal axis system

Concept drawing of the Body-Fixed Reference Frame representation is given in Figure 12.

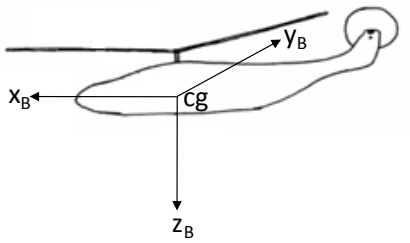

Figure 12 Body-Fixed Reference Frame Representation

2.2.2 Reference Frame Transformations

Sequential rotations are necessary to transform a Earth-Fixed Reference Frame to Body-Fixed Reference Frame. First, Earth-Fixed Reference Frame is rotated by yaw angle, ψ around z_E-axis, then the intermediate frame is rotated by pitch angle, θ around y'_E-axis and finally the intermediate frame is rotated by roll angle, ϕ around x''_E-axis. The conceptual drawing of the transformation is given in Figure 13.

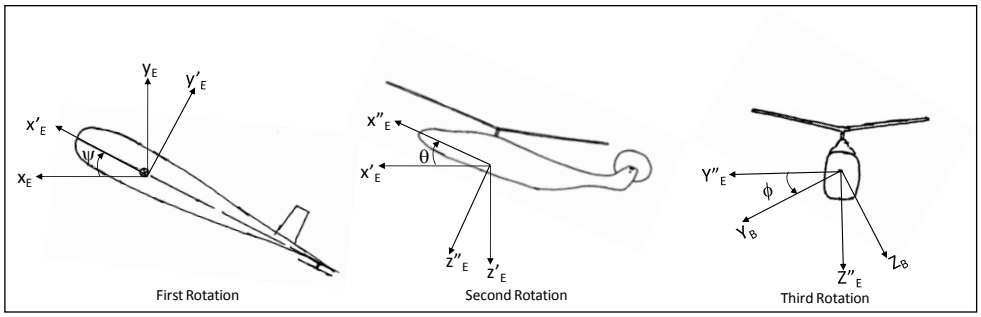

Figure 13 Earth-Fixed Reference Frame to Body-Fixed Reference Frame Transformation

The transformation matrix from Body-Fixed Reference Frame to Earth-Fixed Reference Frame can be written as given in Equation 2.1 [29-30].

$$L_{EB} = \begin{bmatrix} \cos\theta\cos\psi & \sin\phi\sin\theta\cos\psi - \cos\phi\sin\psi & \cos\phi\sin\theta\cos\psi + \sin\phi\sin\psi \\ \cos\theta\sin\psi & \sin\phi\sin\theta\sin\psi + \cos\phi\cos\psi & \cos\phi\sin\theta\sin\psi - \sin\phi\cos\psi \\ -\sin\theta & \sin\phi\cos\theta & \cos\phi\cos\theta \end{bmatrix} \quad (2.1)$$

The relationship between the body angular rates and the Euler angular rates are given in Equation 2.2 [29-30];

$$\begin{bmatrix} \dot{\phi} \\ \dot{\theta} \\ \dot{\psi} \end{bmatrix} = \begin{bmatrix} 1 & \sin\phi\tan\theta & \cos\phi\tan\theta \\ 0 & \cos\phi & -\sin\phi \\ 0 & \sin\phi\sec\theta & \cos\phi\sec\theta \end{bmatrix} \cdot \begin{bmatrix} p \\ q \\ r \end{bmatrix} \tag{2.2}$$

The relationship between the body angular accelerations and the Euler angular accelerations are given in Equation 2.3 ;

$$\begin{aligned} \dot{p} &= \ddot{\phi} - \ddot{\psi}\sin\theta - \dot{\psi}\dot{\theta}\cos\theta \\ \dot{q} &= \ddot{\theta}\cos\phi - \dot{\theta}\dot{\phi}\sin\dot{\phi} + \ddot{\psi}\sin\phi\cos\theta + \dot{\psi}\dot{\phi}\cos\theta\cos\phi - \dot{\psi}\dot{\theta}\sin\theta\sin\phi \\ \dot{r} &= -\ddot{\theta}\sin\phi - \dot{\phi}\dot{\theta}\cos\phi + \ddot{\psi}\cos\phi\cos\theta - \dot{\psi}\dot{\phi}\cos\theta\sin\phi - \dot{\psi}\dot{\theta}\sin\theta\cos\phi \end{aligned} \tag{2.3}$$

These reference frames and the transformation matrices are used in the following chapters for helicoter stability analysis and the controller design studies.

CHAPTER 3

PLANT MODELLING AND STABILITY ANALYSIS

The helicopter model is derived by using AH-1G helicopter data. AH-1G helicopter specifications, a set of descriptive data and the stability and control derivatives are taken from [31]. This data set contains several flight conditions within the flight envelope, namely at different forward velocities, altitudes and loadings. This study is based on the data at nominal loading and level flight sea level conditions. The stability and control derivatives are all given in the Body Fixed Reference Frame. For each case in the set, the derivatives are given with the flight conditions and trim controls, attitude angles and velocities. The data set used in this study is given in APPENDIX B.

By using stability and control matrices, the state space model of AH-1G is generated. State space model structure is referenced to [32].

$$\dot{x} = Ax + Bu \tag{3.1}$$

In [31], the stability & control derivatives are given for various forward velocity values. The stability & control derivatives are interpolated with respect to the helicopter forward velocity and accordingly the linear helicopter model matrices are updated continuously during the simulation.

$$\begin{bmatrix}\dot{u}\\ \dot{w}\\ \dot{q}\\ \dot{\theta}\\ \dot{v}\\ \dot{p}\\ \dot{\phi}\\ \dot{r}\\ \dot{\psi}\end{bmatrix} = \begin{bmatrix} X_u & X_w & X_q - w_e & -g\cdot\cos\theta_e & X_v & X_p & 0 & X_r & 0\\ Z_u & Z_w & Z_q + u_e & -g\cdot\cos\phi_e\cdot\sin\theta_e & Z_v & Z_p & -g\cdot\sin\phi_e\cdot\cos\theta_e & Z_r & 0\\ M_u & M_w & M_q & 0 & M_v & M_p & 0 & M_r & 0\\ 0 & 0 & \cos\theta_e & 0 & 0 & 0 & -\Omega_a\cdot\cos\theta_e & -\sin\theta_e & 0\\ \mathrm{Y_u} & Y_w & Y_q & -g\cdot\sin\phi_e\cdot\sin\theta_e & Y_v & Y_p + w_e & g\cdot\cos\phi_e\cdot\cos\theta_e & Y_r - u_e & 0\\ L'_u & L'_w & L'_q & 0 & L'_v & L'_p & 0 & L'_r & 0\\ 0 & 0 & \sin\phi_e\cdot\tan\theta_e & \Omega_a\cdot\sec\theta_e & 0 & 1 & 0 & \cos\phi_e\cdot\tan\theta_e & 0\\ N'_u & N'_w & N'_q & 0 & N'_v & N'_p & 0 & N'_r & 0\\ 0 & 0 & \sin\phi_e\cdot\sec\theta_e & 0 & 0 & 0 & 0 & 0 & 0\end{bmatrix}\cdot\begin{bmatrix}u\\ w\\ q\\ \theta\\ v\\ p\\ \phi\\ r\\ \psi\end{bmatrix}$$

$$+\begin{bmatrix} X_{\delta c} & X_{\delta b} & X_{\delta a} & X_{\delta p}\\ Z_{\delta c} & Z_{\delta b} & Z_{\delta a} & Z_{\delta p}\\ M_{\delta c} & M_{\delta b} & M_{\delta a} & M_{\delta p}\\ 0 & 0 & 0 & 0\\ Y_{\delta c} & Y_{\delta b} & Y_{\delta a} & Y_{\delta p}\\ L'_{\delta c} & L'_{\delta b} & L'_{\delta a} & L'_{\delta p}\\ 0 & 0 & 0 & 0\\ N'_{\delta c} & N'_{\delta b} & N'_{\delta a} & N'_{\delta p}\\ 0 & 0 & 0 & 0\end{bmatrix}\cdot\begin{bmatrix}\delta_c\\ \delta_b\\ \delta_a\\ \delta_p\end{bmatrix} \tag{3.2}$$

Where;

The force derivatives are normalized by helicopter mass, and the moment derivatives are normalized by helicopter moments of inertia.

$$X_{(\,)} = \frac{1}{m}\cdot\frac{\partial X}{\partial(\,)};\quad Y_{(\,)} = \frac{1}{m}\cdot\frac{\partial Y}{\partial(\,)};\quad Z_{(\,)} = \frac{1}{m}\cdot\frac{\partial Z}{\partial(\,)} \tag{3.3}$$

$$L_{(\,)} = \frac{1}{I_{XX}}\cdot\frac{\partial L}{\partial(\,)};\quad M_{(\,)} = \frac{1}{I_{YY}}\cdot\frac{\partial M}{\partial(\,)};\quad N_{(\,)} = \frac{1}{I_{ZZ}}\cdot\frac{\partial N}{\partial(\,)} \tag{3.4}$$

$$L'_{(\,)} = \frac{I_{ZZ}}{I_{XX}\cdot I_{ZZ} - I_{XZ}^2}L_{(\,)}\cdot I_{XX} + \frac{I_{XZ}}{I_{XX}\cdot I_{ZZ} - I_{XZ}^2}N_{(\,)}\cdot I_{ZZ}; \tag{3.5}$$

$$N'_{(\,)} = \frac{I_{XZ}}{I_{XX}\cdot I_{ZZ} - I_{XZ}^2}L_{(\,)}\cdot I_{XX} + \frac{I_{XX}}{I_{XX}\cdot I_{ZZ} - I_{XZ}^2}N_{(\,)}\cdot I_{ZZ} \tag{3.6}$$

The units of the state space matrix elements are as given in Table 1.

Table 1 State Space Model Symbol Definition

Definiations	Symbols	Units
body translational velocities	u, v, w	ft/s
body translational velocities (equilibrium values)	u_e, v_e, w_e	ft/s
body angular rates (velocities)	p, q, r	rad/s
Euler angles	ϕ, θ, ψ	rad
Euler angles (equilibrium values)	ϕ_e, θ_e, ψ_e	rad
force change wrt. translational velocity	X_u, X_v, X_w	$1/s$
force change wrt. angular velocity	X_p, X_q, X_r	$ft/rad \cdot s$
moment change wrt. translational velocity	M_u, M_v, M_w	$rad/ft \cdot s$
moment change wrt. angular velocity	M_p, M_q, M_r	$1/s$
force change wrt. control	$X_{\delta c}, X_{\delta b}, X_{\delta a}, X_{\delta p}$	$ft/s^2 \cdot in.$
moment change wrt. control	$M_{\delta c}, M_{\delta b}, M_{\delta a}, M_{\delta p}$	$rad/s^2 \cdot in.$
control inputs (lateral, longitudinal, collective, pedal)	$\delta_a, \delta_b, \delta_c, \delta_p$	$in.$

Compared to fixed-wing aircrafts, cross-coupling has more significant effect on rotorcrafts [32]. Therefore the studies are performed without decoupling of the system matrix.

By using the linear model of the helicopter, the stability roots (eigenvalues of the stability matrix) are found. Results are compared with the study in [33] where the stability and control matrices are decoupled as longitudinal and lateral modes and then short period, long period, dutch roll, roll and spiral modes are analyized. Similar results are observed for the coupled system roots (Figure 14). Also, the natural frequency, the damping ratio and the time constant characteristics of the system are calculated (Table 2) and the values are assigned to related modes. The relevant results are given in [33].

Stability analysis shows that the short period mode, the roll mode and the spiral modes are stable for all forward velocities. On the other hand, the phugoid mode and the dutch roll mode become unstable for certain forward flight velocities.

Table 2 Natural Frequency, Damping Ratio and Time Constant Characteristics

Forward Velocity	Short Period Mode		Phugoid Mode		Dutch Roll Mode		Roll Mode	Spiral Mode
	Natural Frequency (rad/s)	Damping Ratio	Natural Frequency (rad/s)	Damping Ratio	Natural Frequency (rad/s)	Damping Ratio	Time Constant (s)	Time Constant (s)
1knot	0.71	0.84	0.36	-0.29	0.54	-0.24	1.22	2.27
20 knot	0.65	0.83	0.32	-0.26	0.70	0.14	0.96	4.88
40 knot	0.72	0.81	0.32	-0.17	0.97	0.28	0.74	8.71
60 knot	0.82	0.70	0.26	-0.06	1.23	0.34	0.69	13.76
80 knot	0.97	0.62	0.25	0.00	1.45	0.37	0.71	19.69
100 knot	1.21	0.51	0.22	0.06	1.60	0.38	0.74	24.15
120 knot	1.49	0.52	0.16	-0.10	1.70	0.34	0.85	12.63
140 knot	1.55	0.51	0.18	0.03	1.91	0.35	1.20	10.47

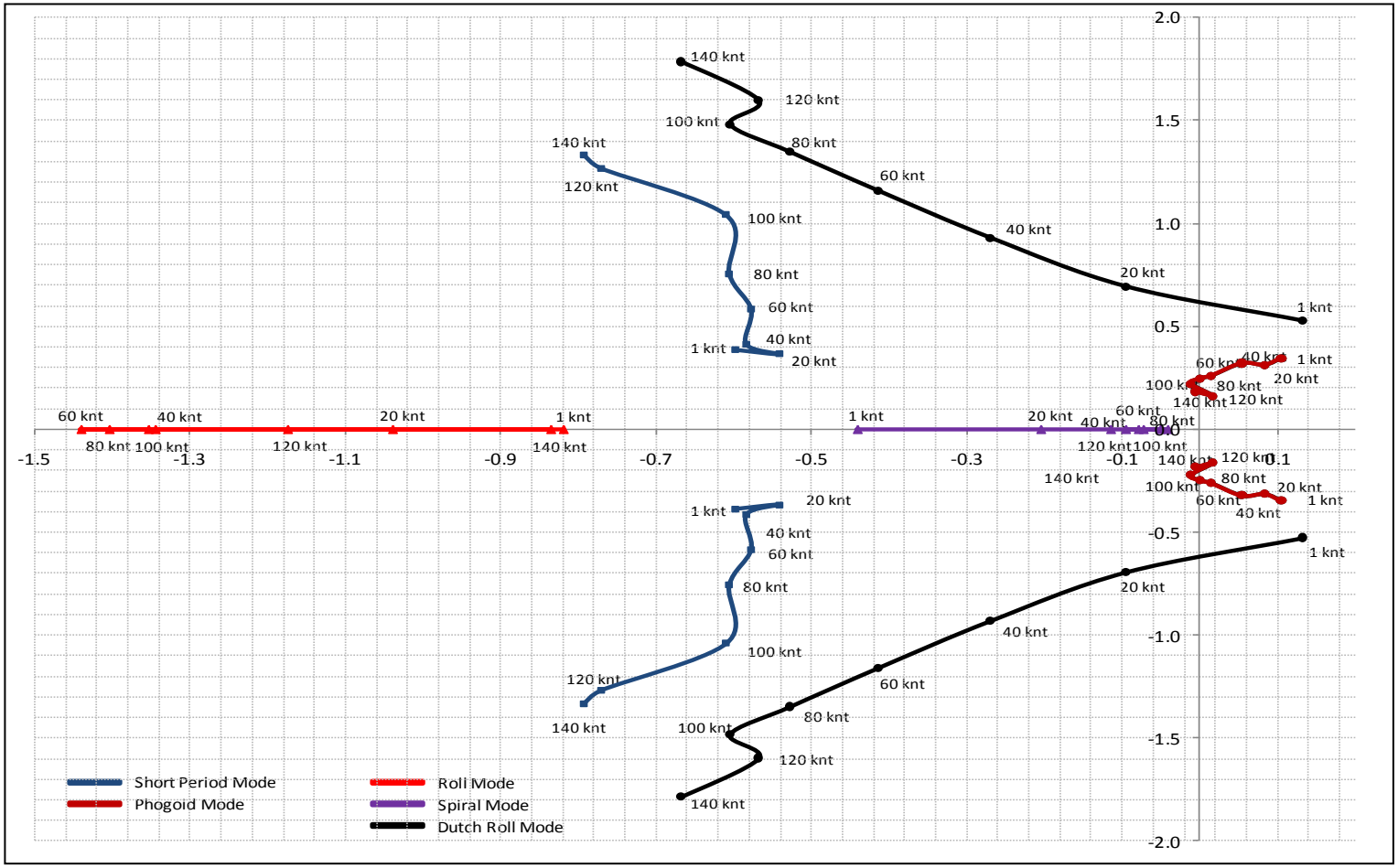

Figure 14 AH-1G Helicopter Pole Locations

CHAPTER 4

CONTROLLER DESIGN

Helicopter dynamic modes resemble those of fixed-wing aircraft. However, cross-couplings have more significant effects on helicopter dynamics than fixed-wing aircraft [33]. Therefore, it is avoided to decouple the longitudinal and lateral dynamics in helicopter controller design [32]. Alternative to the traditional control methods which are widely-used for fixed-wing aircrafts, one of the accepted control method for the nonlinear systems like helicopters is dynamic inversion [8]. According to this method, nonlinear control is achieved by using an inverse transformation of the linearized helicopter model [8]. In this study, the trajectory and the attitude controller which is based on dynamic inversion method is analyzed in three main parts. These are; plant model, inner loop and outer loop. In plant model part, helicopter linear model is introduced. In inner loop part, the inverse transformation technique, helicopter stabilization and attitude control are explained. In outer loop part, the trajectory control technique, guidance algorithm and the controller switching logic are defined. The concept representation of the trajectory and the attitude controller is given in Figure 15.

4.1 Plant Model

Plant model is composed of actuator model, linear helicopter model and state space model interpolation block.

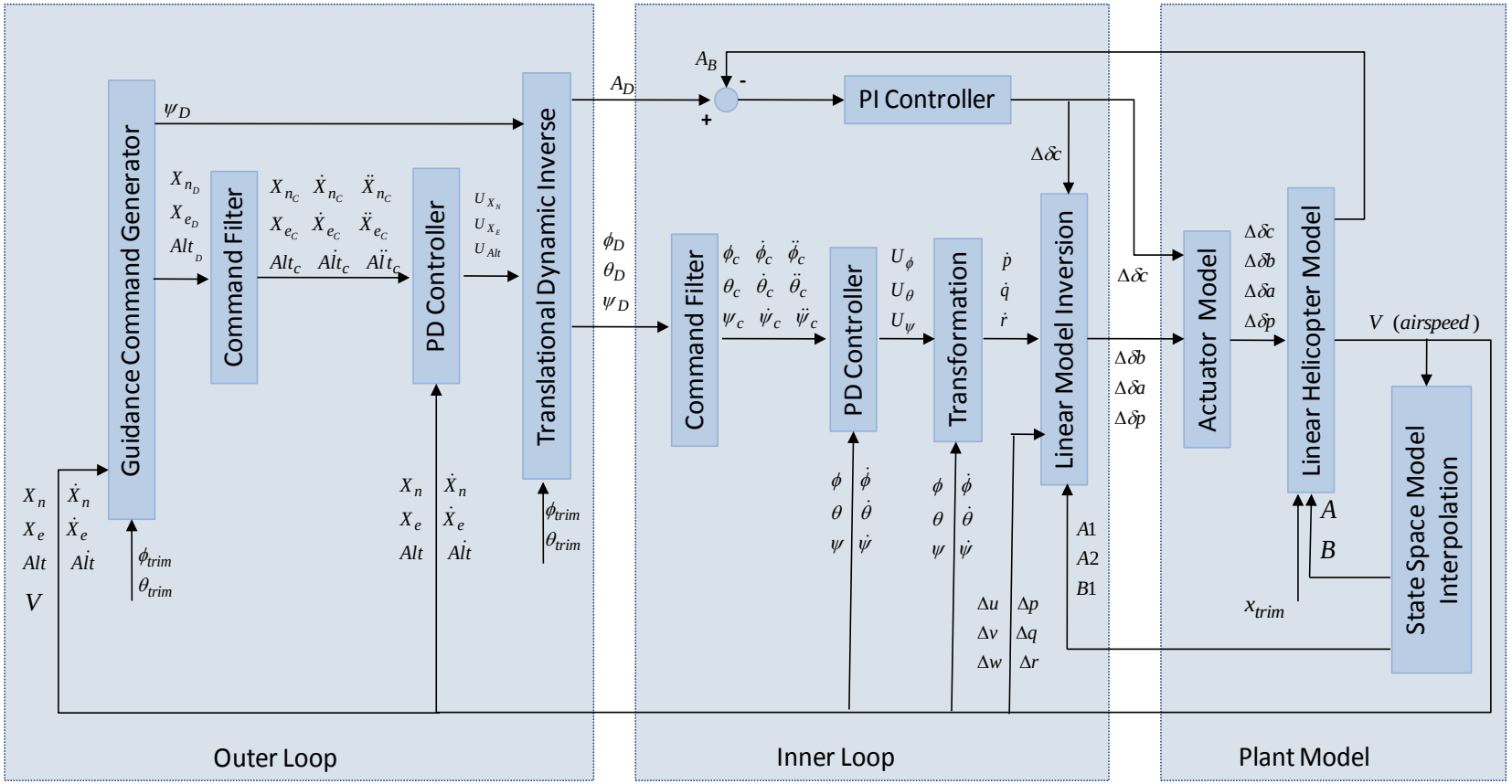

Figure 15 Concept Representation of Trajectory and Attitude Controller

4.1.1 Actuator Model

In this study, the actuator model is represented as a first order low pass filter. According to typical control engineering approach, actuator bandwidth is selected as it is at least five times higher than the helicopter natural frequencies (helicopter natural frequencies are given in Chapter 3). With this assumption, bandwidth is selected as 8 Hz for all actuators (collective, lateral / longitudinal cyclic and the pedal). The actuator transfer function is given in Equation 4.1.

$$TF = \frac{50}{s + 50} \tag{4.1}$$

According to Ref. [31], the actuator deflection limitations of AH-1G helicopter are selected as in Table 3.

Table 3 Actuator Limits

	Collective, δ_c	Longitudinal Cyclic, δ_b	Lateral Cyclic, δ_a	Pedal, δ_p
Deflection Limits (in.)	±5	±6	±6	±3.25

Also, it is assumed that there is no backlash in the actuators in the scope of this study.

4.1.2 Linear Helicopter Model State Space Model Interpolation Block

In this thesis, state space approximation is used to model helicopter dynamics. Helicopter model and state space model interpolation are explained in Chapter 3. Helicopter model is integrated to the simulation with the calculation block given in Figure 16.

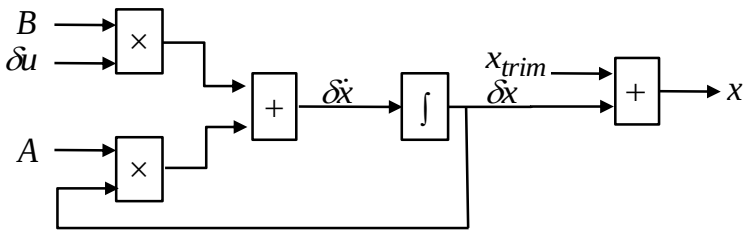

Figure 16 Calculation Block of the Linear Helicopter Model

In linear helicopter model, the helicopter body translational velocities (u, v, w), body angular rates (p, q, r) and Euler angles (ϕ, θ, ψ) are computed according to the above given block. The calculation of the positions (X_n, X_e, X_d) and velocities ($\dot{X}_n, \dot{X}_e, \dot{X}_d$) in Earth-Fixed Reference Frame are performed according to the following paragraph. Acceleration calculations are explained in Paragraph 4.2.5.

Position and Velocity Calculation in Earth-Fixed Reference Frame

In linear helicopter model block, velocity values in Body-Fixed Reference Frame are transformed into the velocity in Earth-Fixed Reference Frame and position values are calculated by integration. Then, position value in “down” direction is converted into “altitude” value by multiplying with “-1”. The related formulation is given in Equation 4.2.

$$V_V = L_{VB} V_B$$

$$\begin{bmatrix} \dot{X}_n \\ \dot{X}_e \\ \dot{X}_d \end{bmatrix} = L_{VB} \begin{bmatrix} u \\ v \\ w \end{bmatrix} \Rightarrow \left(\int \begin{bmatrix} \dot{X}_n \\ \dot{X}_e \\ \dot{X}_d \end{bmatrix} \right) \cdot \begin{bmatrix} 1 & 1 & -1 \end{bmatrix} = \begin{bmatrix} X_n \\ X_e \\ h \end{bmatrix} \tag{4.2}$$

4.2 Inner Loop Controller

Rotational dynamics are stabilized in inner loop by using the inverse transformation of the plant matrices [6]. Inputs of this loop are Euler angles (ϕ, θ, ψ) and the outputs are the actuator commands (δ_c, δ_b, δ_a, δ_p). Euler angles which are generated by the outer loop are passed through the command filter, compared with actual Euler angles and their derivatives (fed from linear helicopter model) and then, the errors are processed by the PD controller. Proportional element of the PD controller increases stability and the derivative element is implemented to improve the transient performance. The outputs of the controller are transformed into the rotational body rates and then, the actuator commands ($\Delta\delta_b$, $\Delta\delta_a$, $\Delta\delta_p$) are obtained by inverse transformation. The collective control channel ($\Delta\delta_c$) which is related with total acceleration demand is slower than the longitudinal, lateral and pedal controls which are connected to fast rotational states. Therefore, collective control is

decoupled from the other three controls. Helicopter acceleration is controlled by a PI controller. Steady state error in acceleration which may lead to divergence of the total velocity of the helicopter is reduced by the integral action.

The internal blocks of the inner loop are explained in the following paragraphs.

4.2.1 Command Filter

Inner loop inputs are the Euler angles which are the outputs of the outer loop. Each Euler angle command is passed through a second order command filter to generate the controller commands. Also, by the second order command filter, the first and the second order derivatives of the Euler angles are generated. These derivatives are the commands of the PD controller. The natural frequency of the command filter is selected as 3 rad/s and damping ratio is selected as 0.8 for each channel.

Command filter block diagram for the theta channel is given in Figure 17.

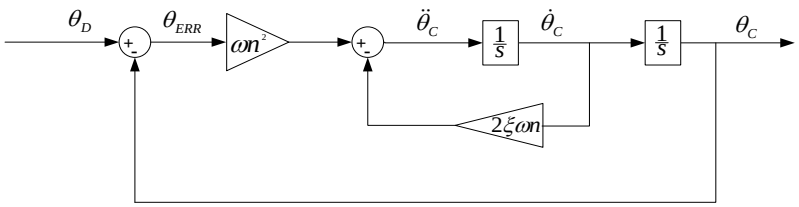

Figure 17 Command Filter Block Diagram for Theta Channel

4.2.2 PD Controller

The command filter outputs and the actual Euler angles and their derivatives are fed to PD controller. The outputs of the PD controller correspond to the second derivatives of the Euler angles. In order to increase the system response, the second order derivatives coming from the command filter are fed forward.

PD controllers are present for all of the channels (phi, theta, psi) in the inner loop. An example illustration of the three channel PD controller is given in Figure 18. The proportional and derivative controller gain selections are described in APPENDIX C. Same gain values are used for each channel and kept constant for all forward velocity conditions.

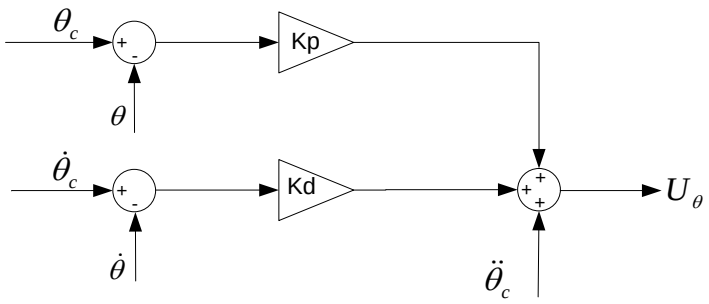

Figure 18 PD Controller Block Diagram for Theta Channel

4.2.3 Transformation

In transformation block, the Euler angular accelerations, which are the outputs of PD controller, are converted into body angular accelerations which are the linear model inversion block commands. The related formulation is given in Equation 4.3.

$$\begin{aligned} \dot{p} &= \ddot{\phi} - \ddot{\psi}\sin\theta - \dot{\psi}\dot{\theta}\cos\theta \\ \dot{q} &= \ddot{\theta}\cos\phi - \dot{\theta}\dot{\phi}\sin\phi + \ddot{\psi}\sin\phi\cos\theta + \dot{\psi}\dot{\phi}\cos\theta\cos\phi - \dot{\psi}\dot{\theta}\sin\theta\sin\phi \\ \dot{r} &= -\ddot{\theta}\sin\phi - \dot{\theta}\dot{\phi}\cos\phi + \ddot{\psi}\cos\phi\cos\theta - \dot{\psi}\dot{\phi}\cos\theta\sin\phi - \dot{\psi}\dot{\theta}\sin\theta\cos\phi \end{aligned} \qquad (4.3)$$

It should be noted that the body angular accelerations ($\dot{p}$, $\dot{q}$, $\dot{r}$) are the outputs of the transformation block, Euler angular accelerations ($\ddot{\phi}$, $\ddot{\theta}$, $\ddot{\psi}$) are the outputs of the PD controller and the Euler angles (ϕ, θ, ψ) and their first derivatives ($\dot{\phi}$, $\dot{\theta}$, $\dot{\psi}$) are the linear helicopter model outputs.

4.2.4 Dynamic Inversion (Linear Model Inversion) Method

Helicopter fast rotational states are stabilized by dynamic inversion method. Dynamic inversion matrices are derived from the decoupled state space representation. The derivation starts from state space model.

$$\dot{x} = Ax + Bu \tag{4.4}$$

Then, the fast rotational and slow translational states are decoupled. Since the dynamic effect of collective is rather slow compared to other three controls, collective control is decoupled from the other states.

$$\dot{x}_1 = A_1 x_1 + A_2 x_2 + B_1 u_1 \tag{4.5}$$

Definitions of the matrices (Equation 4.6) are given in Table 4.

Table 4 Dynamic Model Inversion Method Symbol Definition

Symbols	Definiations
x_1	The state vector containing rotational states ($p,\ q,\ r$)
x_2	The state vector containing translational states and collective control ($u,\ v,\ w,\ \delta_c$)
A_1	Stability matrix containing the effects of rotational states on themselves
A_2	The stability matrix containing the effects of translational states on rotational states
B_1	The control matrix containing the effect of controls on rotational states
u_1	The control vector containing the longitudinal, lateral and pedal controls

$$x_1 = \begin{bmatrix} \Delta p \\ \Delta q \\ \Delta r \end{bmatrix}; \quad x_2 = \begin{bmatrix} \Delta u \\ \Delta v \\ \Delta w \\ \Delta \delta_c \end{bmatrix}; \quad A_1 = \begin{bmatrix} L'_p & L'_q & L'_r \\ M_p & M_q & M_r \\ N'_p & N'_q & N'_r \end{bmatrix}; \quad A_2 = \begin{bmatrix} L'_u & L'_v & L'_w & L'_{\delta_c} \\ M_u & M_v & M_w & M_{\delta_c} \\ N'_u & N'_v & N'_w & N'_{\delta_c} \end{bmatrix};$$

$$B_1 = \begin{bmatrix} L'_{\delta_b} & L'_{\delta_a} & L'_{\delta_p} \\ M_{\delta_b} & M_{\delta_a} & M_{\delta_p} \\ N'_{\delta_b} & N'_{\delta_a} & N'_{\delta_p} \end{bmatrix}; \quad u_1 = \begin{bmatrix} \Delta \delta_b \\ \Delta \delta_a \\ \Delta \delta_p \end{bmatrix} \tag{4.6}$$

If control vector u_1 is left alone in Equation 4.5, the final linear model equation is obtained (Equation 4.7).

$$u_1 = B_1^{-1} \cdot \left[\dot{x}_1 - A_2 x_2 - A_1 x_1 \right] \Rightarrow \begin{bmatrix} \Delta \delta_b \\ \Delta \delta_a \\ \Delta \delta_p \end{bmatrix} = B_1^{-1} \cdot \left(\begin{bmatrix} \dot{p} \\ \dot{q} \\ \dot{r} \end{bmatrix} - A_2 \begin{bmatrix} \Delta u \\ \Delta v \\ \Delta w \\ \Delta \delta_c \end{bmatrix} - A_1 \begin{bmatrix} \Delta p \\ \Delta q \\ \Delta r \end{bmatrix} \right) \tag{4.7}$$

It should be noted that the body angular accelerations ($\dot{p}$, $\dot{q}$, $\dot{r}$) are the outputs of the transformation block, the states Δu, Δv, Δw, Δp, Δq and Δr are fed back from the linear helicopter model to linear model inversion block and the collective control $\Delta \delta_c$ is the output of the acceleration controller (PI controller).

4.2.5 Acceleration Controller (PI Controller)

Helicopter total acceleration is mainly related with main rotor thrust which is produced by collective control. The acceleration command which is generated in the outer loop is compared with the actual acceleration which is obtained from the linear helicopter model and the error is processed by a PI controller to produce the collective control command ($\Delta \delta_c$). Proportional element of the PI controller is required to increase stability and the integrator element is used to reduce the steady state error which may cause divergence in the total velocity. Equations about acceleration control are given below.

Desired acceleration components (U_{Xn}, U_{Xe}, U_{Alt}) which are represented in Earth-Fixed Reference Frame are generated by the translational dynamic inverse block. Explanation about this derivation is given in the following paragraphs. The formulation of the desired acceleration is given as;

$$a_D = \sqrt{U_{Xn}^2 + U_{Xe}^2 + (U_{Alt} - g)^2} \tag{4.8}$$

In the desired acceleration formulation, only the required aerodynamic loads are taken into consideration and therefore, the specific gravity force is excluded here.

In linear helicopter model block, acceleration values in Body-Fixed Reference Frame are transformed into the acceleration in Earth-Fixed Reference Frame (Equation 4.9).

$$\bar{a}_B = \begin{bmatrix} \frac{F_x}{m} \\ \frac{F_y}{m} \\ \frac{F_z}{m} \end{bmatrix} + L_{BV} \begin{bmatrix} 0 \\ 0 \\ g \end{bmatrix} = \begin{bmatrix} \dot{u} \\ \dot{v} \\ \dot{w} \end{bmatrix} + \begin{bmatrix} 0 & -r & q \\ r & 0 & -p \\ -q & p & 0 \end{bmatrix} \cdot \begin{bmatrix} u \\ v \\ w \end{bmatrix}$$

$$\Rightarrow \begin{bmatrix} a_x \\ a_y \\ a_z \end{bmatrix} = L_{VB} \begin{bmatrix} \frac{F_x}{m} \\ \frac{F_y}{m} \\ \frac{F_z}{m} \end{bmatrix} = L_{VB} \left(\begin{bmatrix} \dot{u} \\ \dot{v} \\ \dot{w} \end{bmatrix} + \begin{bmatrix} 0 & -r & q \\ r & 0 & -p \\ -q & p & 0 \end{bmatrix} \cdot \begin{bmatrix} u \\ v \\ w \end{bmatrix} \right) - \begin{bmatrix} 0 \\ 0 \\ g \end{bmatrix} \tag{4.9}$$

Definitions of the symbols are given in Table 5.

Table 5 Symbol Definitions for Acceleration Calculation

Symbols	Definiations
$\vec{a}_B$	Helicopter actual acceleration vector in Body-Fixed Reference Frame
$F_x,\ F_y,\ F_z$	Aerodynamic and Propulsive Forces in Body-Fixed Reference Frame
L_{EB}	Transformation Matrix from Body-Fixed Reference Frame to Earth-Fixed Reference Frame
$u, v, w, \dot{u}, \dot{v}, \dot{w}, p, q, r, \phi, \theta, \psi$	Linear Helicopter Model Outputs
$a_x,\ a_y,\ a_z$	Actual Acceleration Components in Earth-Fixed Reference Frame

Total actual acceleration formulation in Earth-Fixed Reference Frame is given in Equation 4.10.

$$a = \sqrt{a_x^2 + a_y^2 + a_z^2} \tag{4.10}$$

4.3 Outer Loop Controller

Trajectory control and guidance decisions are performed in this loop. The position (north / east positions and altitude) commands, heading angle commands and the controller switching judgment are formed in guidance command generator block. Position controls are provided through a PD controller. Helicopter heading angle which is produced by guidance command generator block is directly passed from the outer loop to inner loop without any change.

4.3.1 Guidance Command Generator

The flight trajectories are created according to the selected attack pattern and firing types of Cobra helicopter and the firing attitudes are derived from ballistic trajectories of 2.75” rockets. The logic flowchart of the guidance algorithms is shown in Figure 19.

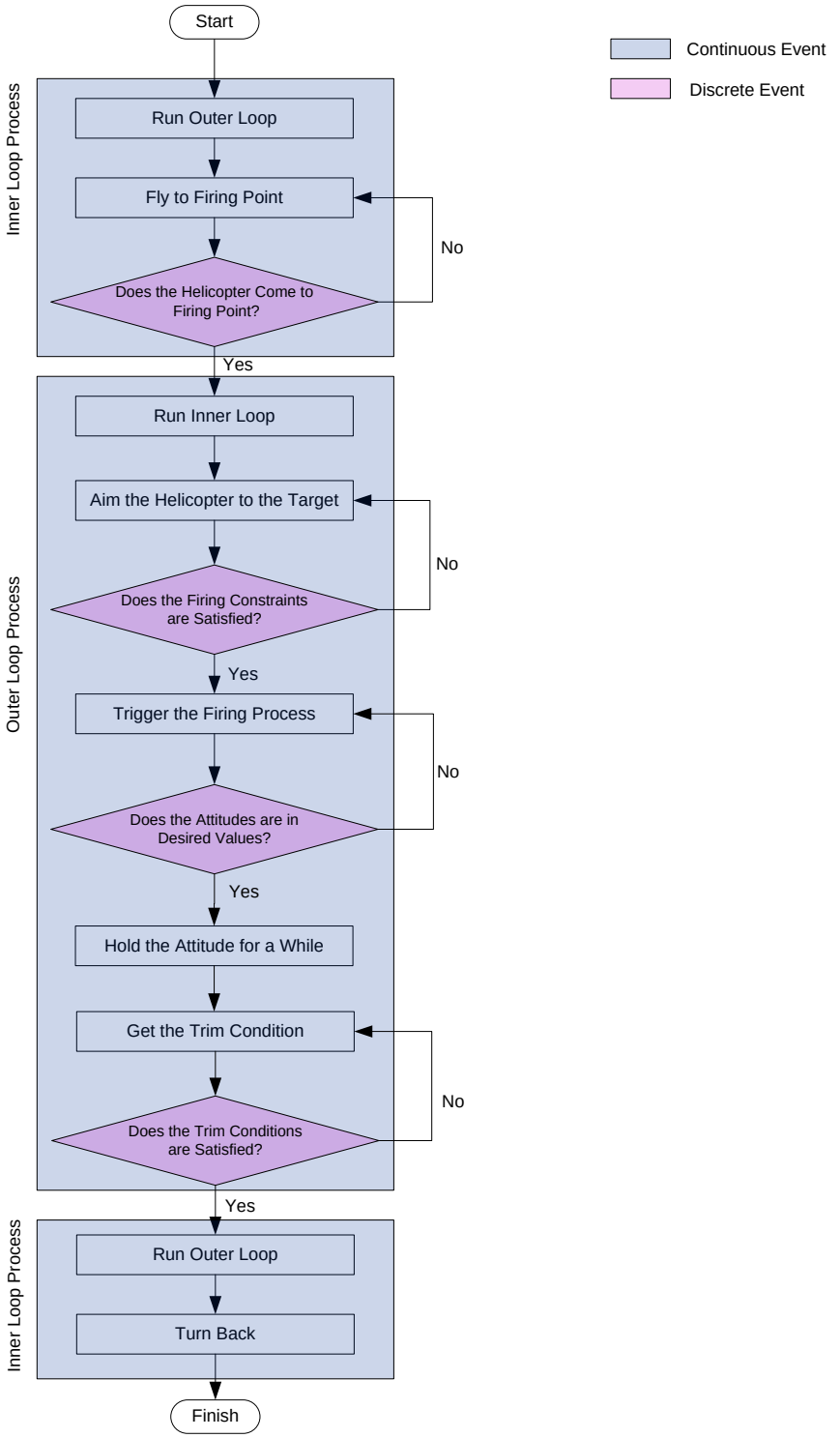

Figure 19 Logic Flowchart of Guidance Algorithm

The guidance algorithms are studied in three main groups according to firing types.

4.3.1.1 Guidance Algorithm for Hover Fire

The helicopter starts flying with trajectory control. The commands of the trajectory control are desired north / east positions, altitude and the direction (heading angle) of the flight. Helicopter continues to fly with trajectory control until the commanded positions and the heading angle are satisfied. In addition to this requirement, it is expected that helicopter reaches to 0 knot forward velocity at the firing point which is the hover firing requirement Velocity control is performed inherently by assuming that the forward velocity is equal to the first derivative of the forward position (see Equation 4.11).

$$V_n = \frac{X_n}{t} \tag{4.11}$$

When the helicopter reaches to the firing point, if the requirements are satisfied, the Guidance Algorithm switches the controller from trajectory control (outer loop) to the attitude control (inner loop). Controller switching concept is shown in Figure 20.

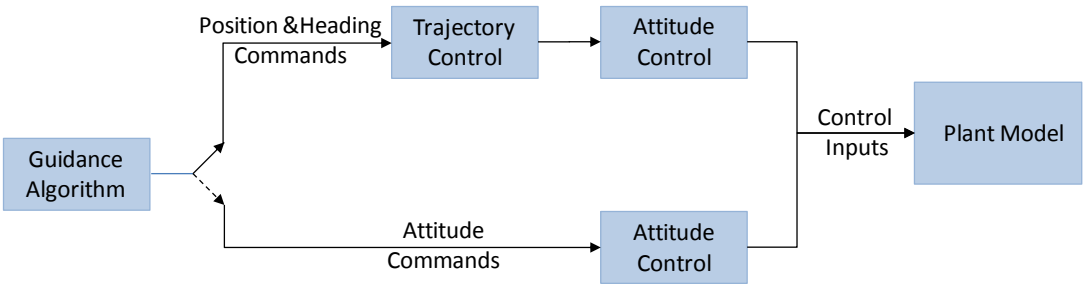

Figure 20 Controller Switching Concept

Requirements (Discrete decisions) to Switch Controller from Outer Loop to Inner Loop

- Actual position (north/east/altitude) and heading angle are equal to commanded values within the design tolerance
- Helicopter is in hover condition
- Helicopter is in trim condition

Trim condition is inherently gained by setting the controller commands (positions and heading angle) in steady state form.

Guidance algorithm determines the required Euler angles at the firing instant for relevant target range. When the actual Euler angles reaches to the desired ones within the design tolerance, the firing is triggered and the attitude angles are hold for a few seconds to make sure that the rocket is separated from the helicopter. It must be noticed that the rocket firing and separation dynamics are not modeled here. However it is known from the 2.75" rocket ignition system characteristics that the rocket is ignited within 40 – 50 ms and the rocket leaves the launcher within 100 ms after trigger pull [34].

The last criterion to pass from the attitude control (inner loop) to trajectory control (outer loop) is taking the helicopter back to the trim conditions. This trim condition is obtained by setting the Euler angles to the values just before the previous controller switching. When the trim conditions are satisfied, helicopter attitudes are again hold for a while and after that, the controller is switched from the attitude control (inner loop) to trajectory control (outer loop).

At this step, the helicopter heading angle is commanded to make a 180° turn in counter clockwise direction. In this way, the helicopter retreats. After that, helicopter keeps its direction and altitude until it reaches to the last waypoint. When the helicopter arrives the simulation is terminated.

4.3.1.2 Guidance Algorithm for Running Fire

Guidance algorithm logic for running fire is quite similar with those for hover fire. One of the main differences of running fire from hover fire is that the helicopter must have a specified forward velocity instead of 0 knot at the firing instant. The second major difference is that when helicopter controller is switched (after firing) from attitude control (inner loop) to trajectory control (outer loop); it tracks a circular flight

pattern until it turns back to the retreating flight direction. Conceptual drawing of this flight pattern is given in Figure 21.

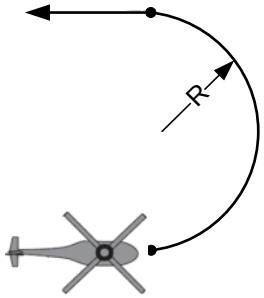

Figure 21 Conceptual Drawing of U-turn for Running Fire

The relation between helicopter heading rate, helicopter forward velocity and the radius of curvature can be written as (Equation 4.12);

$$\dot{\psi} = \frac{V}{R} \tag{4.12}$$

4.3.1.3 Guidance Algorithm for Diving Fire

Guidance algorithm logic for diving fire is quite similar with those for running fire. The main difference between these two flight types is, in spite of running fire, flight altitude is variable in diving flight. Before firing, helicopter dives until it reaches to the firing point and after firing it ascends again.

Before helicopter reaches to the firing point, altitude command is generated according to the flight path angle (Figure 22). The related equation can be given as (Equation 4.13);

$$\text{Descending Altitude} = \text{Descending Range} \cdot \sin\gamma \tag{4.13}$$

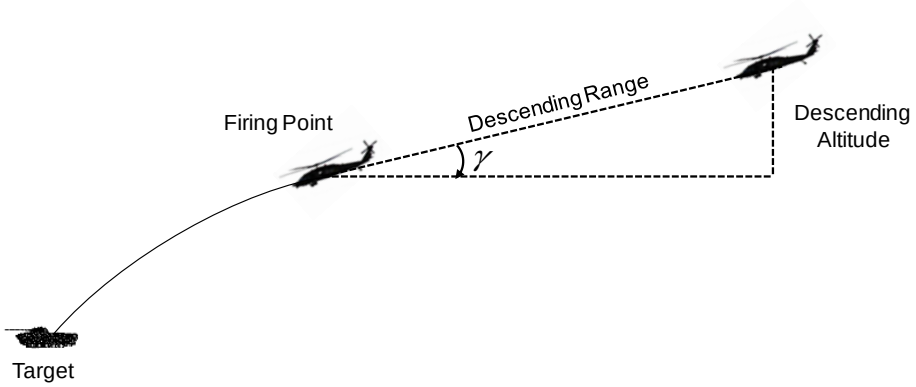

Figure 22 Flight Path Angle Relations with Descending Altitude and Descending Range

4.3.2 Command Filter

The function of the outer loop command filter is the same as the function of filter in the inner loop. The filter inputs are the helicopter desired positions (north, east, altitude) and the outputs are the filtered position demands and the associated first and second order derivatives which are going to be the commands of PD controller in the outer loop.The natural frequency and the damping ratio of the command filter are chosen as 0.7 rad/s and 0.8 respectively for each channel.

An example illustration of the three channel command filter is given in Figure 23.

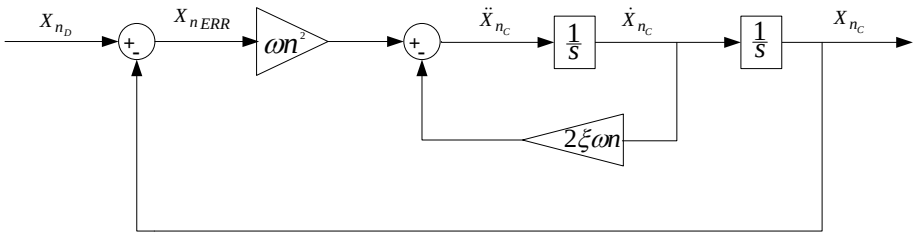

Figure 23 Command Filter Block Diagram for North Position Channel

4.3.3 PD Controller

The PD controller inputs are the command filter outputs, the actual positions and their first derivatives (the linear helicopter model outputs). The outputs of the

controller correspond to the second derivative of the positions. To increase the system response to the inputs, the second order derivatives coming from the command filter are fed forward.

PD controllers are present for all channels (north / east position and altitude) in the outer loop. An example illustration of the three channel PD controller is given in Figure 24.

The proportional and derivative controller gain selections are described in APPENDIX C. Same gain values are used for each channel and kept constant for all forward velocity conditions.

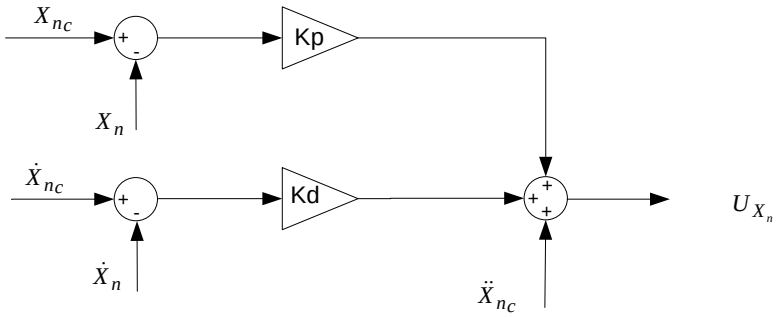

Figure 24 PD Controller for North Position Channel

4.3.4 Translational Dynamic Inverse

In this block, the PD Controller outputs are converted into Euler angle commands (pitch and roll angle). The formulations are explained below.

$$\begin{bmatrix} \ddot{X}_n \\ \ddot{X}_e \\ \ddot{Alt} \end{bmatrix} = L_{EB} \cdot \begin{bmatrix} F_x / m \\ F_y / m \\ F_z / m \end{bmatrix} + \begin{bmatrix} 0 \\ 0 \\ g \end{bmatrix} \Rightarrow \begin{bmatrix} U_{X_n} \\ U_{X_e} \\ U_{Alt} - g \end{bmatrix} = \mathrm{L}_{\mathrm{VB}} \begin{bmatrix} F_x / m \\ F_y / m \\ F_z / m \end{bmatrix} \tag{4.14}$$

Where,

X_n, X_e, Alt : Positions in Earth-Fixed Reference Frame

L_{EB}: Transformation Matrix from Body-Fixed Reference Frame to Earth-Fixed Reference Frame

F_x, F_y, F_z: Aerodynamic Forces and Thrust in Body-Fixed Reference Frame

U_{X_n}, U_{X_e}, U_{Alt}: Outer loop PD controller outputs (Acceleration commands in Earth-Fixed Reference Frame)

Formulation of pitch and roll angle commands (Equation 4.15) is derived from Equation 4.14 under some assumptions. These are;

- Lateral / longitudinal cyclic and pedal control forces are much smaller compared to the collective control force
- F_x and F_y are very small compared to F_z [8];

$$\phi_D = \sin^{-1}\left(\frac{-U_{X_n}\sin\psi_D + U_{X_e}\cos\psi_D}{\sqrt{U_{X_n}{}^2 + U_{X_e}{}^2 + (U_{Alt}-g)^2}}\right) + \phi_{trim}$$

$$\theta_D = \tan^{-1}\left(\frac{U_{X_n}\cos\psi_D + U_{X_e}\sin\psi_D}{(U_{Alt}-g)}\right) + \theta_{trim} \qquad (4.15)$$

Where ψ_D is the heading command, θ_D and ϕ_D are pitch and roll commands respectively.

CHAPTER 5

SIMULATION RESULTS

The trajectory and attitude controller performance is analyzed in simulation environment. Three test cases are developed according to the Cobra helicopter tactical usage. The firing type, the helicopter forward velocity and helicopter relative altitude, target range and the helicopter pitch angle values are taken as basic criterions to generate these test cases. With the selected helicopter forward velocity, relative altitude and target range, the required helicopter pitch angle is determined from [27]. The test cases are tabulated in Table 6.

Table 6 Test Cases[2]

Scenario	Firing Type	Forward Velocity	Relative Altitude	Target Range	Pitch Angle	Target Motion
1	Hover Fire	0 knot	150 ft	Mid Range (~3km)	0.5 deg	Moving
2	Running Fire	60 knot	300 ft	Mid Range (~3km)	-0.5 deg	Stationary
3	Diving Fire	60 knot	3000 ft	Mid Range (~3km)	-16 deg	Stationary

The selection of roll angle (at target alignment phase) is done by the classical convention of “wings level” (zero roll) approach. Yaw (heading) angle is selected such that the helicopter nose is directly pointing to the target. For all of the firing scenarios, target direction with respect to the helicopter is assumed to be North-East (45 deg clockwise). However, it is assumed that the target is not stationary for Scenario 1. Therefore the “moving target” correction is added to the desired yaw angle requirement (North-East direction in heading). For “moving target” calculations, it is assumed that the helicopter is hovering, the target range is 3 km and the target is moving with a constant speed, 70 km/s (nominal value for tanks or light armoured personnel carriers). The concept drawing of the yaw angle correction for moving target condition is given in Figure 25.

[2] Forward velocity, relative altitude and pitch angle values are the values at target alignment phase

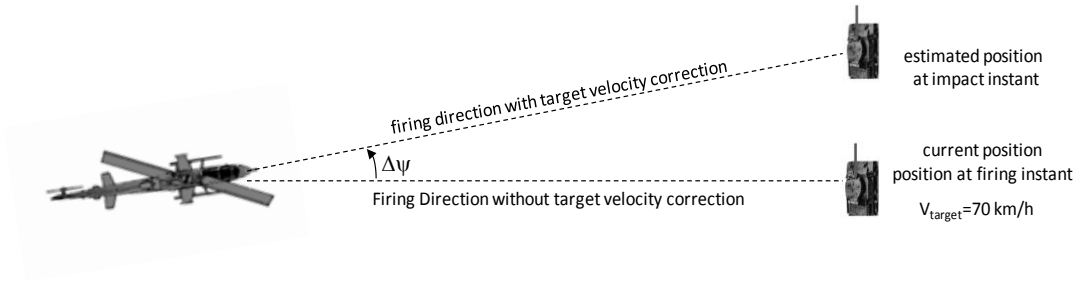

Figure 25 The Concept Drawing of The Yaw Angle Correction for Moving Target Condition

The heading angle correction is calculated as;

$$\Delta\psi = \tan^{-1}\left(\frac{\text{change in target position}}{\text{target range}}\right) = \tan^{-1}\left(\frac{\text{target speed}\cdot\text{rocket flight time}}{\text{target range}}\right)$$

$$= \tan^{-1}\left(\frac{70\cdot 7}{3}\left[km/h\right]\cdot[s]\cdot\left[1/km\right]\right) \cong 2.5\,\text{deg} \qquad (5.1)$$

Where,

The rocket flight time is taken as 7s according to the ballistic charts [27].

With these calculations, by adding the moving target correction, the helicopter yaw angle requirement becomes 47.5 deg at firing instant for Scenario 1.

5.1 Test Cases

5.1.1 Scenario 1 (Hover Fire Test)

Initial conditions are defined as; helicopter forward velocity is 1 knot, helicopter heading is to the north. The helicopter flies to the firing point which is 3000 ft away from the initial point with north-east heading and the altitude is 150 ft above from the initial position. First, the helicopter accelerates until it reaches to 40 knot forward velocity, and then continues to fly with a constant speed and then it starts to decelerate until it reaches approximately to 0 knot forward velocity at firing point. When the helicopter arrives to firing point, switching from trajectory control to attitude control occurs. Then, the helicopter changes its attitudes according to the firing aiming angles which is 0.5 degree pitch and 0 degree roll. When the desired attitudes are reached, rocket firing is triggered and the helicopter is commanded to

hold this attitude for a second to guarantee that the rocket is separated from the helicopter at desired attitudes. Then, the helicopter attitudes are commanded to turn back to the conditions just before the previous switching. The reason of this action is to force the helicopter to turn back to the trim condition. The helicopter attitudes are again hold at these values for a second and then the controller is switched back to trajectory control. Then, the helicopter performs a 180 degree heading turn (counterclockwise direction is positive) to retreat. When the helicopter closes to its initial position less than 1000 ft in the horizontal plane, it initiates a descent that will continue until ground level altitude.

In these simulations, the position tolerances are set to 10 ft in each direction (north, east, altitude) and the attitude angle tolerances are taken as 1 degree in each direction (roll, pitch, yaw) in order to perform discrete events like controller switching and fire triggering. These tolerances and the attitude hold durations are selected considering the actual applications of Cobra pilots. Simulation results are given in Figure 26 - Figure 31.

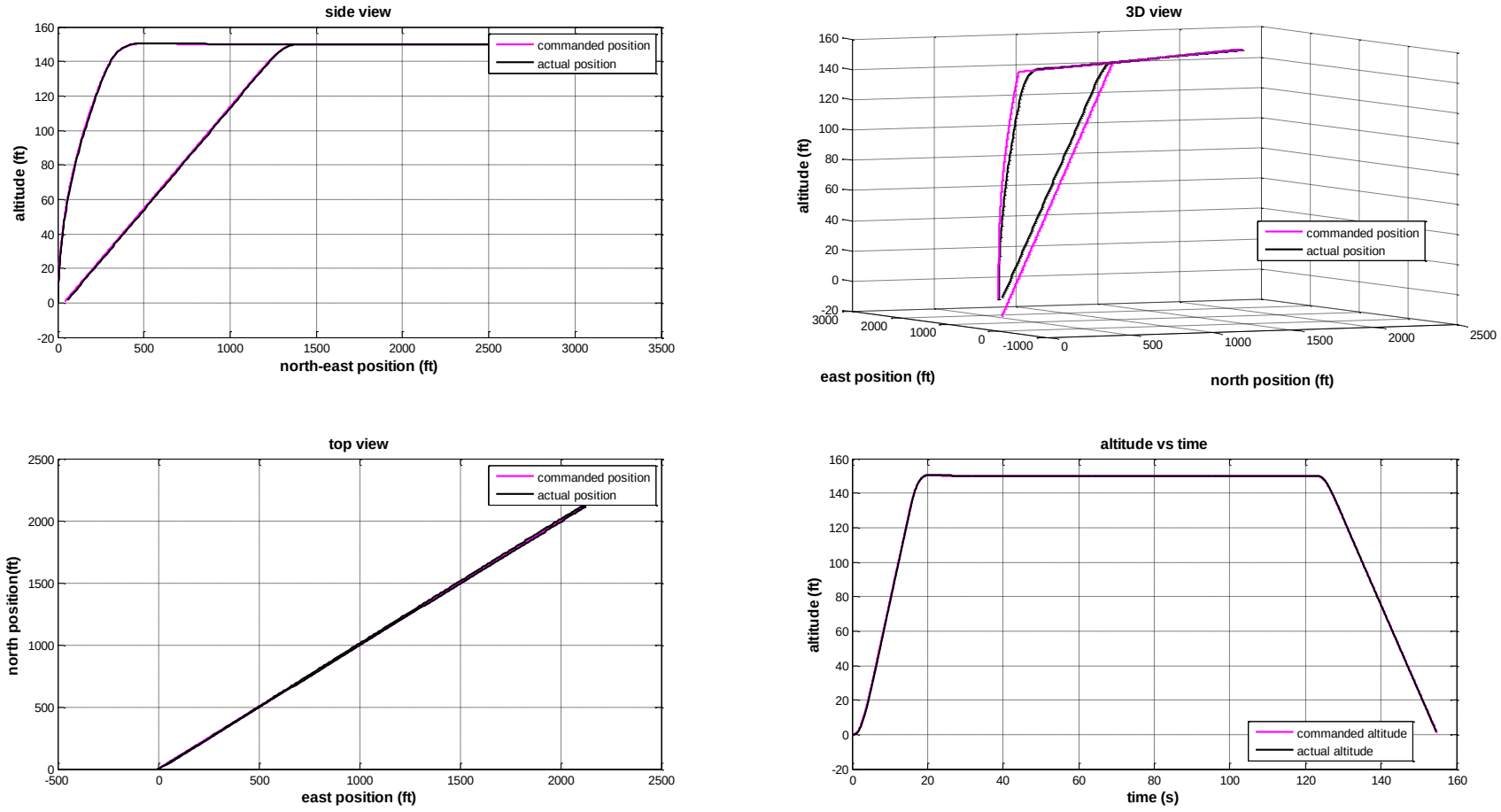

Figure 26 Scenario 2 North / East Positions and Altitude

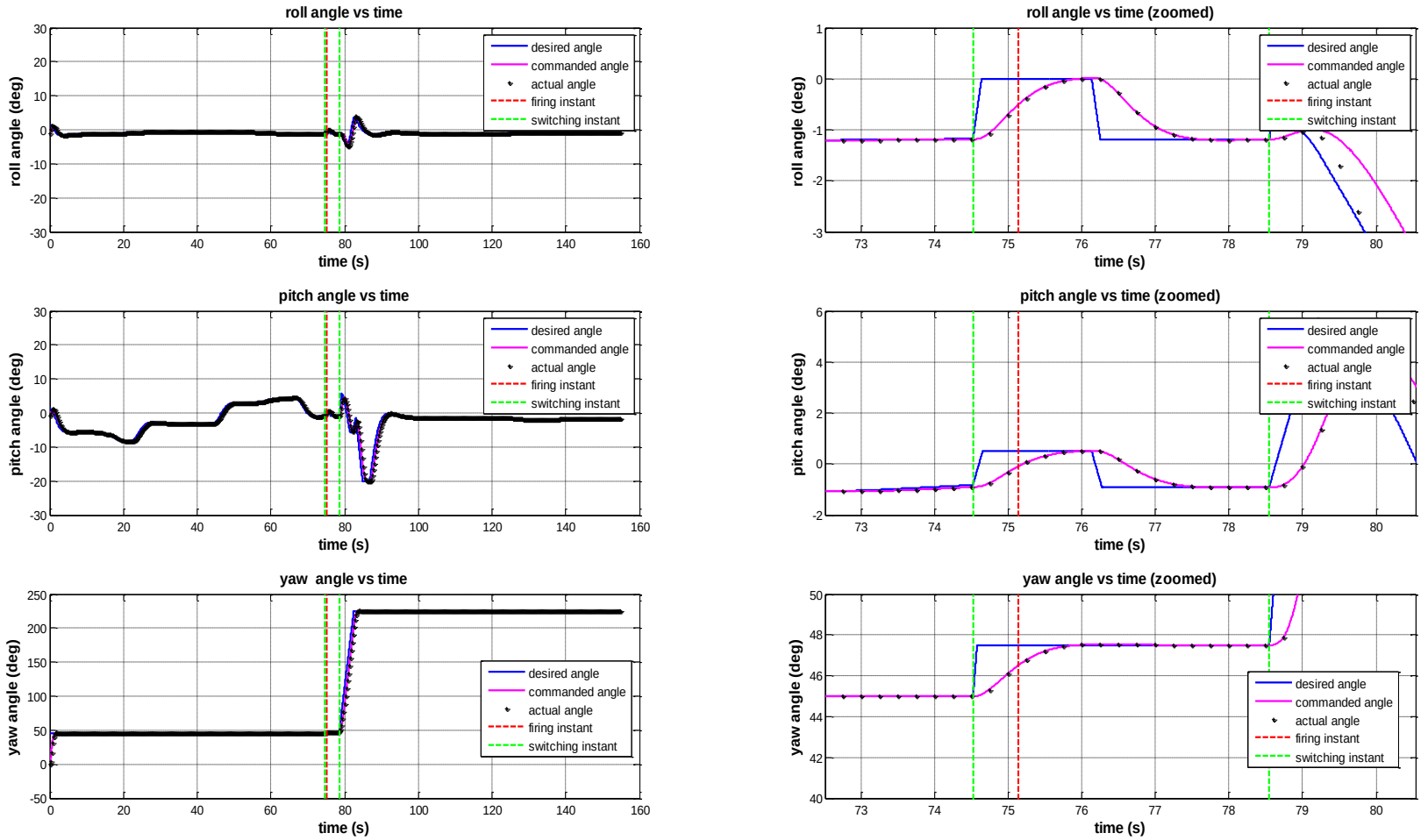

Figure 27 Scenario 1 Euler Angles

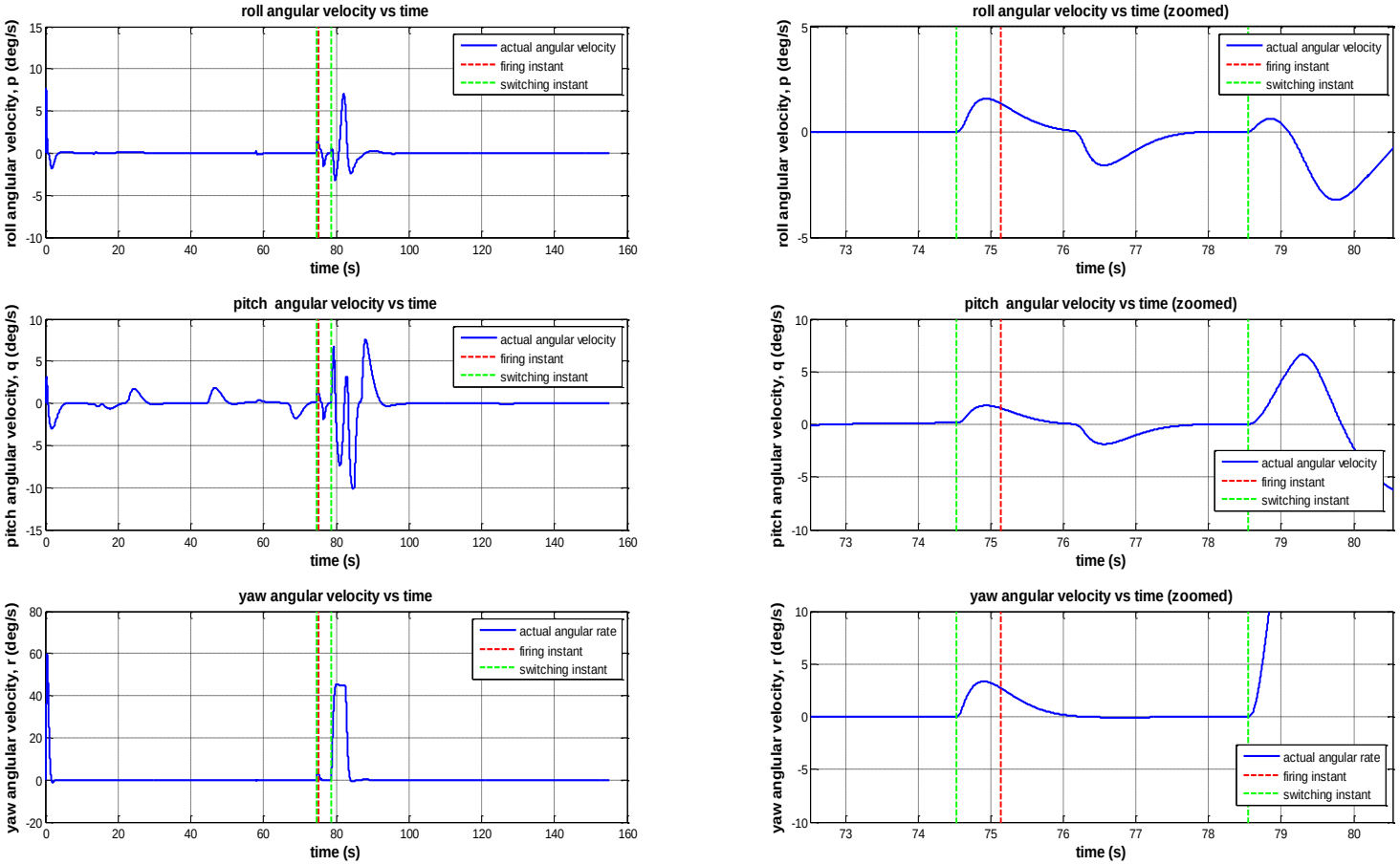

Figure 28 Scenario 1 Angular Velocities

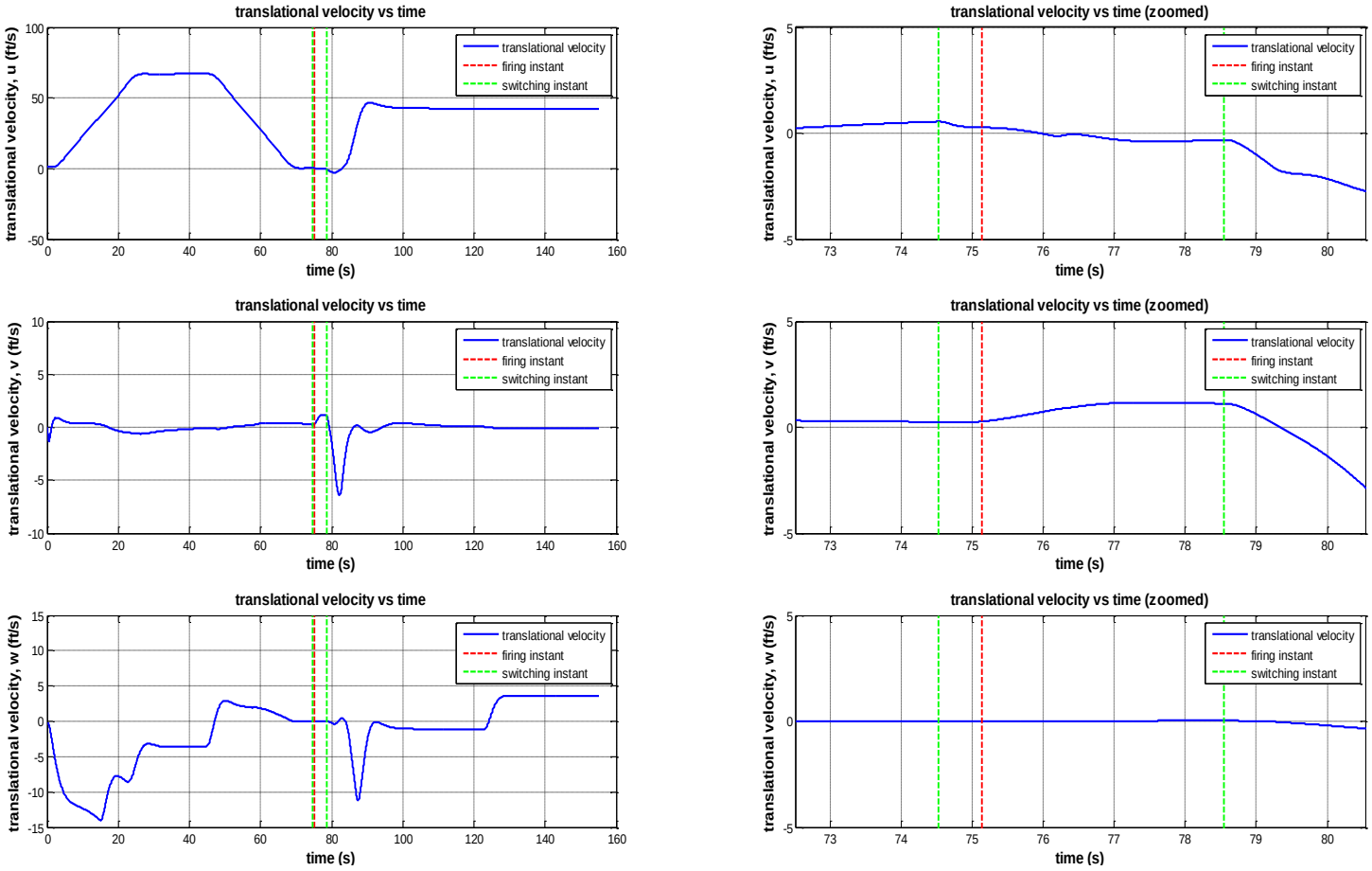

Figure 29 Scenario 1 Translational Velocities

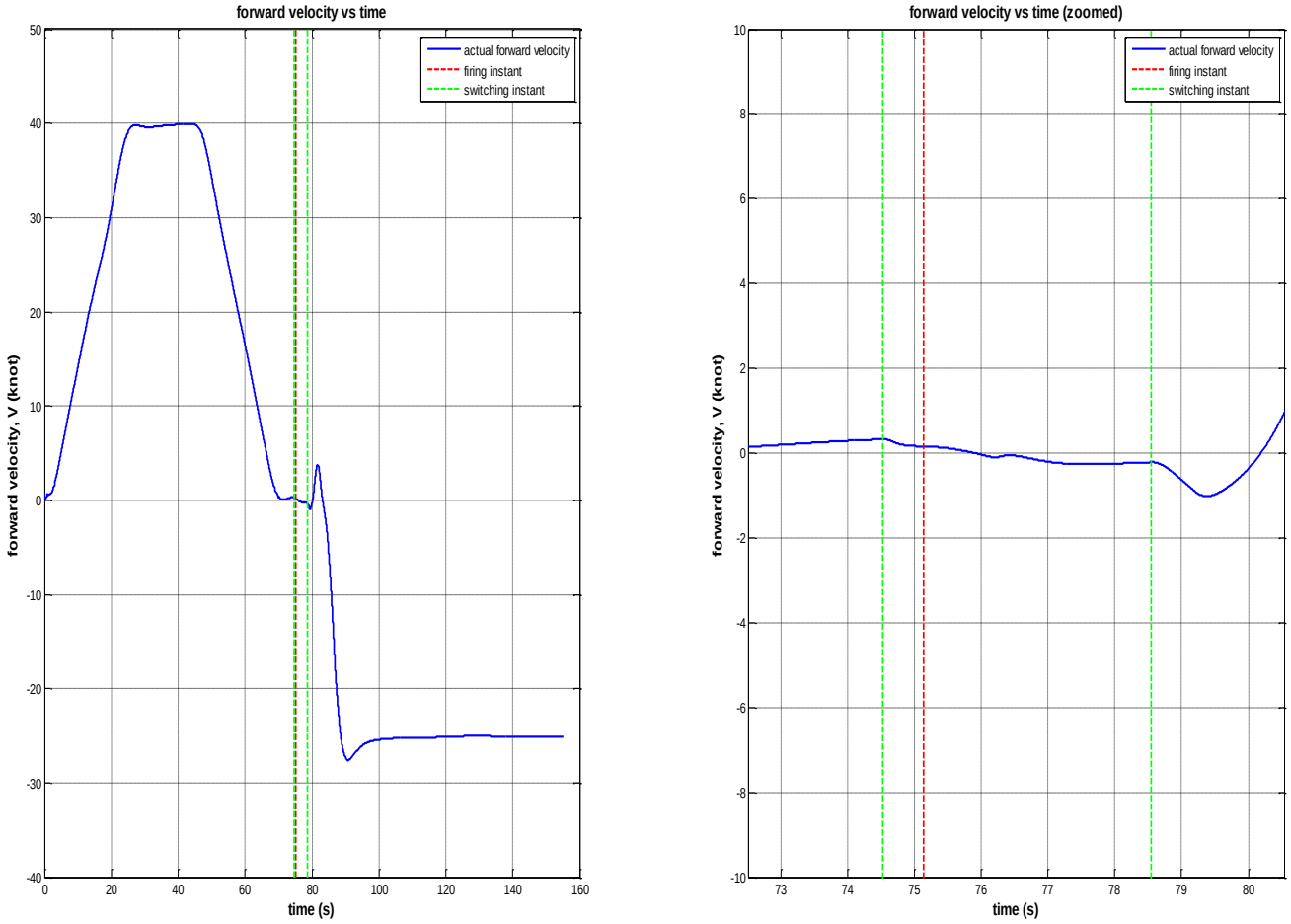

Figure 30 Scenario 1 Helicopter Forward Velocity

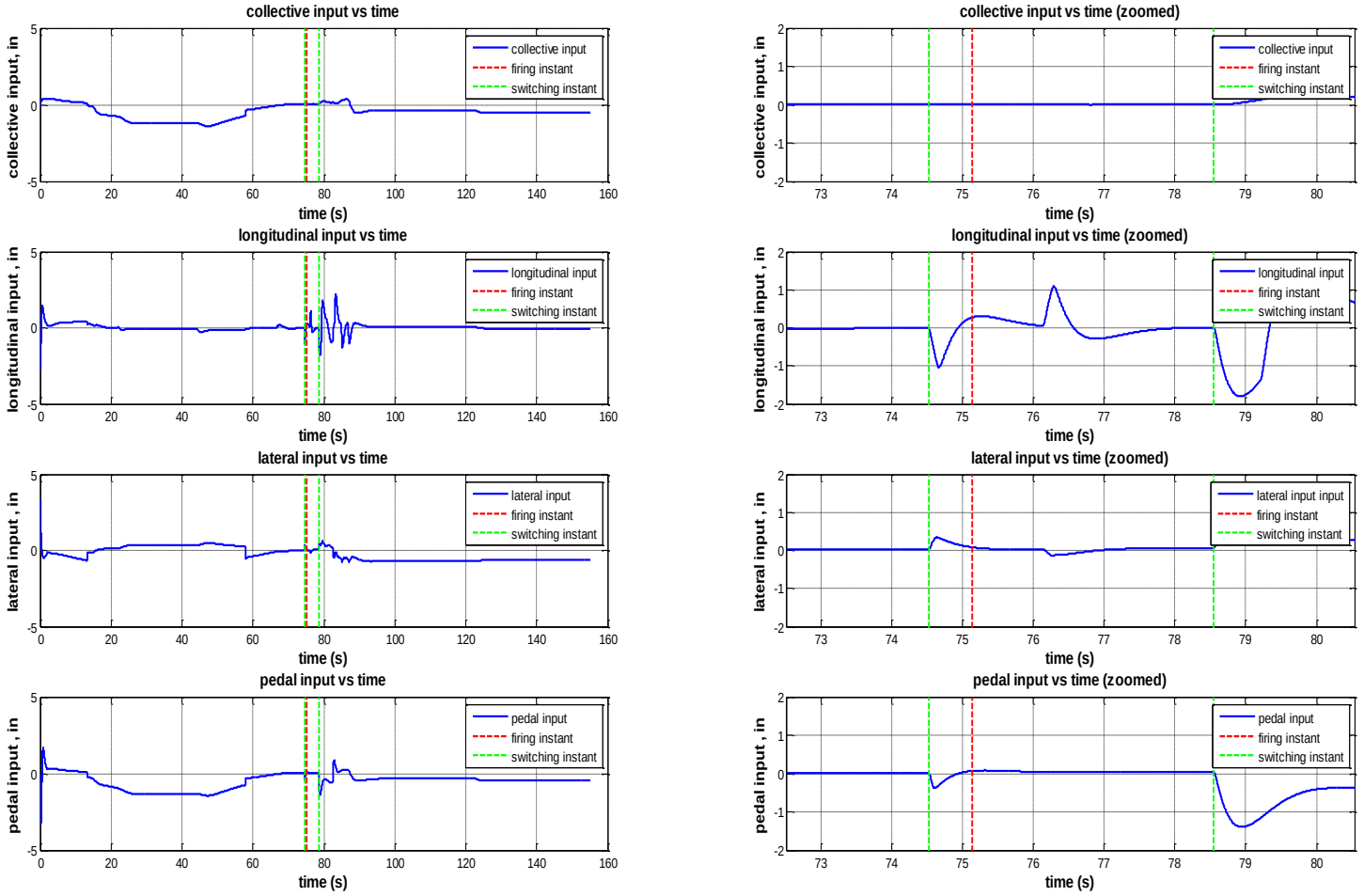

Figure 31 Scenario 1 Helicopter Control Inputs

The hover firing performance of the controller is evaluated under given test conditions by analyzing scenario 1 results. According to Figure 26, the trajectory tracking performance of the system is quite satisfactory to accomplish the mission; target engagement. In fact, the commanded and the actual trajectories are almost equal for hover test simulation. Four distinct maneuvers are performed until the helicopter reaches firing point. These are the yaw rate change in the first two seconds of the flight, the climb rate change in the 20th second of the flight (Figure 26) and the forward acceleration change in the 25th and the 45th seconds of the flight (Figure 30). The yaw rate change mainly affects the yaw angle (Figure 27). In addition, the coupling affects are occurred on the roll and the pitch angles (Figure 27), on the roll and the pitch angular velocities (Figure 28) and on all of the translational velocities (Figure 29). Although the climb rate maneuver mainly affects the body vertical velocity (Figure 29), the pitch angle (Figure 27) and the pitch angular velocity (Figure 28) are also affected. The change in forward acceleration mainly affects the body forward velocity (Figure 29). In addition, the pitch angle (Figure 27) and the pitch angular velocity (Figure 28) are also affected by this maneuver. The coupling effects of the climb and forward acceleration maneuvers on roll and yaw channels and on the body side velocity are insignificant (Figure 27, Figure 28 and Figure 29). Three other different maneuvers are performed in retreating phase. Two of them are commanded at the beginning of this phase: the 180 degree heading turn and forward acceleration. The coupling effects of these maneuvers are observed in the roll and the pitch channel and in all of the translational velocities (Figure 27, Figure 28 and Figure 29). The final maneuver of trajectory controller is the descent rate change in the125th second of the flight (Figure 26). This maneuver mainly affects the body vertical velocity (Figure 29).

Attitude controller is also works with a satisfactory performance to complete the mission. According to the design requirements, the commanded Euler angles must be satisfied with design tolerance at the firing instant. This is accomplished by an attitude controller (inner loop of the system). The results of the scenario 1 represent that the helicopter Euler angle values are achieved (Figure 27) at firing instant which occurs at the 75th second of this flight.

The guidance algorithm commands are generated to satisfy the trim condition just before the controller switching actions. Consequently, at the 74th and the 78th

seconds of the flight, the trim is achieved. This statement is confirmed by analyzing the helicopter Euler angles, angular velocities, translational velocities and the control inputs. According the Figure 27, Figure 29 and Figure 31, helicopter Euler angle, translational velocity and the control input values are constant during the controller switching instants. Also the helicopter angular velocities converge to zero deg/s (Figure 28) at these instants.

5.1.2 Scenario 2 (Running Fire Test)

Initial conditions are defined as; helicopter forward velocity is 1 knot, helicopter heading is to the north. The helicopter flies to the firing point which is 6000 ft away from the initial point with north-east heading and the altitude is 300 ft above from the initial position. In order to reach the firing point; first, the helicopter accelerates from 1 knot to 60 knot and then it keeps its forward velocity around 60 knot. When the helicopter arrives to firing point, switching from trajectory control to attitude control occurs and the helicopter changes its attitudes according to the firing aiming angles which are -0.5 degree pitch and 0 degree roll. When the attitudes are reached, rocket firing is triggered and the helicopter is commanded to hold this attitude for a second to guarantee that the rocket is separated from the helicopter at desired aiming angles. Then, the helicopter attitudes are commanded to turn back to the conditions just before the previous switching. The reason of this action is to force the helicopter to turn back to the trim condition. The helicopter attitudes are hold at these values for a second and then the controller is switched back to trajectory control. Then, the helicopter performs forward flight in north east direction. When the flight time is more than 5 seconds from firing time, the helicopter performs a u-turn with 2000 ft radius of curvature to retreat. When the helicopter closes to its initial position less than 4000 ft in north direction, it initiates a descent that will continue until ground level altitude.

In these simulations the position tolerances are set to 10 ft in each direction (north, east, altitude) and the attitude angle tolerances are taken as 1 degree in each direction (roll, pitch, yaw) in order to perform discrete events like controller switching and fire triggering. Simulation are given in Figure 32-Figure 37.

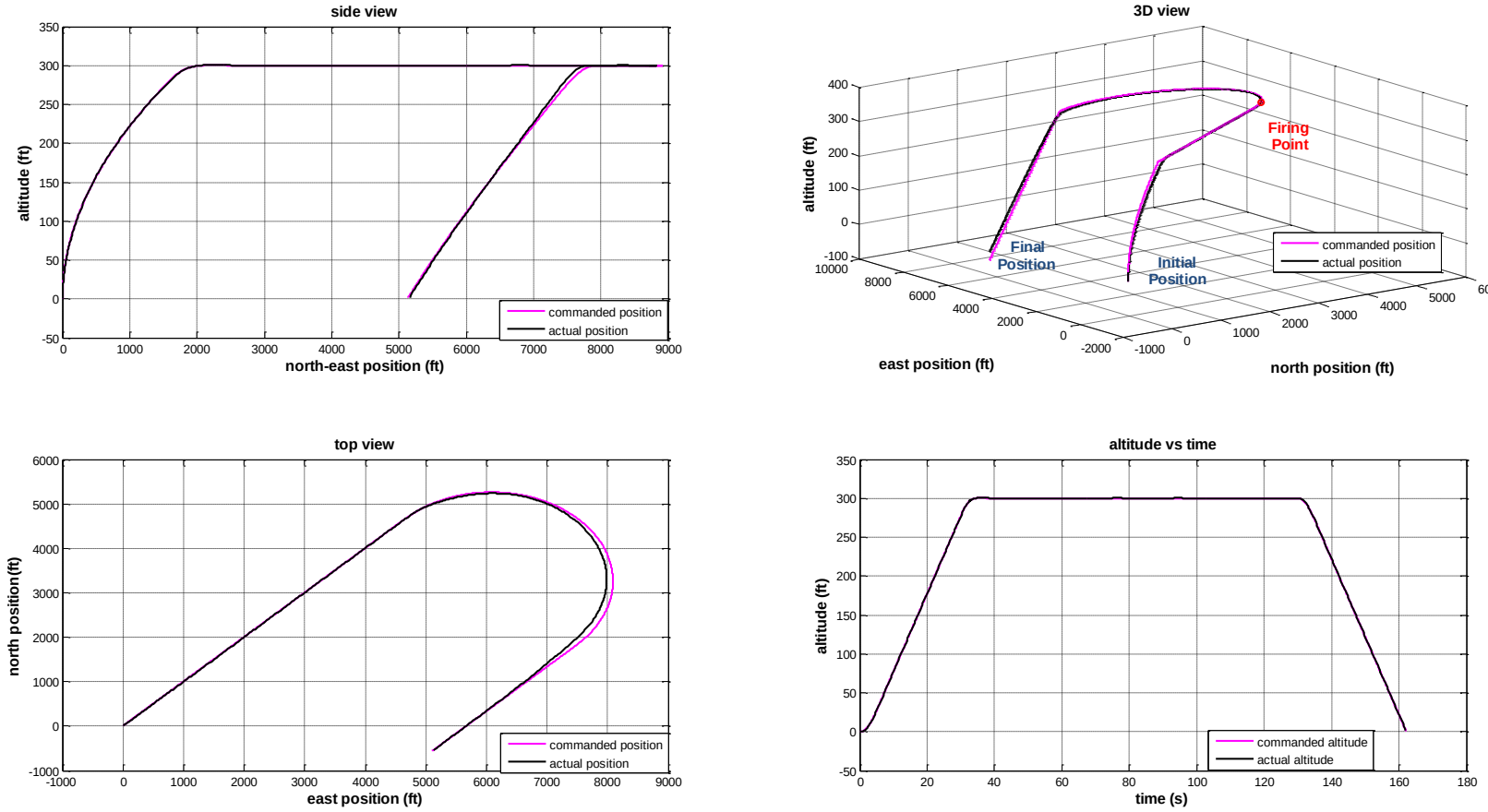

Figure 32 Scenario 2 North / East Positions and Altitude

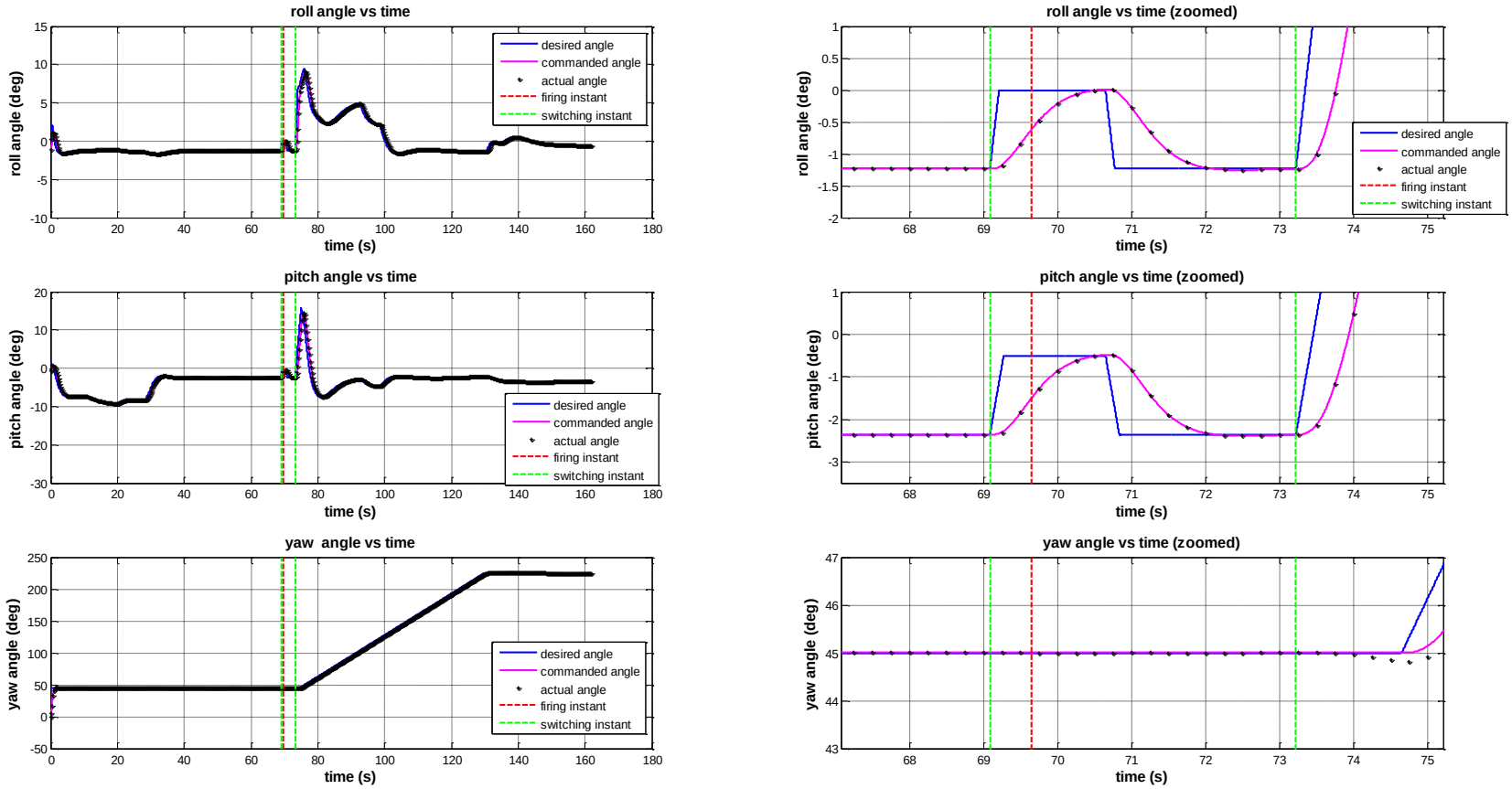

Figure 33 Scenario 2 Euler Angles

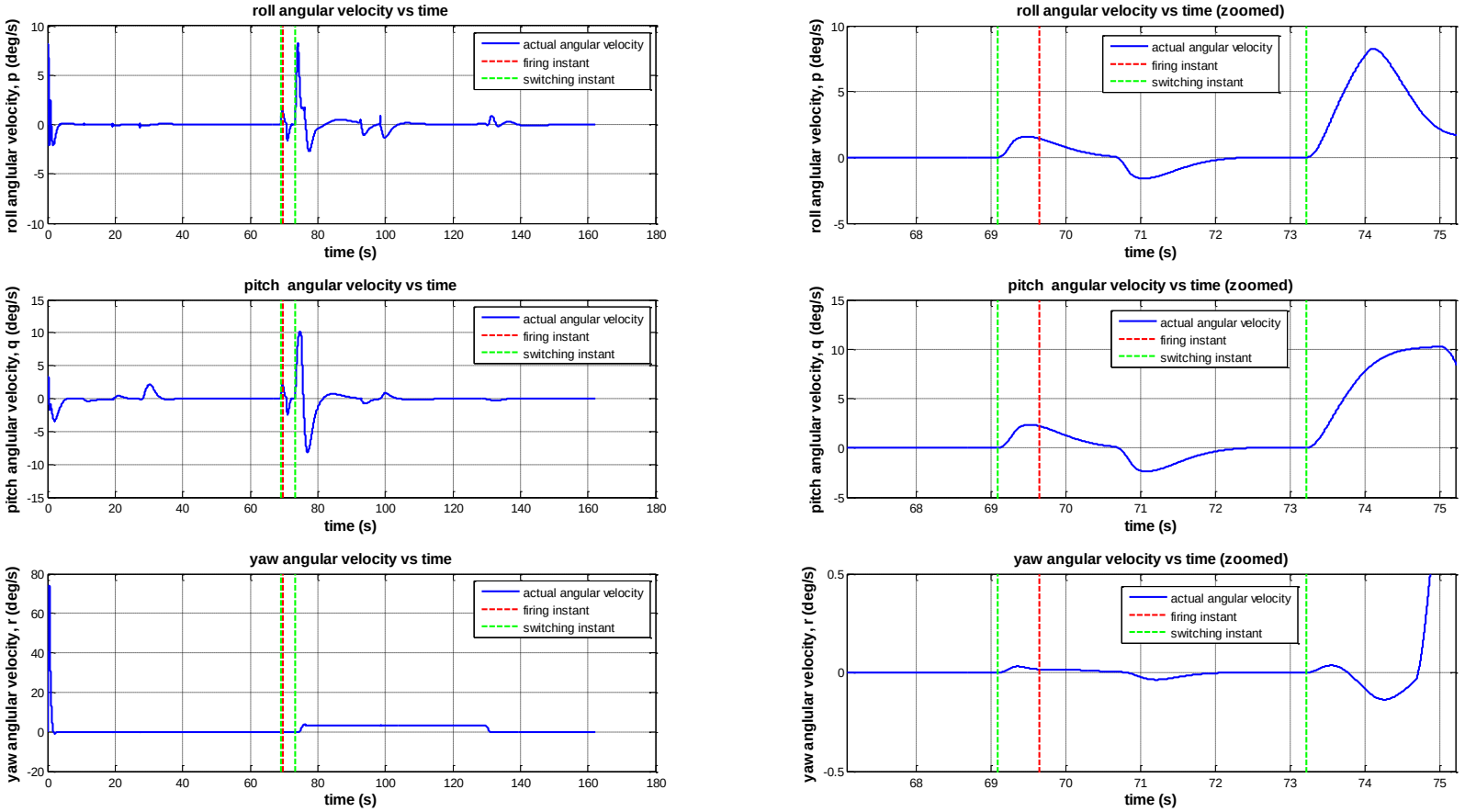

Figure 34 Scenario 2 Angular Velocities

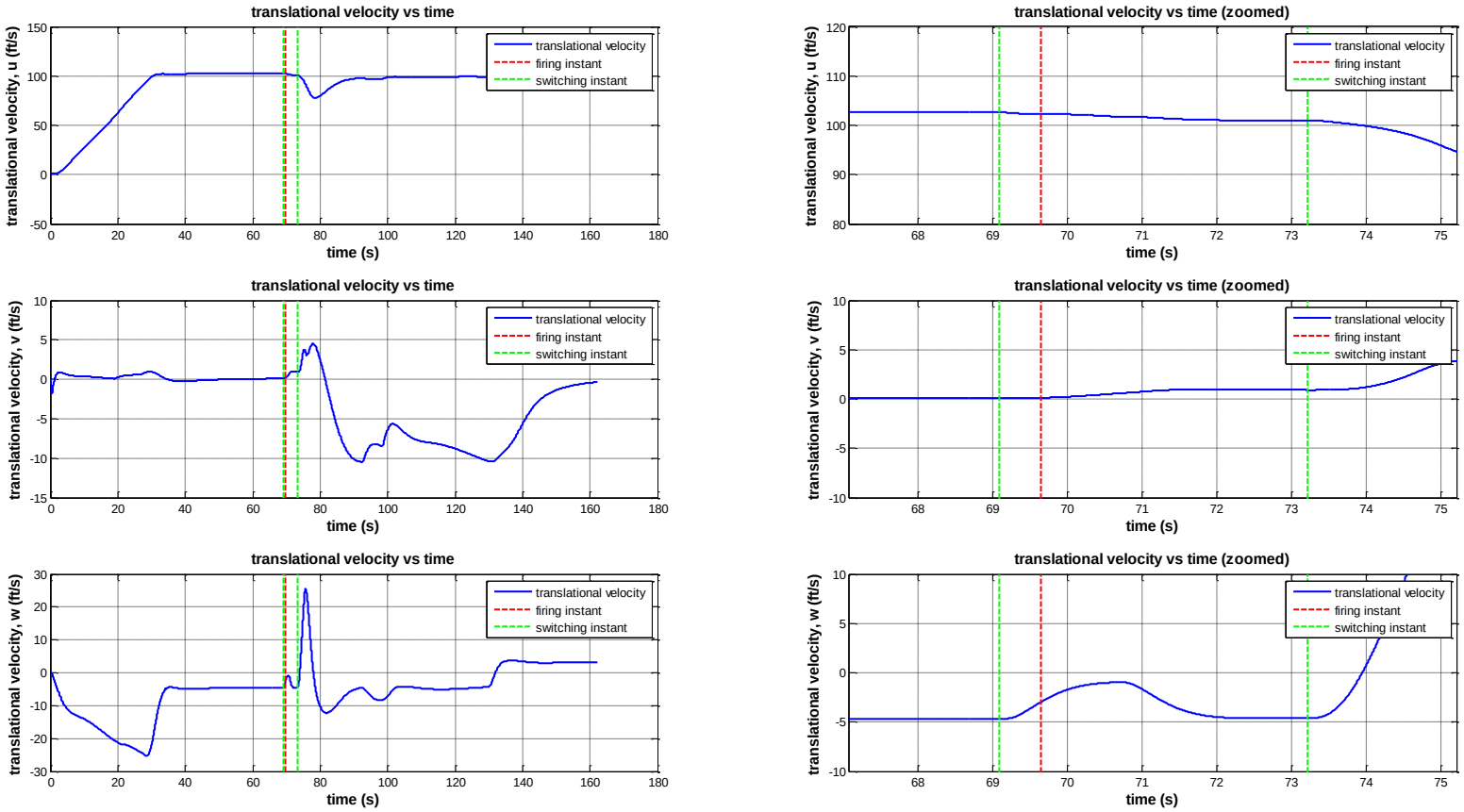

Figure 35 Scenario 2 Translational Velocities

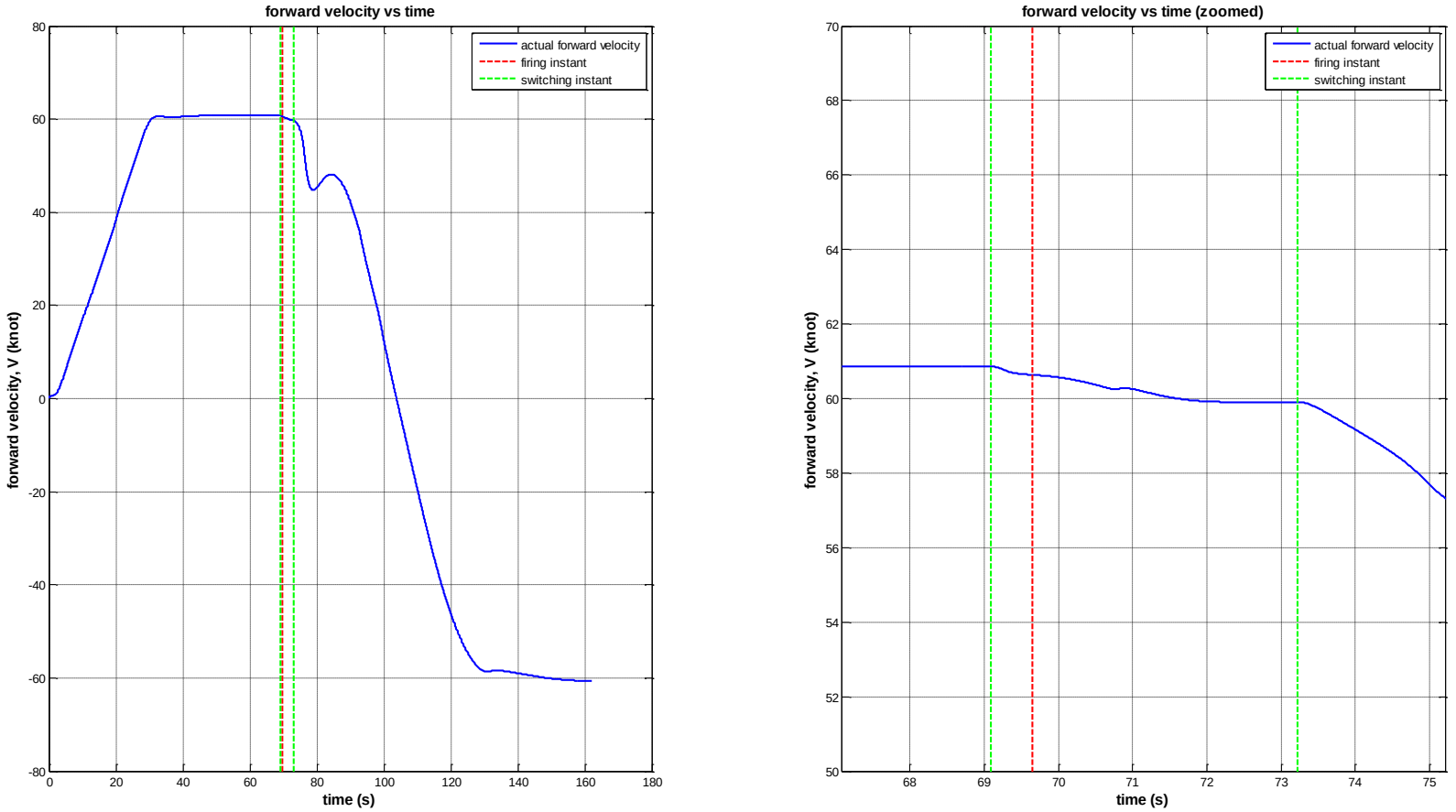

Figure 36 Scenario 2 Helicopter Forward Velocity

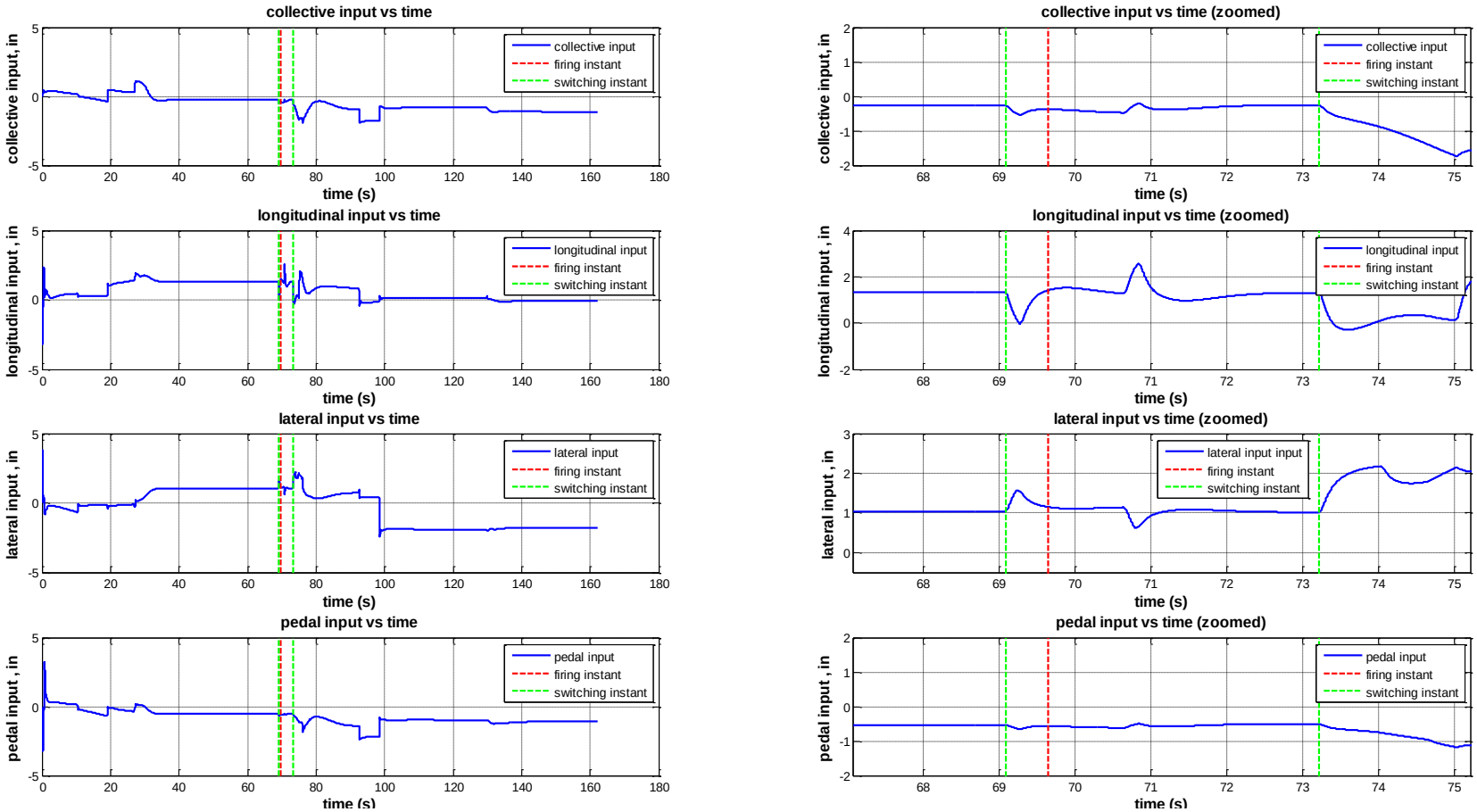

Figure 37 Scenario 2 Helicopter Control Inputs

The running fire performance of the controller is evaluated according to scenario 2 results. Similar interpretations with hover fire simulation results can be made for running fire test case. According to Figure 32, the helicopter trajectory tracking performance is sufficient to execute the mission. Three distinct maneuvers are performed until the helicopter reaches firing point. These are the yaw rate change in the first two seconds of the flight, the climb rate change and forward acceleration change in the 33th second of the flight (Figure 32, Figure 36). The comments about these similar maneuvers of the scenario 1 are also valid for this case (Figure 33, Figure 34 and Figure 35). Two other different maneuvers are performed in retreating phase. One of them is commanded at the beginning of this phase: the u-turn maneuver. The coupling effects of this maneuver are observed in the roll and the pitch channels and in all of the translational velocities (Figure 33, Figure 34 and Figure 35). The effects of this maneuver are continued until the 129th second of the flight where the u-turn is completed. The final maneuver of trajectory controller is the descent rate change in the 131th second of the flight (Figure 32). This maneuver mainly affects the body vertical velocity (Figure 35).

The results of the scenario 2 represent that the helicopter commanded Euler angles are also tracked with satisfactory performance by attitude controller (Figure 33).

In scenario 2, the requirement to trim the system just before the controller switching instants is satisfied. The comments of scenario 1 are also valid for this case. This conclusion is made according to the results of Figure 33, Figure 34, Figure 35 and Figure 37.

5.1.3 Scenario 3 (Diving Fire Test)

Initial conditions are defined as; helicopter forward velocity is 1 knot, helicopter heading is to the north and helicopter altitude is 3500 ft above the ground level. The helicopter flies to the firing point which is 6000 ft away from the initial point with north-east heading and the altitude is 500 ft below from the initial position. In order to reach the firing point; first, the helicopter accelerates from 1 knot to 60 knot and then it keeps its forward velocity around 60 knot. When the helicopter arrives to firing point, switching from trajectory control to attitude control occurs and the

helicopter changes its attitudes according to the firing aiming angles which is -16 degree pitch and 0 degree roll. When the attitudes are reached, rocket firing is triggered and the helicopter is commanded to hold this attitude for a second to guarantee that the rocket is separated from the helicopter at desired aiming angles. Then, the helicopter attitudes are commanded to turn back to the conditions just before the previous switching. The reason of this action is to force the helicopter to turn back to the trim condition. The helicopter attitudes are hold at these values for a second and then the controller is switched back to position control. Then, the helicopter performs forward flight in north east direction and it climbs with 10 ft/s climb rate at the same time. When the flight time is more than 5 seconds from firing time, the helicopter performs a u-turn with 2000 ft radius of curvature to retreat with the same climb rate. Then the helicopter continues to fly until it arrives to the initial point in north direction.

In these simulations the position tolerances are set to 50 ft in each direction (north, east, altitude) and the attitude angle tolerances are taken as 1 degree in each direction (roll, pitch, yaw) in order to perform discrete events like controller switching and fire triggering. Simulation are given in Figure 38-Figure 43.

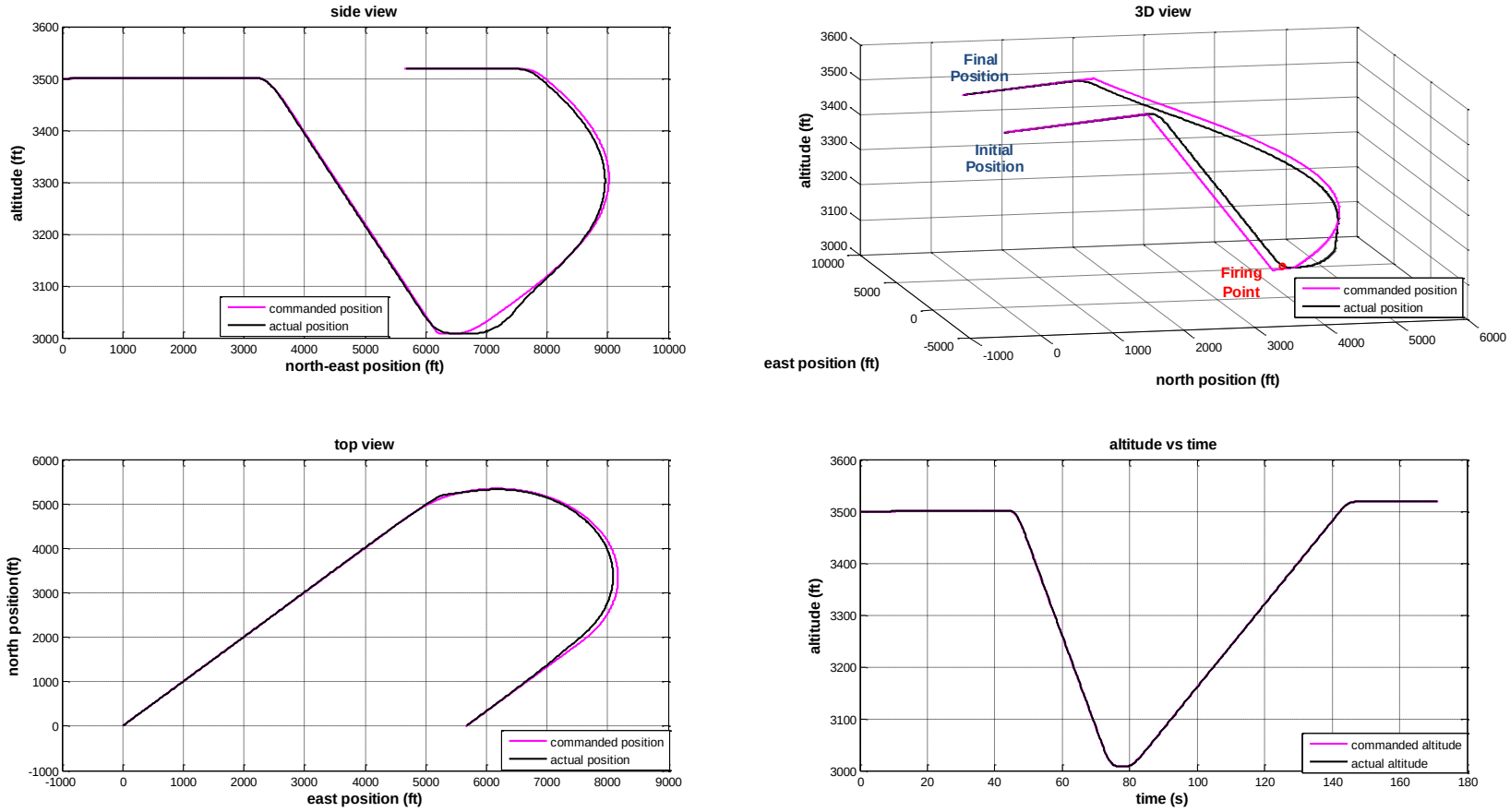

Figure 38 Scenario 3 North / East Positions and Altitude

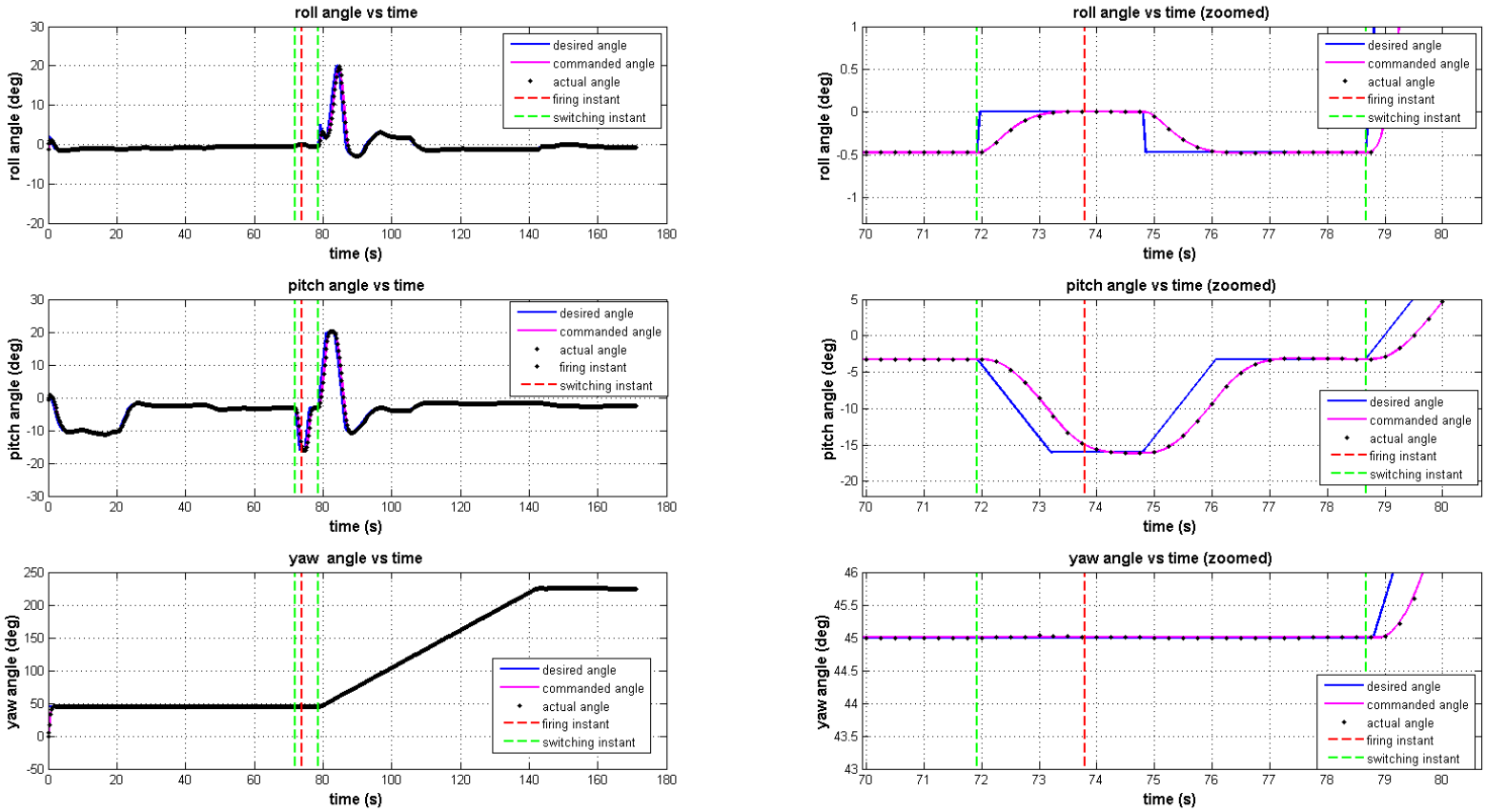

Figure 39 Scenario 3 Euler Angles

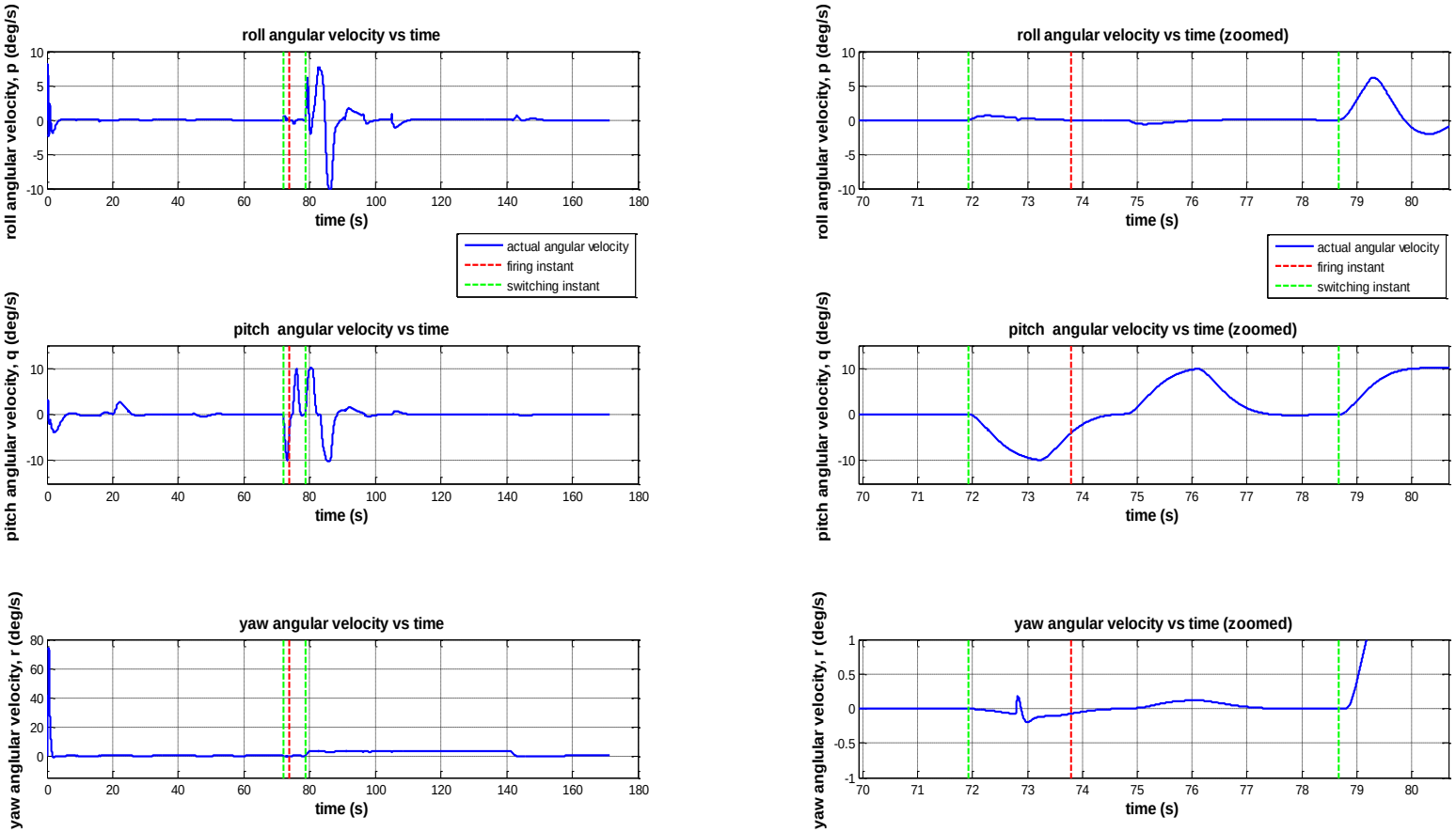

Figure 40 Scenario 3 Angular Velocities

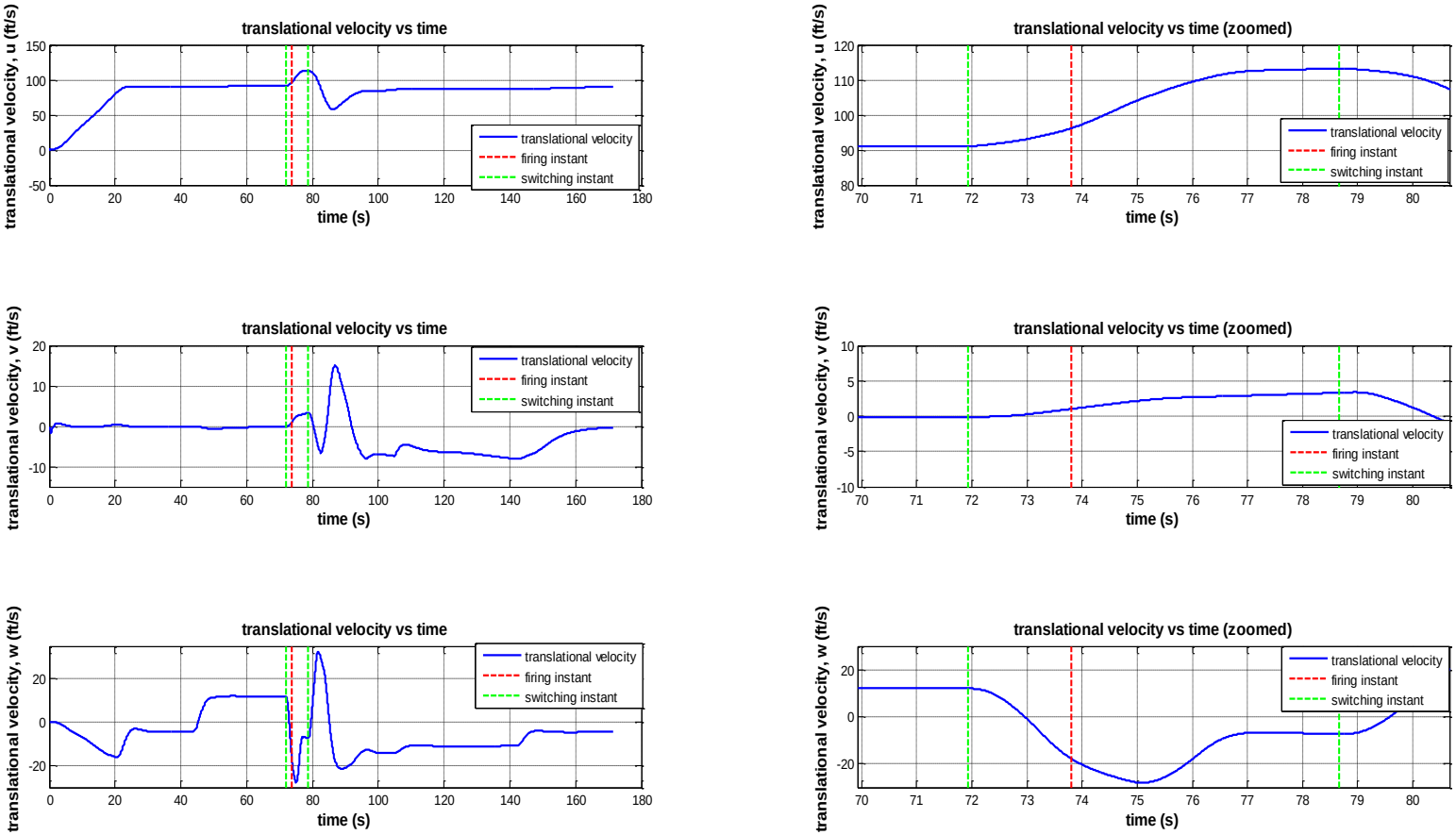

Figure 41 Scenario 3 Translational Velocities

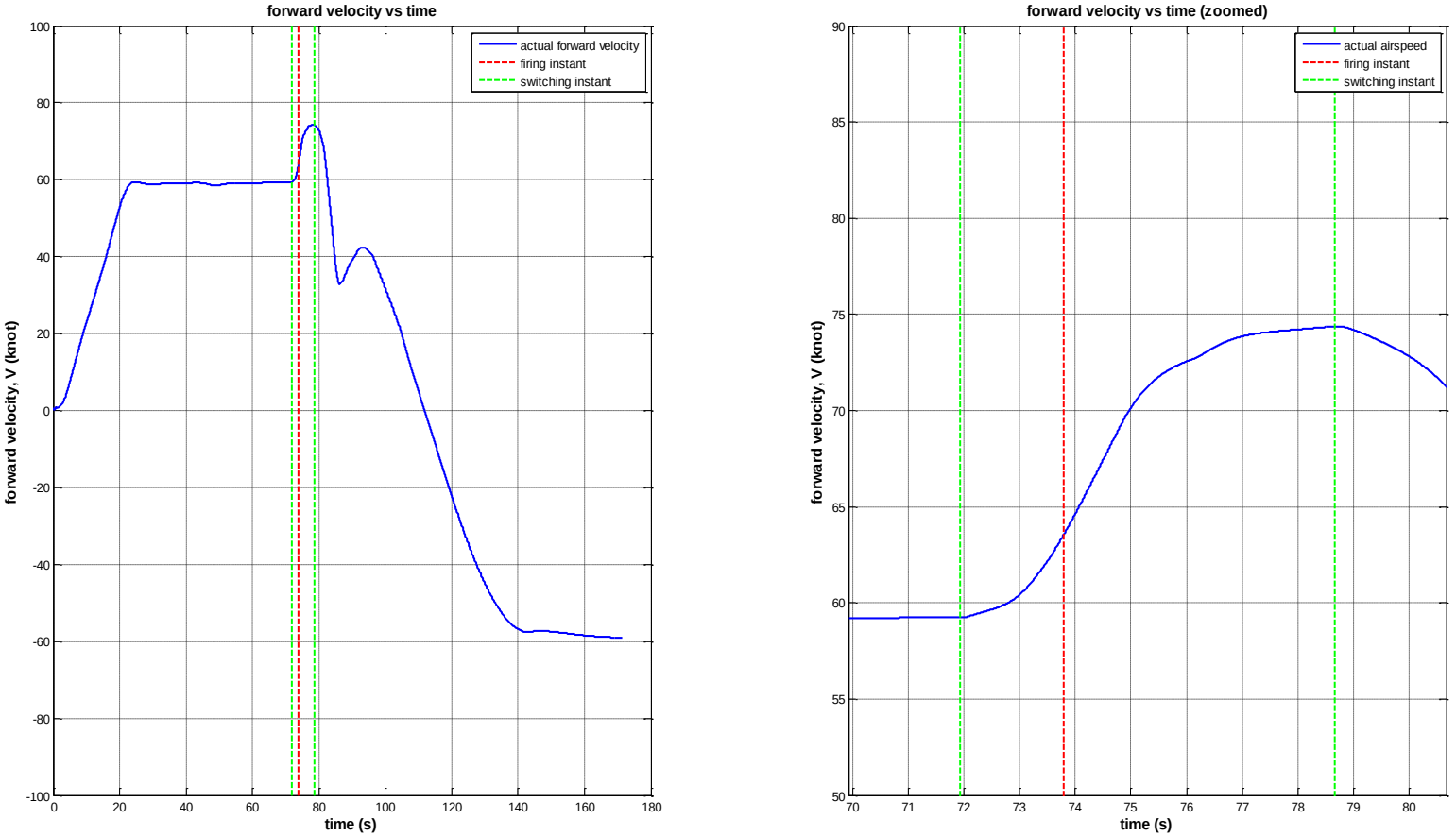

Figure 42 Scenario 3 Helicopter Forward Velocity

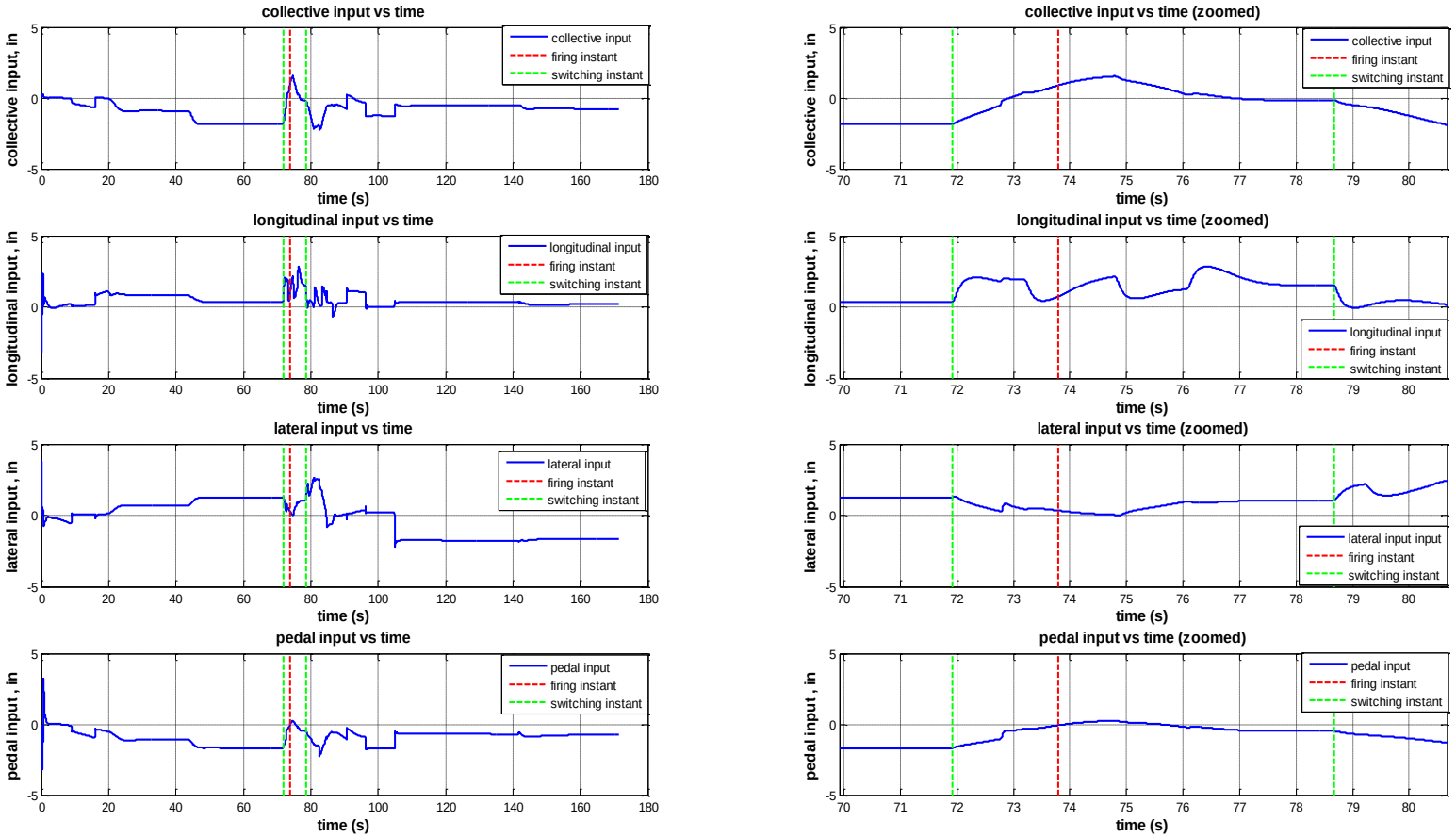

Figure 43 Scenario 3 Helicopter Control Inputs

The diving fire performance of the controller is evaluated according to scenario 3 results. Similar interpretations with hover and running fire simulation results (scenario 1 and scenario 2) can be made for this test case. According to Figure 38, the helicopter trajectory tracking performance is sufficient to execute the mission. Three distinct maneuvers are performed until the helicopter reaches firing point. These are the yaw rate change in the first two seconds of the flight, the forward acceleration change in the 24th second of the flight and the descent rate change in the 45th second of the flight (Figure 39, Figure 42 and Figure 38). The comments about these similar maneuvers of the scenario 1 and the scenario 2 are also valid for this case (Figure 39, Figure 40 and Figure 41). Three other different maneuvers are performed in retreating phase. Two of them are commanded at the beginning of this phase: the u-turn maneuver and climbing. The coupling effects of this maneuver are observed in the roll and the pitch channels and in all of the translational velocities (Figure 39, Figure 40 and Figure 41). The effects of this maneuver are continued until the 141th second of the flight where the u-turn is completed. The last maneuver of trajectory controller is to terminate the climbing by altitude hold command in the 145th second of the flight (Figure 38). This maneuver mainly affects the body vertical velocity (Figure 41).

The results of the scenario 3 represent that the helicopter commanded Euler angles are also tracked with satisfactory performance by attitude controller (Figure 39).

In scenario 3, the requirement to trim the system at controller switching instants is satisfied. The comments of scenario 1 and scenario 2 are also valid for this case. This conclusion is made according to the results of Figure 39, Figure 40, Figure 41 and Figure 43.

5.2 Simulations without Switching at Trim Points

As it is discussed before, in order to switch the controller from the inner to the outer loop, the helicopter attitudes are required to turn back to the trim conditions just before the previous switching. The scenario 2 test is repeated to analyze the controller performance under the conditions where the attitudes are not commanded to turn back their initial values. According to the results, there is no performance

degradation observed in this case. There is not a significant difference between both trajectories tracked by the helicopter. Also the angular rate, the angular velocity and the translational velocity values are quite similar in magnitude and in order. The reason for these results are explained as following; the attitude commands have already been achieved by the helicopter and the flight becomes steady just before the switching instants (after firing command, then the attitudes are hold for a second to guarantee the safe separation of the rocket and consequently the helicopter reaches the steady motion). However, even the simulation looks promising; it might not guarantee the safe switching action for the more challenging test conditions. Simulation results are given in Figure 44 - Figure 49.

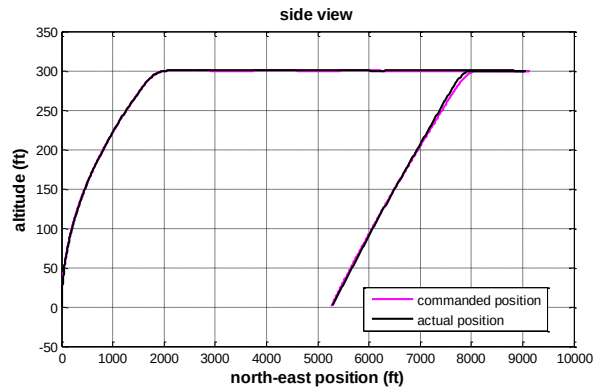

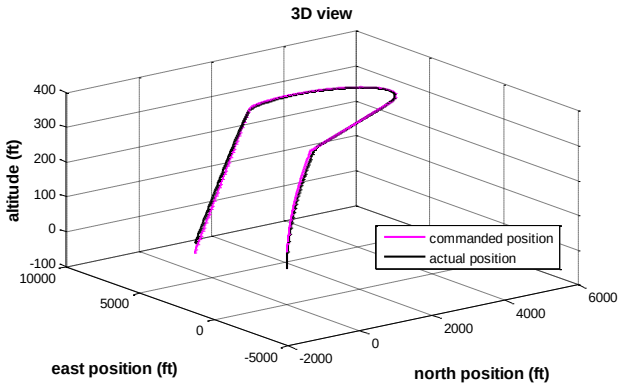

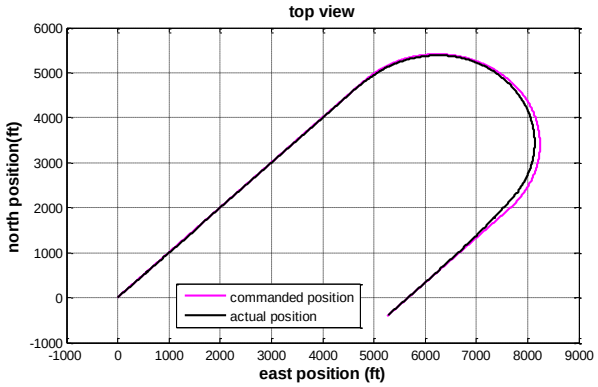

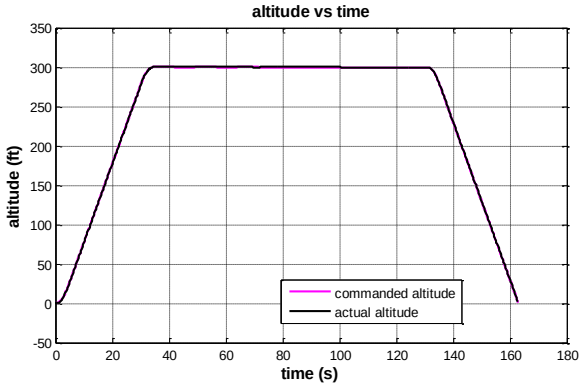

Figure 44 Scenario 2 North / East Positions and Altitude (switching without trim)

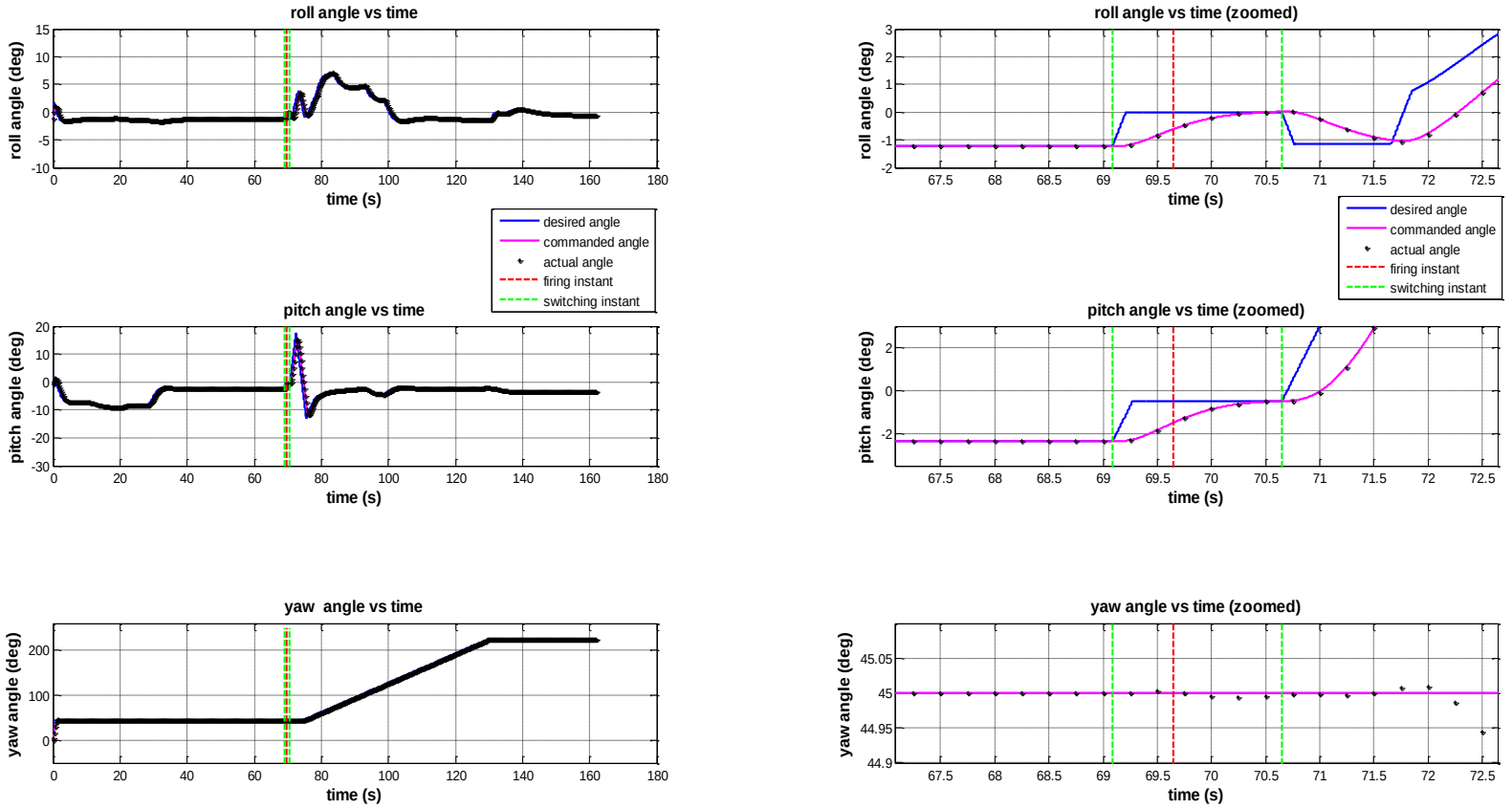

Figure 45 Scenario 2 Euler Angles (switching without trim)

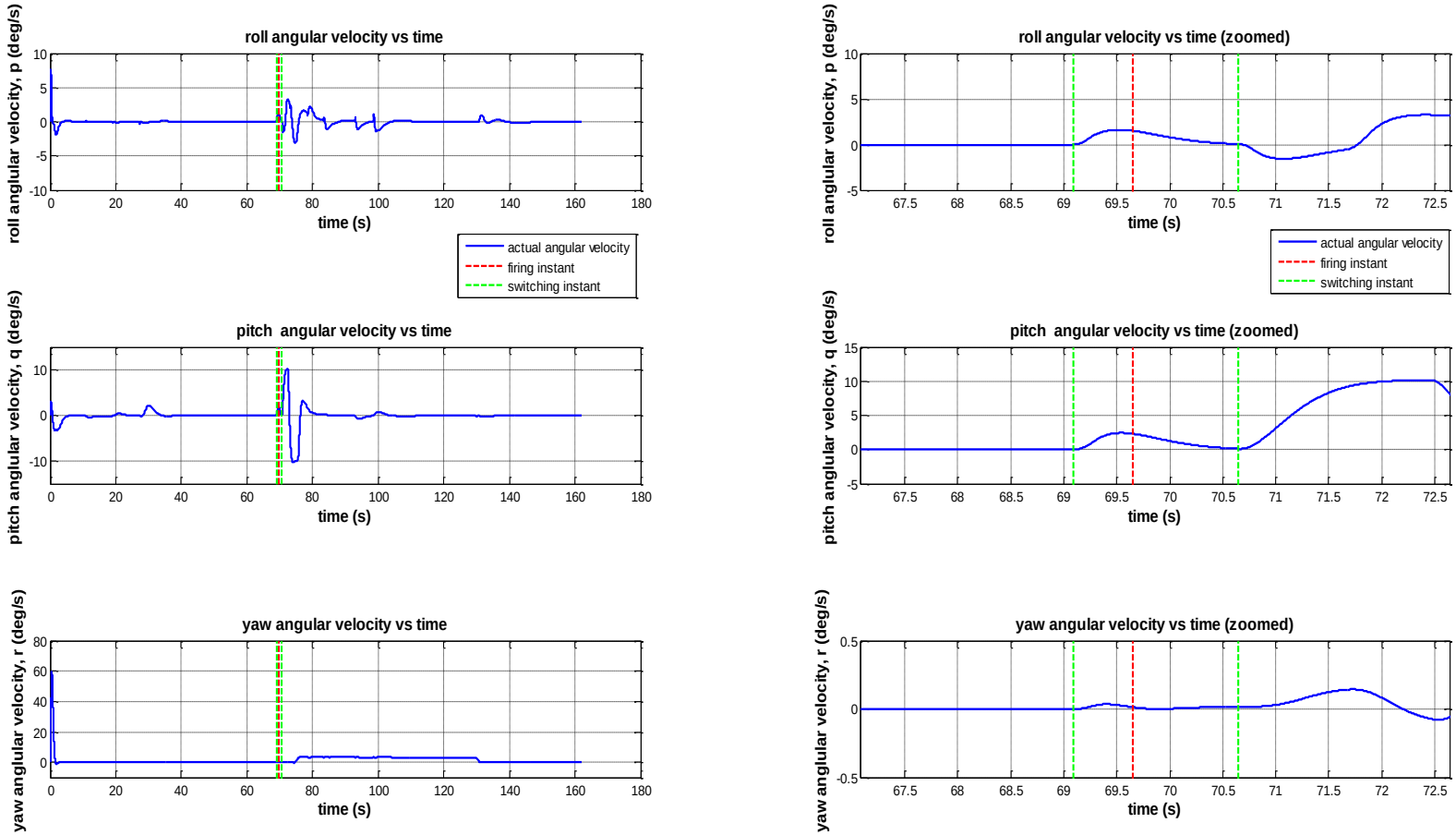

Figure 46 Scenario 2 Angular Velocities (switching without trim)

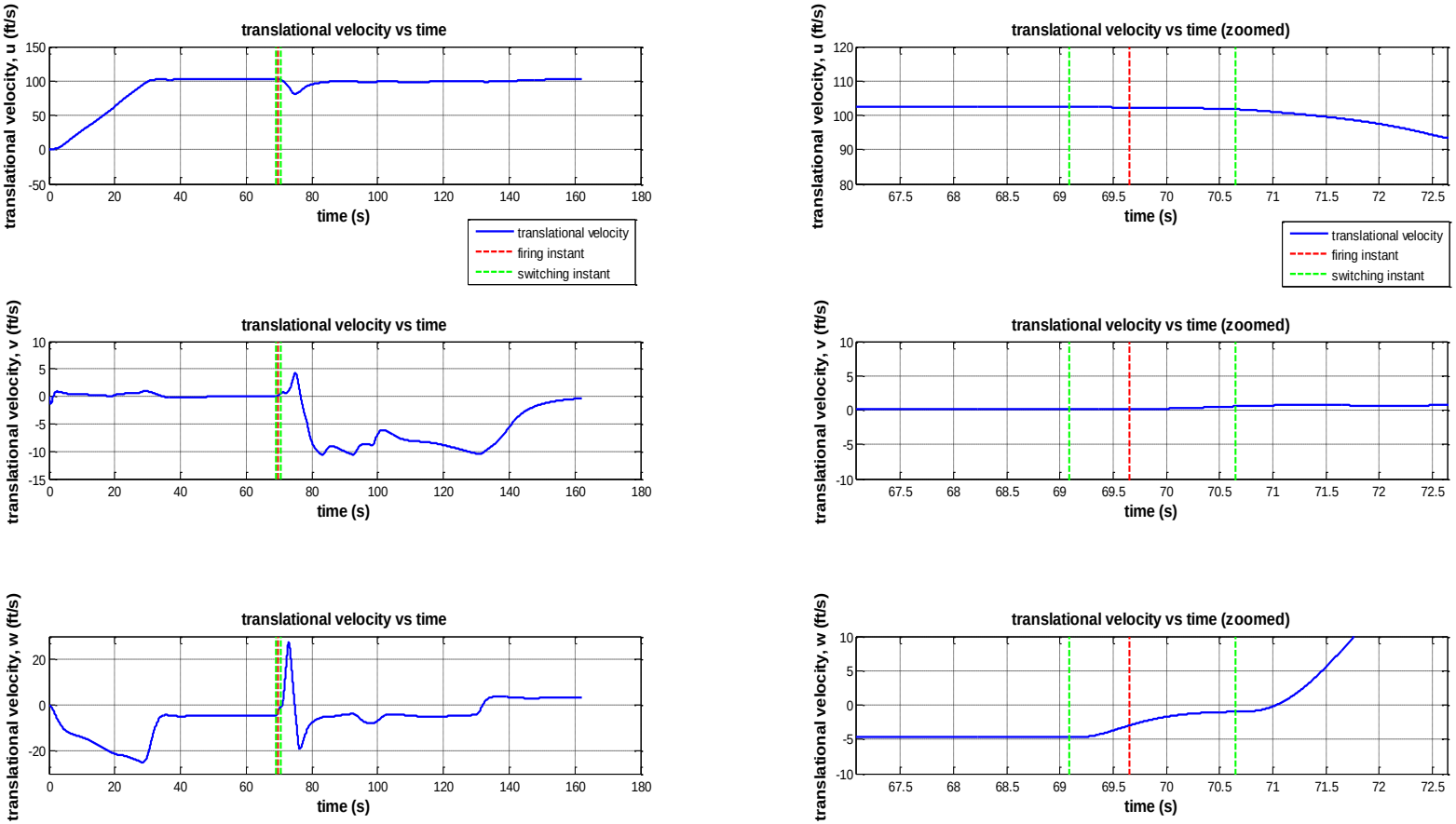

Figure 47 Scenario 2 Translational Velocities (switching without trim)

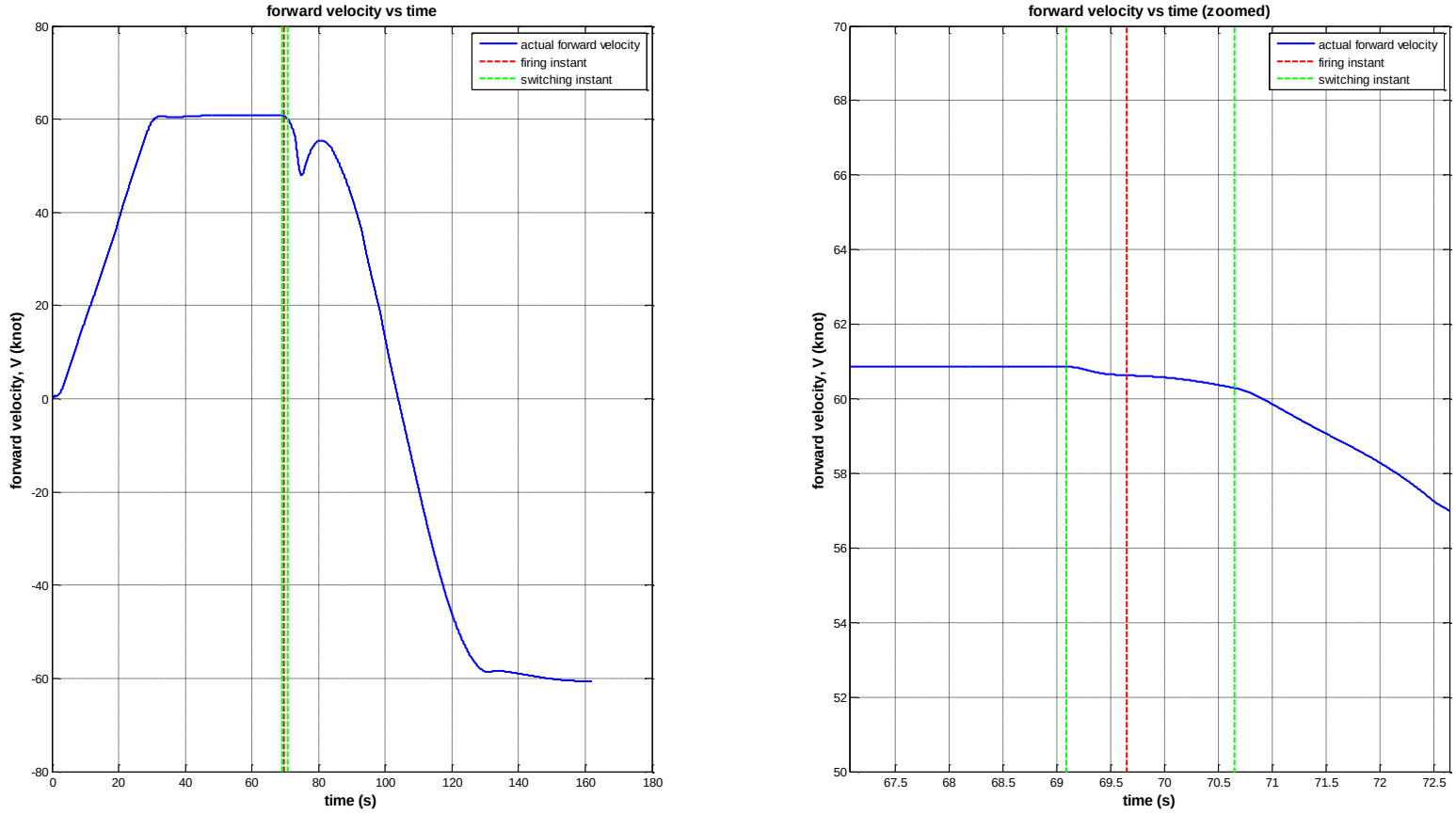

Figure 48 Scenario 2 Helicopter Forward Velocity (switching without trim)

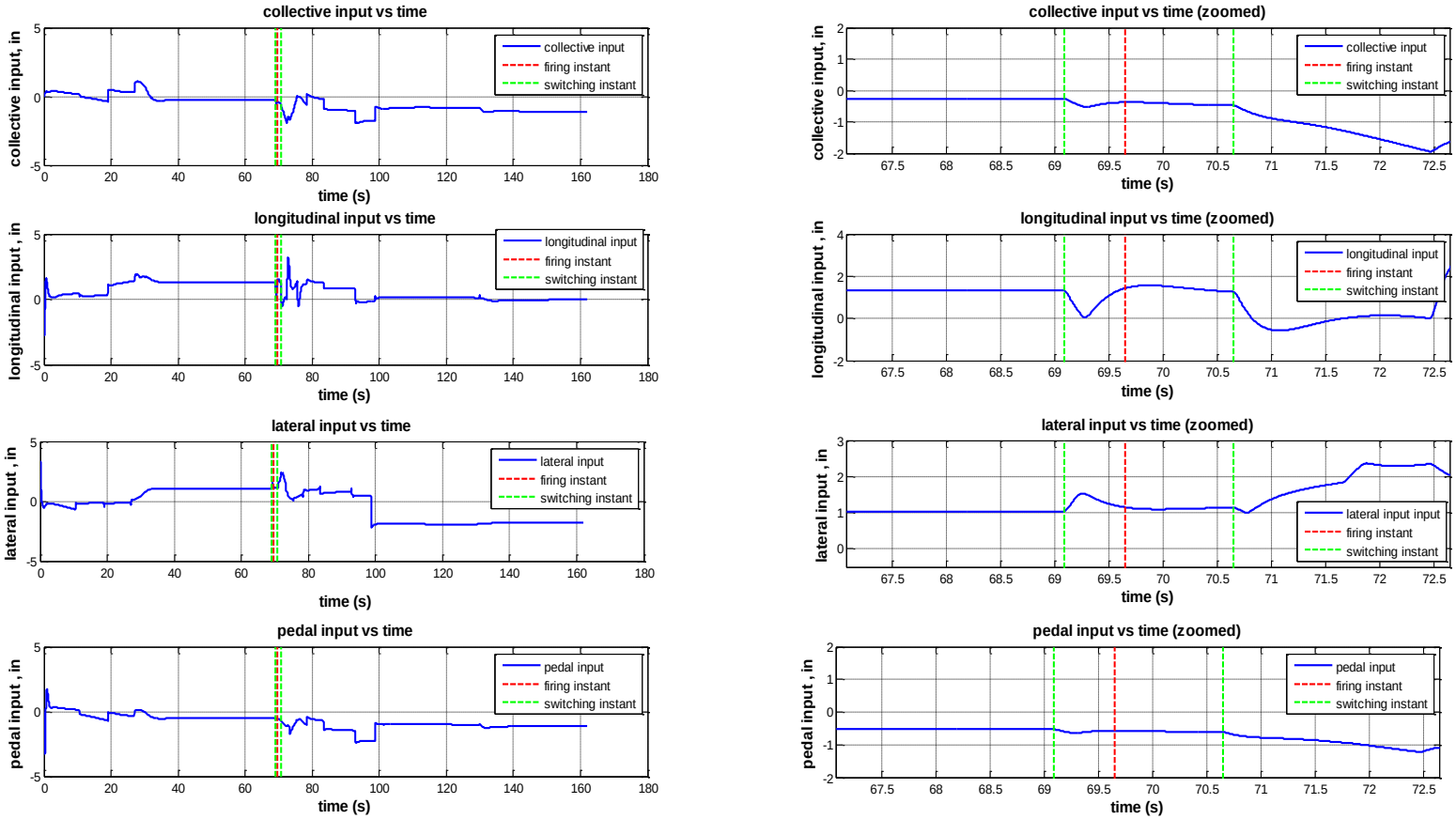

Figure 49 Scenario 2 Helicopter Control Inputs (switching without trim)

5.3 Uncertainty Analysis

In this study, the sensitivity analysis is performed to analyze the effect of the stability and the control derivatives on the system performance. This analysis is done for the derivatives regarding 1 knot forward velocity condition. The derivatives used in the linear helicopter model are multiplied with several constants (positive and negative) to model the uncertainty and the effects of these uncertainties on the inner loop performance are evaluated. According to this work, the stability derivatives M_u, L_u, N_u, Z_w, M_w, L_w, N_w, M_q, L_q, N_q, M_v, Y_v, L_v, N_v, M_p, L_p, N_p, N_r and the control derivatives $M_{\delta b}$, $L_{\delta b}$, $N_{\delta b}$, $L_{\delta a}$, $N_{\delta a}$, $M_{\delta p}$, $L_{\delta p}$, $N_{\delta p}$ are found as important on the roll, pitch and yaw channel performance. Then by giving ±25 % and ±50 % uncertainties (related coefficients are 1.25, 0.75, 1.5, 0.5) to these derivatives which cause the change in the eigenvalue locations of the helicopter, the Euler angle responses of the inner loop to the step input are analyzed and the results are plotted in Figure 50.

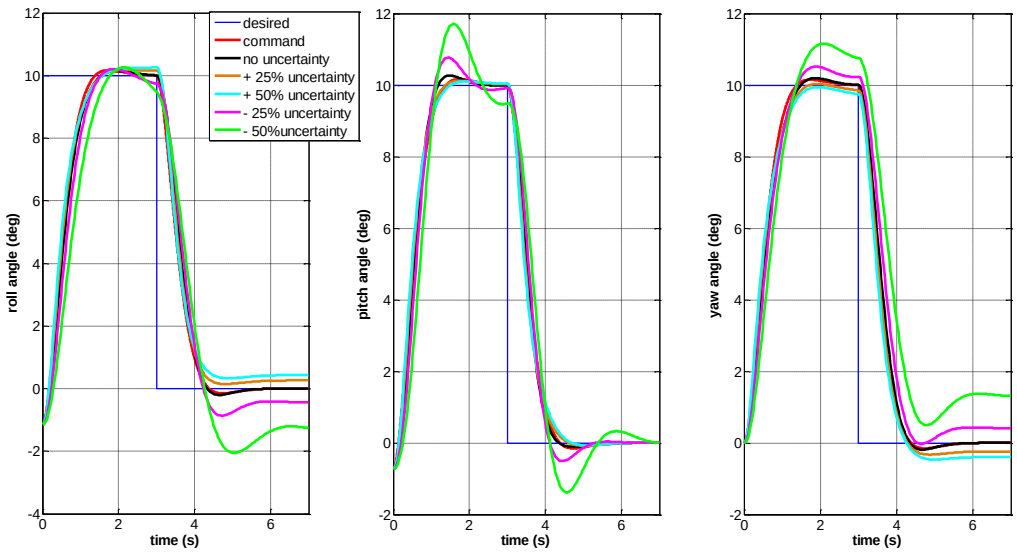

Figure 50 Euler Angles with Uncertainty

According to Figure 50, when there are uncertainties (within the limits given above) in the linear helicopter model, an instability occurs in the roll and yaw channels. The oscillations increase for pitch channel with higher uncertainty conditions.

Then the scenario 1 test (hover fire test) is repeated for these uncertainty conditions and the results are compared in Figure 51 - Figure 54. Figure 51 shows that the trajectory tracking performance of the controller is quite satisfactory under given uncertainty conditions. In fact, the instability builds up quite slowly (doubling time is bigger than 10 s for the worst case) and therefore the deviations can be compensated with the outer loop control.

In order to track the commanded trajectory, the required roll and yaw angle values deviates from the nominal values (case with no uncertainty) with increasing uncertainty (Figure 52, Figure 53). However, the behaviors of the pitch angle change during the simulations are almost the same with the nominal case (Figure 54).

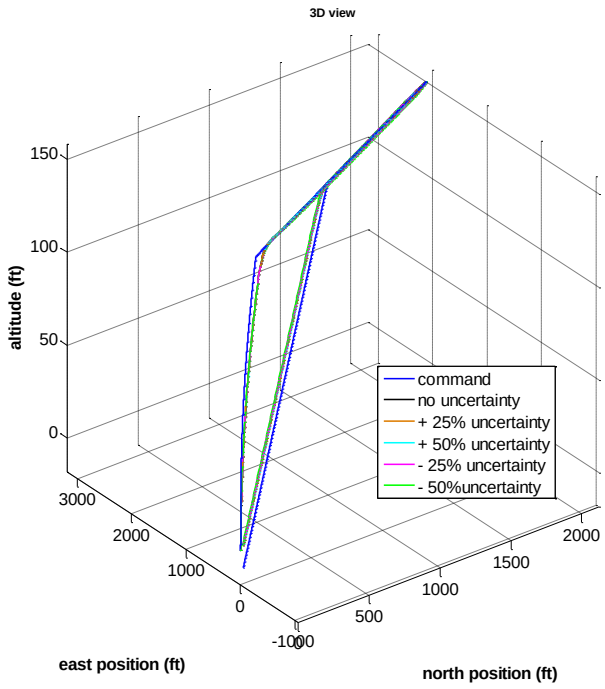

Figure 51 Scenario 1 North and East Positions with Uncertainty

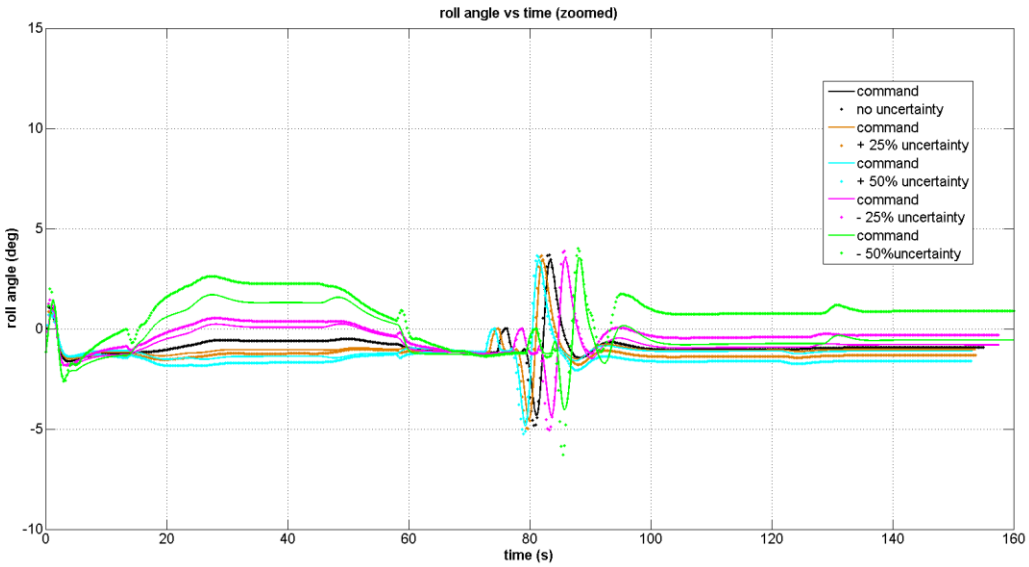

Figure 52 Scenario 1 Roll Angle with Uncertainty

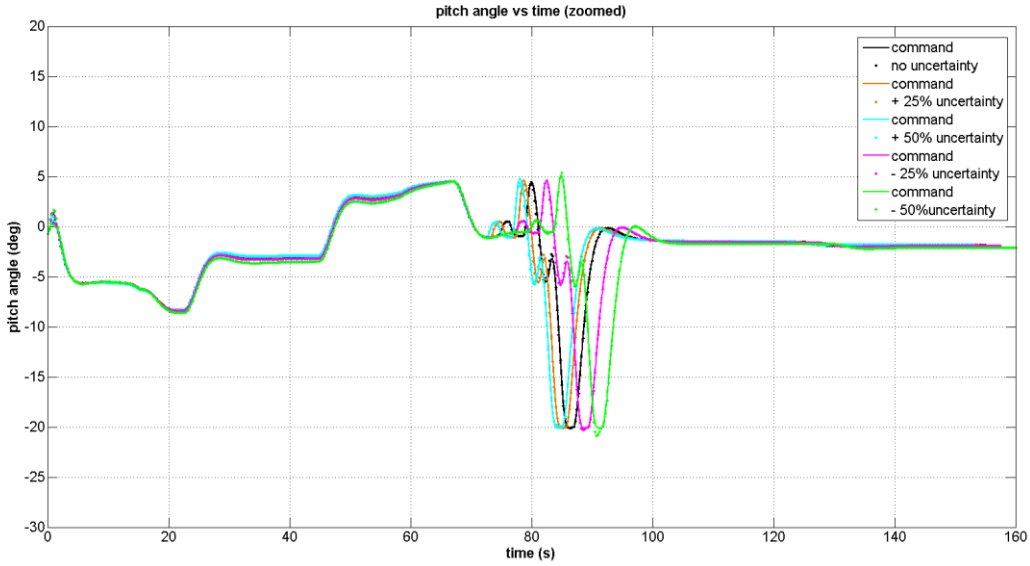

Figure 53 Scenario 1 Pitch Angle with Uncertainty

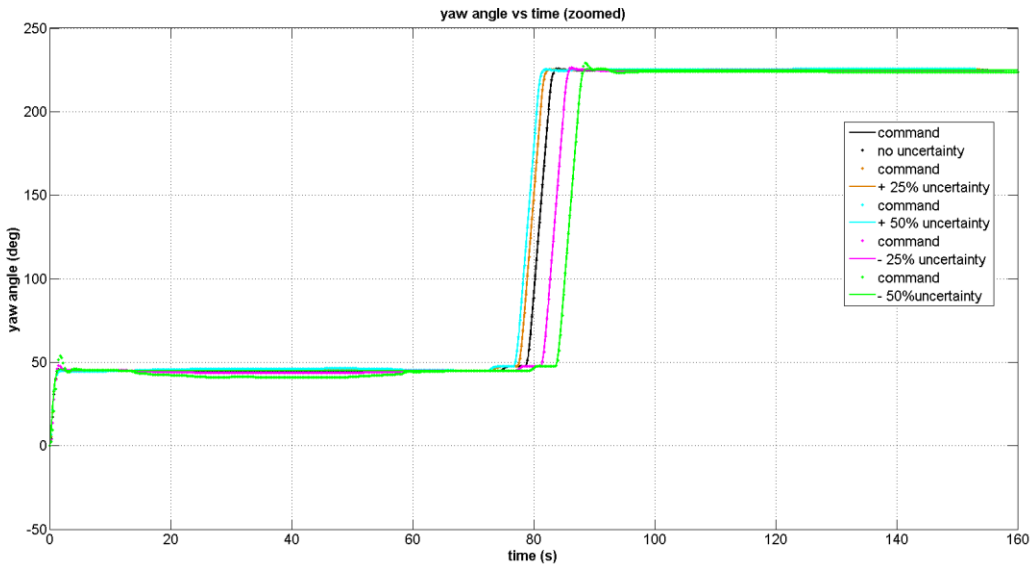

Figure 54 Scenario 1 Yaw Angle with Uncertainty

In this thesis, the system is tested to analyze the controller performance where there is not an exact pole-zero cancellation between the inner loop and the plant model. In order to show that an exact pole zero cancellation does not exist, the transfer functions representing the model error are added to the system. Concept drawing of the model error transfer function in the controller architecture is given in Figure 55.

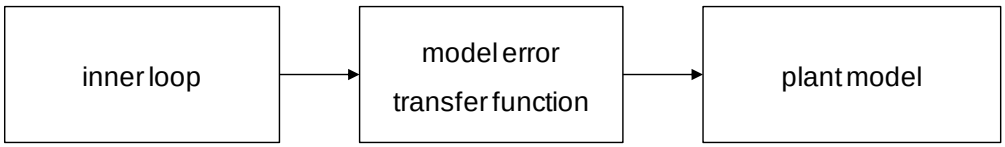

Figure 55 Concept Drawing of the Model Error Transfer Function in the Controller Architecture

The modeling error transfer functions are generated for roll, pitch and the yaw channels. The numerator of the roll channel model error transfer function is selected as to cancel out the roll mode pole of the helicopter and the denominator of it is determined as any number near to that pole (but not at the same location to prevent exact pole zero cancellation). The same principle is executed to generate the pitch and roll channel model error transfer functions. The poles of the short period mode

and the dutch roll mode are used to generate the pitch and yaw channel model error transfer functions respectively. The numeric values of the model error transfer functions are given in APPENDIX D. Then the Euler angle responses of the inner loop to the step input are analyzed at 1 knot forward velocity condition and the results are plotted in Figure 56. According to the results shown in Figure 56, even the stability is preserved when there is a model error in pitch channel (short period mode), an instability is observed if the model error is added to the roll channel (roll mode) or to the yaw channel (dutch roll mode). The instability caused by the model error in roll channel is compensated with outer loop control. In this case, even there is degradation in Euler angle tracking performance (Figure 58), it is shown that the trajectory tracking performance of the controller is quite satisfactory (Figure 57) under given model error condition. However, the instability caused by the model error in yaw channel can not be compensated with the outer loop control (Figure 58-Figure 60) but it is evaluated that the oscillation starts to builds up after almost 15th second of the simulation (Figure 56).

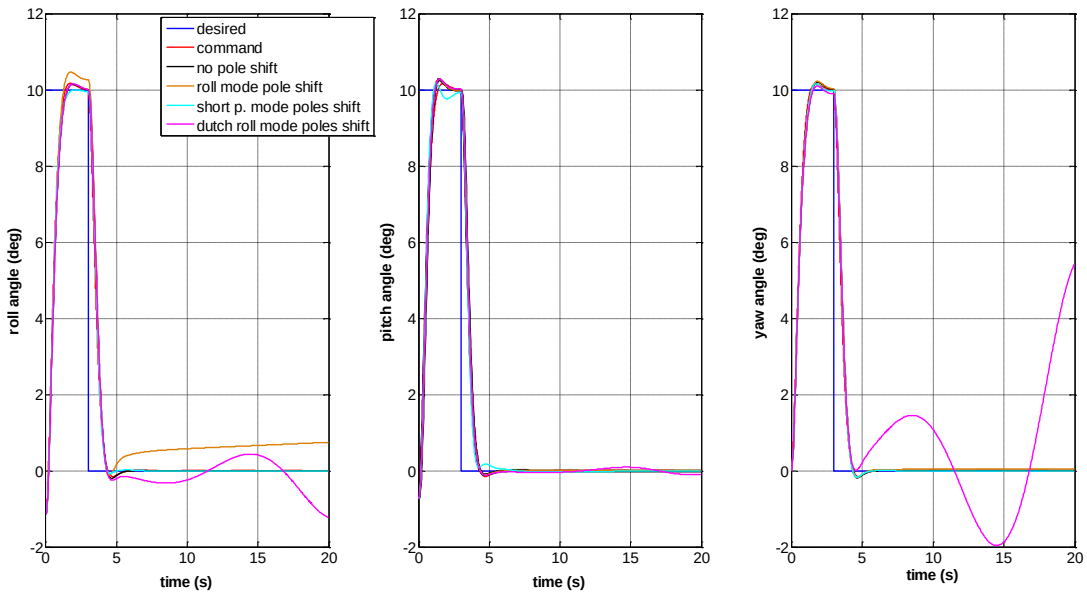

Figure 56 Euler Angles Responses with Model Error

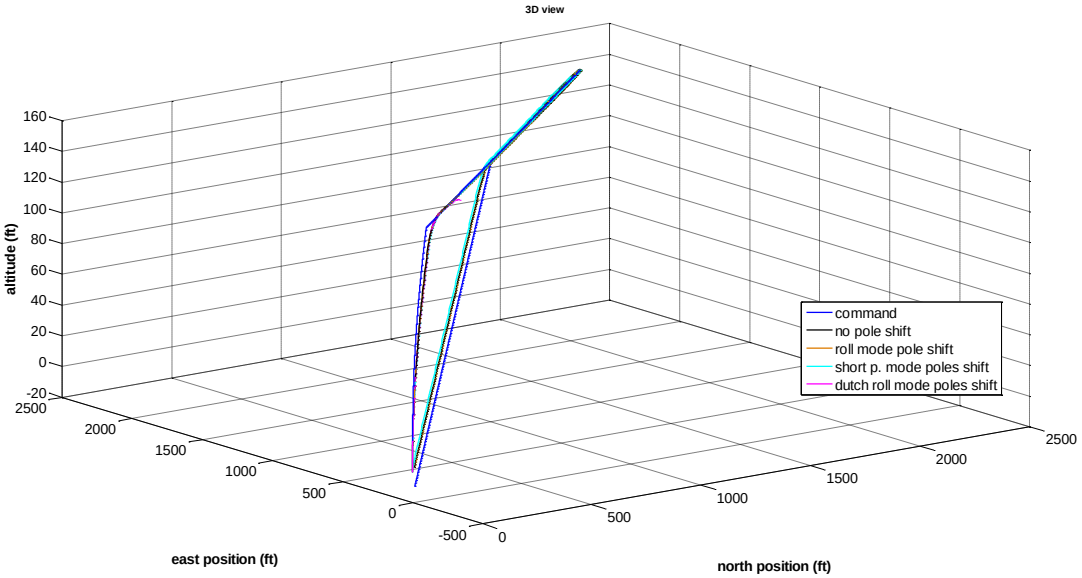

Figure 57 Scenario 1 North and East Positions with Model Error

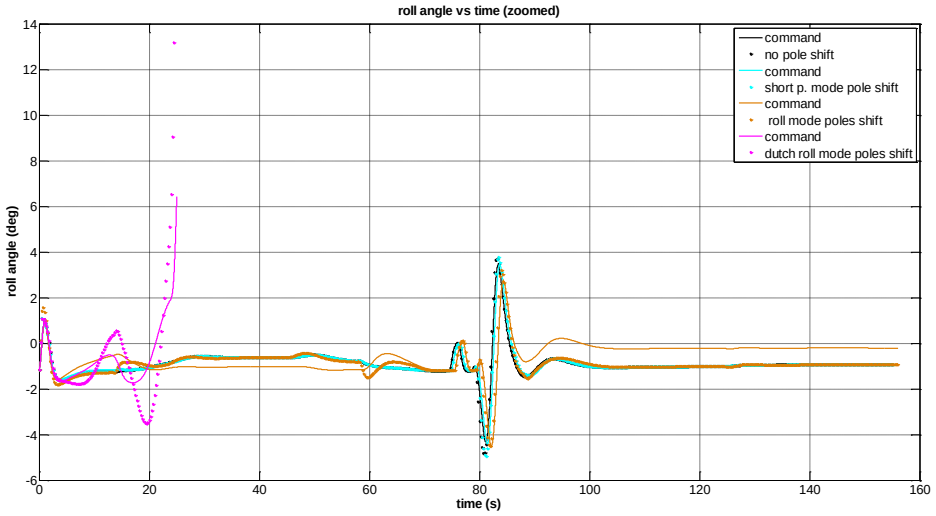

Figure 58 Scenario 1 Roll Angle with Model Error

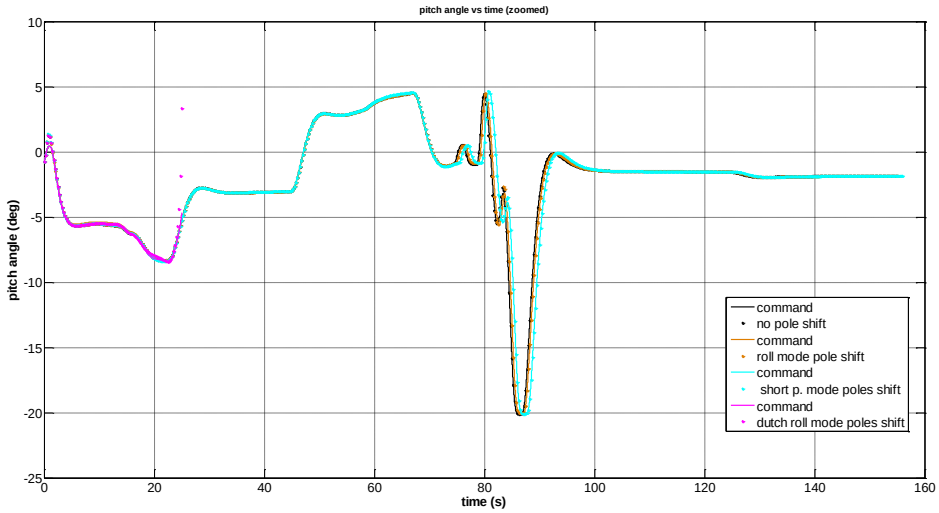

Figure 59 Scenario 1 Pitch Angle with Model Error

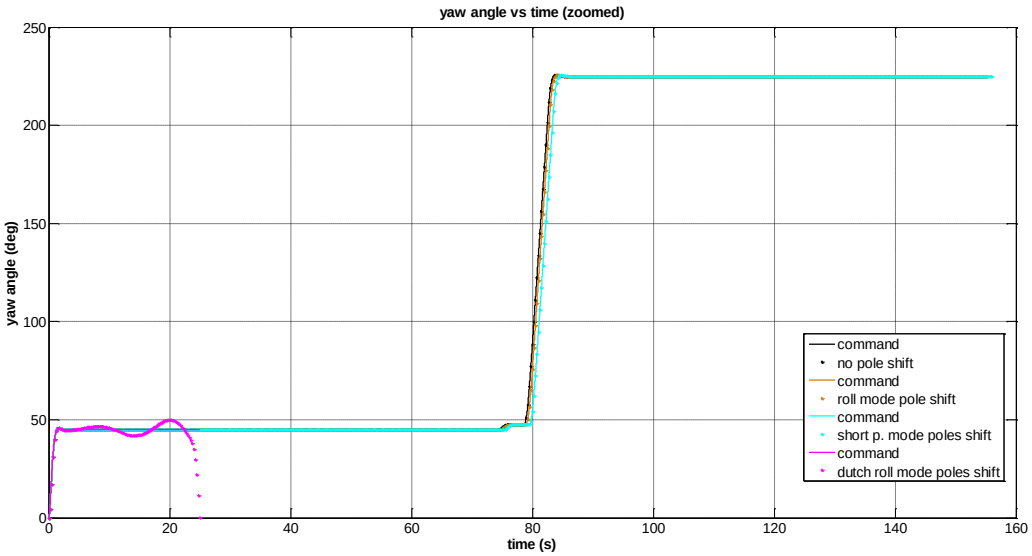

Figure 60 Scenario 1 Yaw Angle with Model Error

5.4 Simulation with Nonlinear Helicopter Model

In this study, the scenario 1 test is repeated with nonlinear helicopter simulation model[3] developed in [6]. Then the scenario 1 test results are compared for the cases with linear and nonlinear helicopter models. The resulting graphs are given in Figure 61-Figure 71.

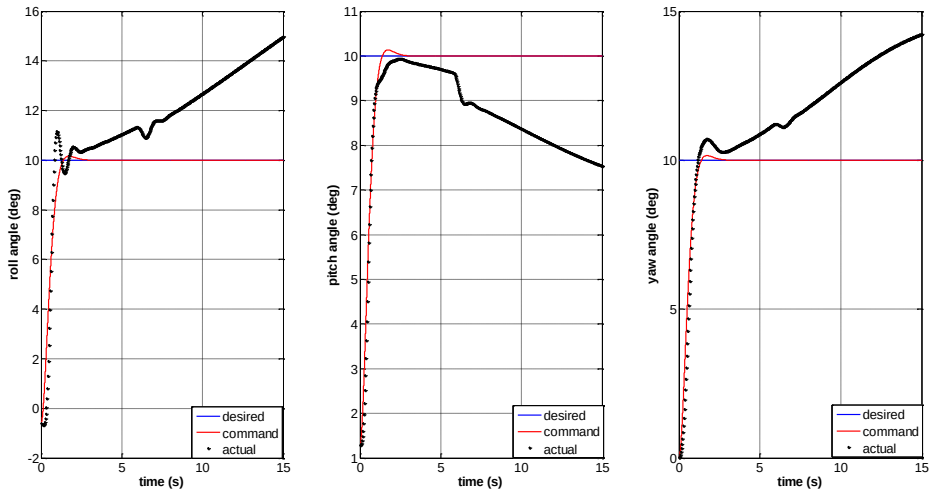

Figure 61 Euler Angles Responses with Nonlinear Model

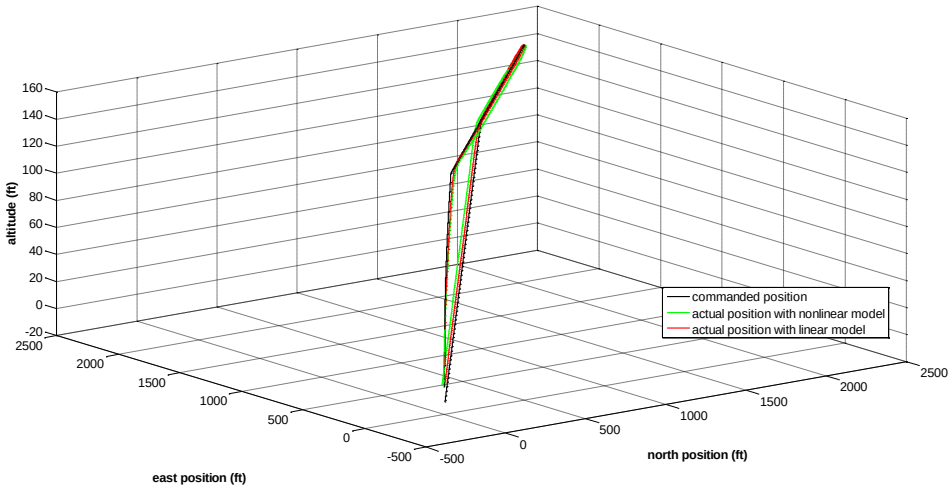

Figure 62 Scenario 1 North / East Positions and Altitude

[3] This nonlinear helicopter model developed in [6] is updated with AH-1G data which is given in APPENDIX A

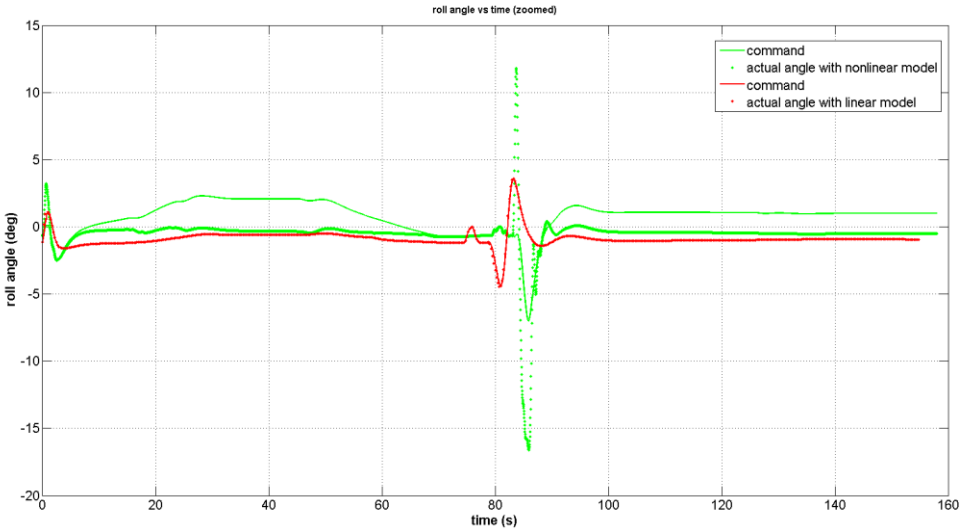

Figure 63 Scenario 1 Euler Angles (Roll Angle)

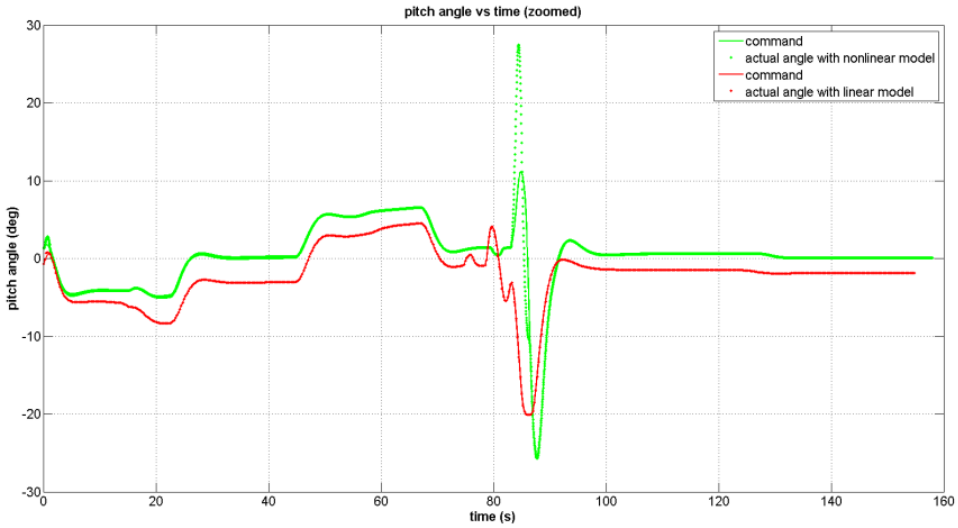

Figure 64 Scenario 1 Euler Angles (Pitch Angle)

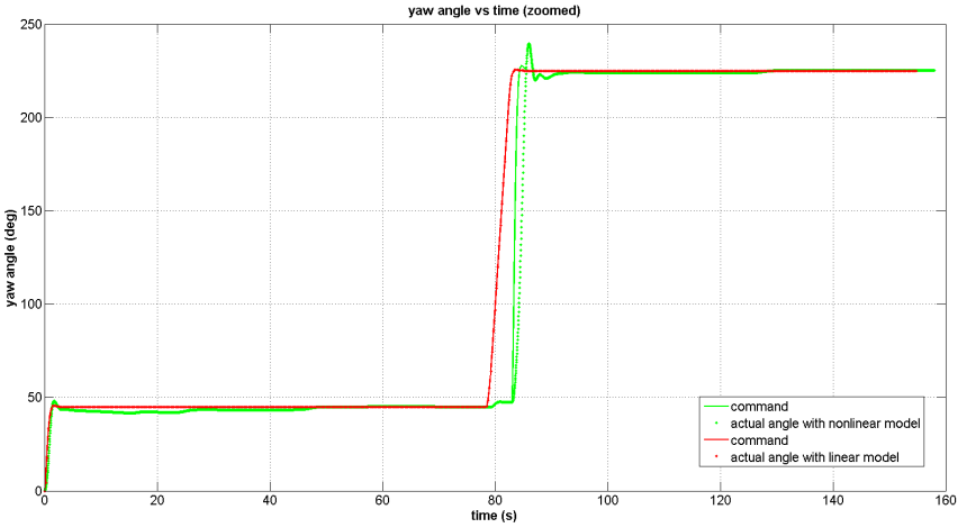

Figure 65 Scenario 1 Euler Angles (Yaw Angle)

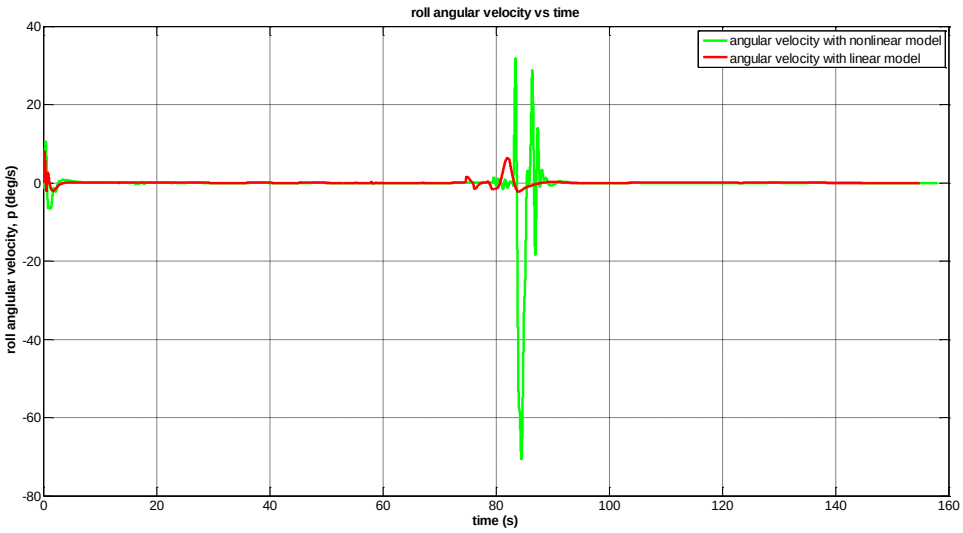

Figure 66 Scenario 1 Angular Velocities (Roll)

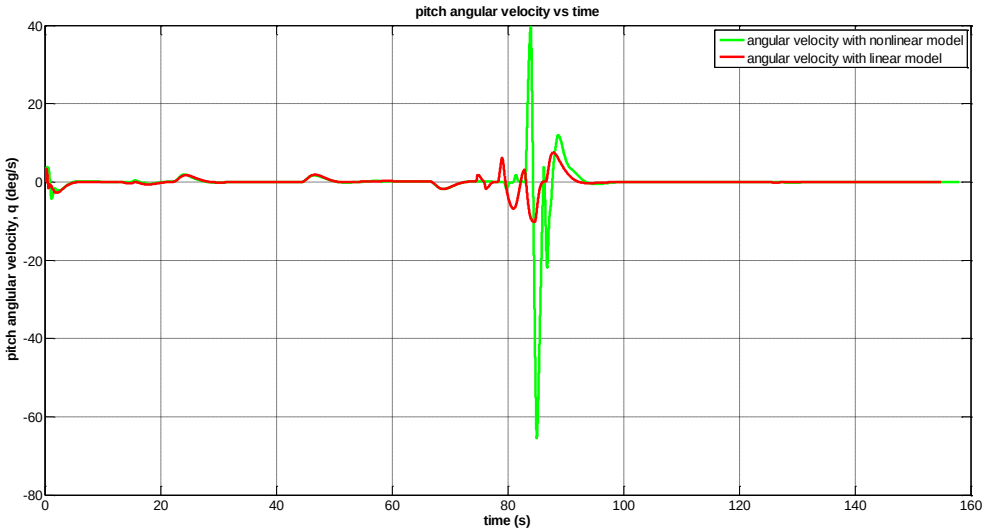

Figure 67 Scenario 1 Angular Velocities (Pitch)

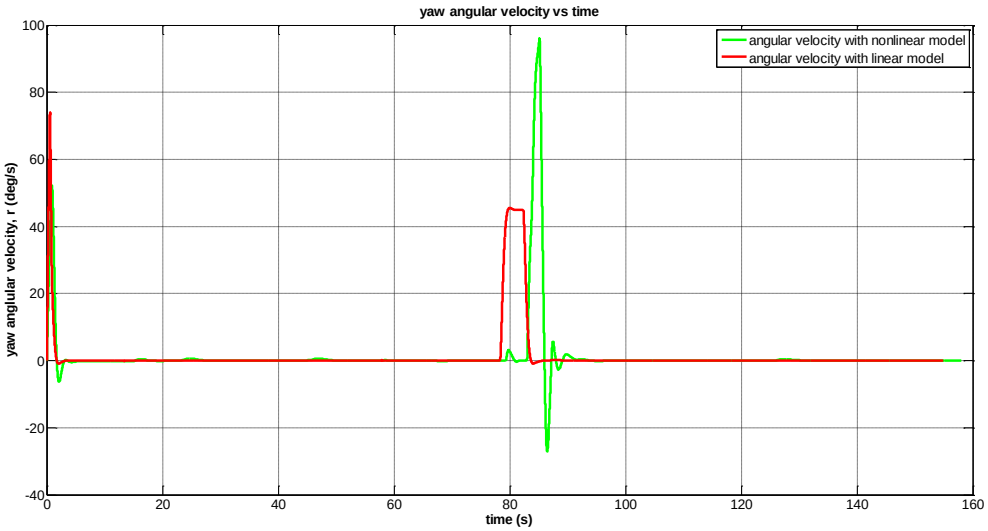

Figure 68 Scenario 1 Angular Velocities (Yaw)

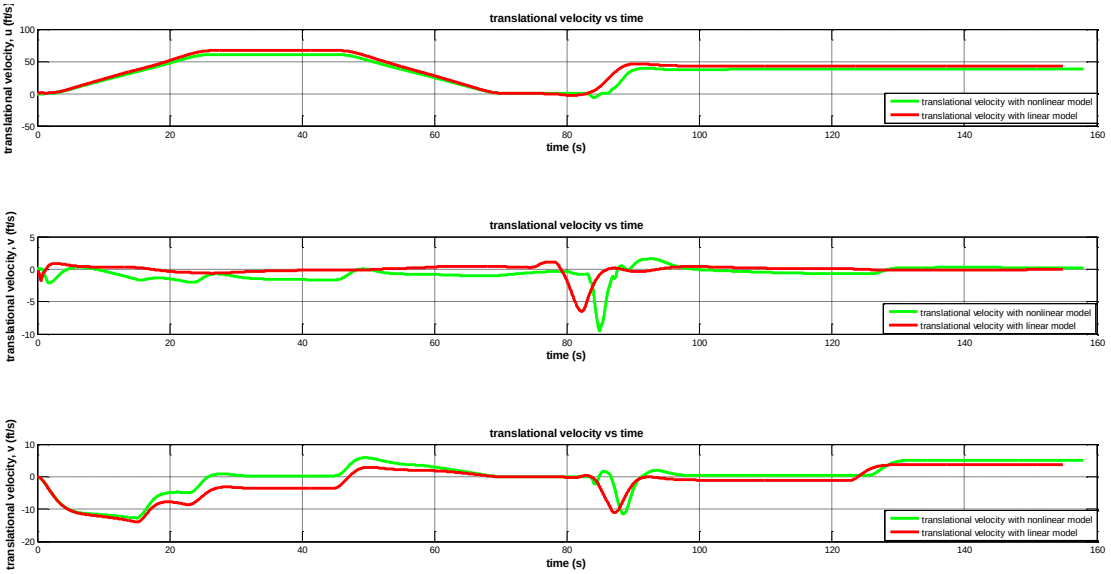

Figure 69 Scenario 1 Translational Velocities

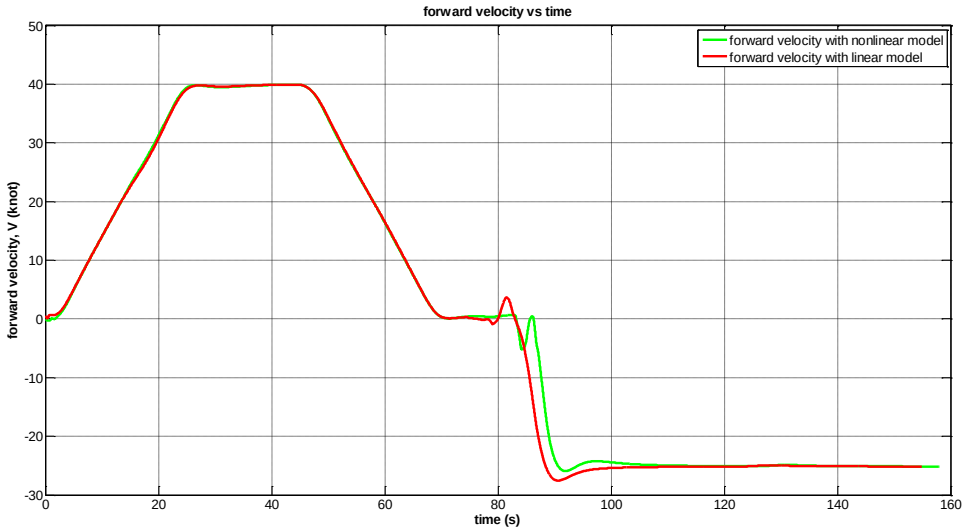

Figure 70 Scenario 1 Helicopter Forward Velocity

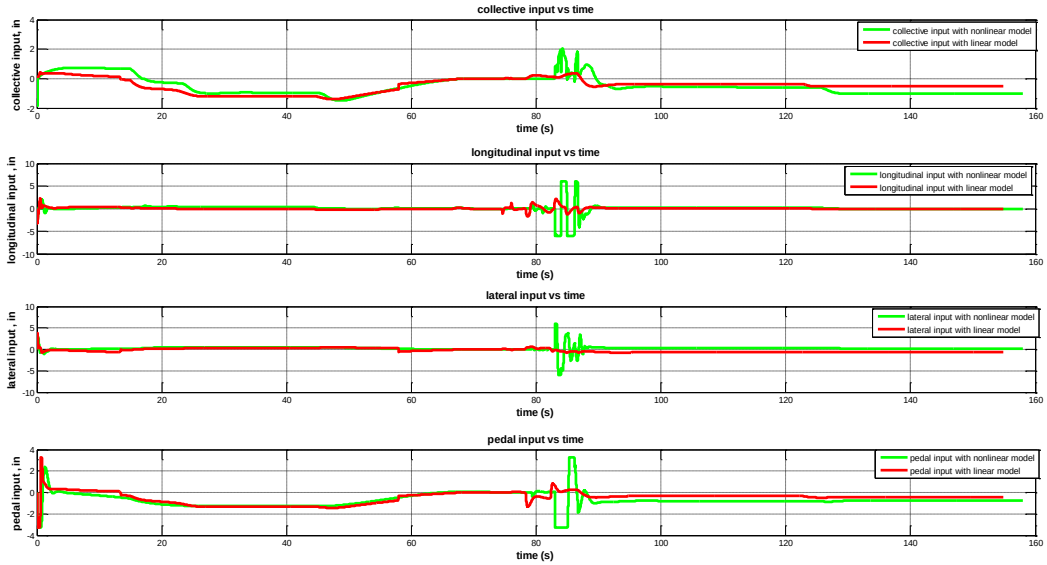

Figure 71 Scenario 1 Helicopter Control Inputs

According to Figure 62, if the step inputs with 10 deg/s magnitude are commanded to the inner loop (with nonlinear helicopter model), an unstable responses are observed (Figure 62). However the instability builds up quite slowly (doubling time is bigger than 15 s) and the stability is achieved by outer loop control. Figure 62 shows that the commanded positions are tracked sufficiently by this controller.

During the scenario 1 simulation (with nonlinear helicopter model), the error in Euler angle tracking (difference between command and the response) increases with increasing helicopter forward velocity. Figure 63, Figure 64, Figure 65 and Figure 70 shows that the tracking error is higher from about 15th to 60th and from about 90th to 160th seconds of the flight than the rest of the flight. This can be explained as following; even though the helicopter dynamics is changing with forward velocity, the inner loop still uses the same stability and the control derivatives (which belong to 1 knot forward velocity condition). This uncertainty results with degradation in Euler angle tracking performance. Also, the controller performance is poor in quality at maneuvering instants (from about 80th to 90th seconds of the flight) where the coupling affects increase in the helicopter dynamics. Consequently, the helicopter angular rates reaches higher values (>60deg/s) at these maneuvering instants (Figure 66-Figure 68). In addition, Figure 71 shows that the required longitudinal

and pedal control inputs reach to their limit values (given in Chapter 4) to execute this maneuver (from about 80^{th} to 90^{th} seconds of the flight).

The simulation results show that the overall performance of the controller with the nonlinear helicopter model is satisfactory.

CHAPTER 6

CONCLUSION

The aim of this thesis was to design the trajectory and the attitude controller for a helicopter to perform the mission; target engagement.

The problem was studied for an unmanned helicopter similar to the AH-1G helicopter. Therefore, the mission scenarios are developed by referencing the tactical operations of the AH-1G helicopter. According to this, the AH-1G helicopter attack patterns and 2.75” rockets firing procedure were analyzed. The attack pattern was based on u-turn maneuver and the firing types were selected as hover fire, running fire and diving fire.

As a hybrid system, mission scenarios for target engagement were based on two types of motion primitives: trim conditions and maneuvers. Trim conditions were defined as the equilibrium points of the system and maneuvers were described as the finite time transitions between two trim conditions and the stabilization was guaranteed by switching the system only at the trim conditions.

After analyzing the stability of AH-1G helicopter, dynamic inversion based controller was developed in this thesis. According to this method, the helicopter attitudes were controller with the inner loop and the trajectory was controlled with the outer loop. Also an algorithm was introduced to enable the controller and guidance system to switch from inner loop to outer or vice versa to provide the necessary maneuvers for the target engagement.

Then, three test cases were developed for three different firing types and the simulations were performed to tune and evaluate the controller performance. Also an uncertainty analysis is performed to analyze the controller performance under given uncertainty conditions. Finally, the controller is tested with nonlinear helicopter model which is developed in [6].

6.1 Future Works

It is recommended to study on the following topics to improve this study.

- Adaptive methods like neural network should be utilized here to compensate for the inversion errors.

- In this study, inertial and navigation system sensors are not modeled. In other words, these sensors are assumed to be ideal. Errors and noise which sensors produce can be modeled. In addition, the actuator model used in this study is very simple. Actuator limitations and nonlinearities such are friction/backlash should be modeled.

- The controller should be tested with more challenging scenarios.

REFERENCES

[1] E. Frazzoli, "*Robust Hybrid Control for Autonomous Vehicle Motion Planning*", Doctor of Philosophy at the Massachusetts Institute of Technology, June 2001

[2] A. Karimoddini, H. Lin, B. M. Chen, T. H. Lee "*Developments in Hybrid Modeling and Control of Unmanned Aerial Vehicles*", IEEE International Conference on Control and Automation Chiristchurch, New Zealand, December 9-11, 2009

[3] T. Schouwenaars, B. Mettler, E. Feron, and J.How, "*Robust Motion Planning Using a Maneuver Automation with Built-in Uncertainties*", Massachusetts Institute of Technology

[4] T. Schouwenaars, B. Mettler, E. Feron, and J.How, "*Hybrid Model for Trajectory Planning of Agile Autonomous Vehicles*", Journal Of Aerospace Computing, Information, And Communication, Vol. 1, December 2004

[5] E. Frazzoli, M. A. Dahleh, E. Feron "*A Hybrid Control Architecture for Aggressive Maneuvering of Autonomous Helicopters*", Proceeding of the 38th Conference on Desicion&Control, Phoenix, Arizona USA, December 1999

[6] O.Tarımcı, "*Adaptive Controller Applications for Rotary Wing Aircraft Models of Varying Simulation Fidelity*", MSc Thesis, Middle East Technical University, 2009.

[7] B. Morton, D. Enns, "*Stability of Dynamic Inversion Control Laws Applied to Nonlinear Aircraft Pitch-Axis Models*", Instituto for Mathematics and Its Applications University of Minnesota, July 1994

[8] J. V. R. Prasad, A. J. Calise, Y. P. and Corban, J. E., "*Adaptive Nonlinear Control Synthesis and Flight Test Evaluation on an Unmanned Helicopter*," IEEE International Conference on Control Applications, 1999

[9] A. J. Calise, R. T. Rysdyk, "*Nonlinear Adaptive Flight Control using Neural Networks*", Georgia Institute of Technology, School of Aerospace Engineering Atlanta, GA

[10] S.A. Snell, D.F. Enns and W.L. Garrard, "*Nonlinear Inversion Flight Control for a Supermaneuverable Aircraft*," AIAA J. of Guidance, Control, and Dynamics, vol. 15, no. 4, pp. 976-984, 1992

[11] M.W. McConley, B.D. Appleby, M.A. Dahleh, ,and E.Feron, "*A Computationally Efficient Lyapunov-Based Scheduling Procedure for Control of Nonlinear Systems with Stability Guarantees*", IEEE Transactions on Automatic Control, January 2000

[12] V. Gavrilets, I. Marinos, B. M. and Feron, E., "*Control Logic for Automated Aerobatic Flight of Miniature Helicopter*", AIAA Guidance, Navigation and Control Conference, 2002

[13] V. Gavrilets, I. Marinos, B. M. and Feron, E., "*Flight Test and Simulation Results for an Autonomous Aerobatic Helicopter*", AIAA/IEEE Digital Avionics Systems Conference, 2002

[14] R.J. Adams, J. M. Buffmgton and S. S. Banda., "*Design of Nonlinear Control Laws for High-Angle-of-Attack Flight*", Journal of Guidance, Control and Dynamics, Vol. 17, No. 4, July-August 1994

[15] B. Morton, D. Enns, B. Y Zhang, " *Stability of Dynamic Inversion Control Laws Applied to Nonlinear Aircraft Pitch-Axis Models*", Institute for Mathematics and Its Applications University of Minnesota,1994

[16] D. Enns, T.Keviczky, "*Dynamic Inversion Based Flight Control for Autonomous RMAX Helicopter*", Proceedings of the 2006 American Control Conference, Minneapolis, Minnesota, USA, June 14-16, 2006

[17] E. Johnsonand and S. Kannan, "*Adaptive Trajectory Control for Autonomous Helicopters*", Georgia Institute of Technology, Atlanta

[18] E. Johnson and S. Kannan, "*Adaptive Flight Control for an Autonomous Unmanned Helicopter*", AIAA Guidance, Navigation, and Control Conference and Exhibit, 5-8 August 2002

[19] A.J. Calise and R.T. Rysdyk, "*Nonlinear Adaptive Flight Control Using Neural Networks*", IEEE Controls Systems Magazine, 1998

[20] D. Yılmaz, "*Evaluation and Comparison of Helicopter Simulation Models with Different Fidelities*", MSc Thesis, Middle East Technical University, 2008

[21] *"Unmanned Combat Armed Rotorcraft"*, last accessed date: 01/09/ 2011, http://en.wikipedia.org/wiki/Unmanned_Combat_Armed_Rotorcraft

[22] *"Unmanned Combat Armed Rotorcraft [UCAR]",* last accessed date: 01/09/2011, http://www.globalsecurity.org/military/systems/aircraft/ucar.htm

[23] *"Weaponizing Unmanned Combat Helicopters*", last accessed date: 01/09/2011, http://defense-update.com/features/du-1-7/armedUAVs_11.htm

[24] "*Fire-X Medium-Range Vertical Unmanned Aircraft System*" last accessed date:01/09/2011,http://www.as.northropgrumman.com/products/fire-x/index.html

[25] Directory of Military Rockets and Missiles, "*Air-Launched 2.75-Inch Rockets*", last accessed date: 01/09/2011, http://www.designation-systems.net/dusrm/app4/275in-rockets.html (Directory of U.S. Military Rockets and Missiles)

[26] R. G. Sanfelice and E. Frazzoli, "*A Hybrid Control Framework for Robust Maneuver-based Motion Planning*", 2008 American Control Conference, Seattle, Washington, USA, June 11-13, 2008

[27] AH-1 Tactical Manual, NWP 3-22.5-AH1

[28] Headquarters, Department of The Army, TC 1-213, "*Aircraft Training Manual Attack Helicopter, AH-1*", 1992

[29] B. Etkin, "*Dynamics of Atmospheric Flight*",1972

[30] R. C. Nelson, "*Flight Stability and Automatic Control*",1989

[31] R.K. Heffley, W.F. Jewell, J.M. Lehman and R.A.A Van Winkle, "*Compilation and Analysis of Helicopter Handling Qualities Data, Volume One: Data Compilation, Systems Technology, Inc. TR 1087-1*", 1979

[32] G. D. Padfield, Helicopter Flight Dynamics: *The Theory and Application of Flying Qualities and Simulation Modeling*, AIAA Education Series, 1996

[33] J. LOPEZ, "*Assessment Of The AH-1G Cobra Using Modern Rotorcraft Handling Qualities Specifications (ADS-33E) and Development Of New Flight Control Laws*", 2007

[34] "*Hydra-70 Rocket System Integration Information*", last accessed date: 01 /09/2011, http://www.fas.org/man/dod-101/sys/missile/docs/hydra_info2.pdf,

APPENDIX A

AH-1G COBRA HELICOPTER

The Bell AH-1 Cobra (Figure A-1) is a two-bladed, turbo-shaft single turbine engine attack helicopter manufactured by Bell Helicopter [35]. It is first used in the US Army in Vietnam War in 1967 and is still one of the most numerous helicopter types in service today [35, 33]. The AH-1G was designed for combat and to protect unarmed troop helicopters. AH-1G helicopters are;

- 2× 7.62 mm (0.308 in) multi-barrel Miniguns, or 2 × M129 40 mm Grenade launchers, or one of each, in the M28 turret
- 2.75 in (70 mm) rockets - 7 rockets mounted in the M158 launcher or 19 rockets in the M200 launcher
- M18 7.62 mm Minigun pod or XM35 armament subsystem with XM195 20 mm cannon

The AH-1G is flown by two crews. They are the pilot and the copilot/gunner. A Stability and Control Augmentation System (SCAS) is added to the system to ease the pilot work load [33].

Figure A-1 AH-1G Cobra Helicopter

A.1 AH-1G Cobra Helicopter Data

AH-1G helicopter data is taken from [31]. Values used in stability analysis and controller design are given in Figure A-2, Figure A-3 and Table A-1 – Table A-10.

Table A-1 AH-1G Descriptive Data

MAIN ROTOR	
Blades	2
Radius	6.706 m (22 ft)
Chord	0.686 m (2.25 ft)
Section	9.33% thickness, special symmetrical section
Hub type	Teetering
Undersling	11.4 cm (4.5 in)
Twist	-10 deg
Pitch flap coupling (δ_3)	Zero
Shaft tilt	Zero
Design rpm	314 to 324 (power on), 294 to 339 (power off)*
Hub location	FS 200, WL 152.76'
Blade flapping inertia	1873.44 kg-m^2 (1381.8 slug-ft^2)
TAIL ROTOR	
Blades	2
Radius	1.295 m (4.25 ft)
Chord	0.214 m (0.701 ft)
Twist	Zero
Gear ratio	5.123
Hub location	FS 520.7, WL 118.27, BL -14.85
WING	
Area	2.583 m^2 (27.8 ft^2)
Aspect ratio	3.91
Center of pressure location	FS 192.0, BL 39.0, WL 62.0
Incidence	14 deg
Dihedral	3.5 deg
ELEVATOR (EACH SIDE, EXCLUDING FUSELAGE CARRY-THROUGH)	
Area	0.683 m^2 (7.35 ft^2)
Aspect ratio	1.49
Center of pressure location	FS 398.5, BL ± 22.07, WL 56.0
Incidence	Variable
VERTICAL STABILIZER	
Area	1.728 m^2 (18.60 ft^2)
Aspect ratio	1.56
Center of pressure location	FS 501.0, WL 84.0

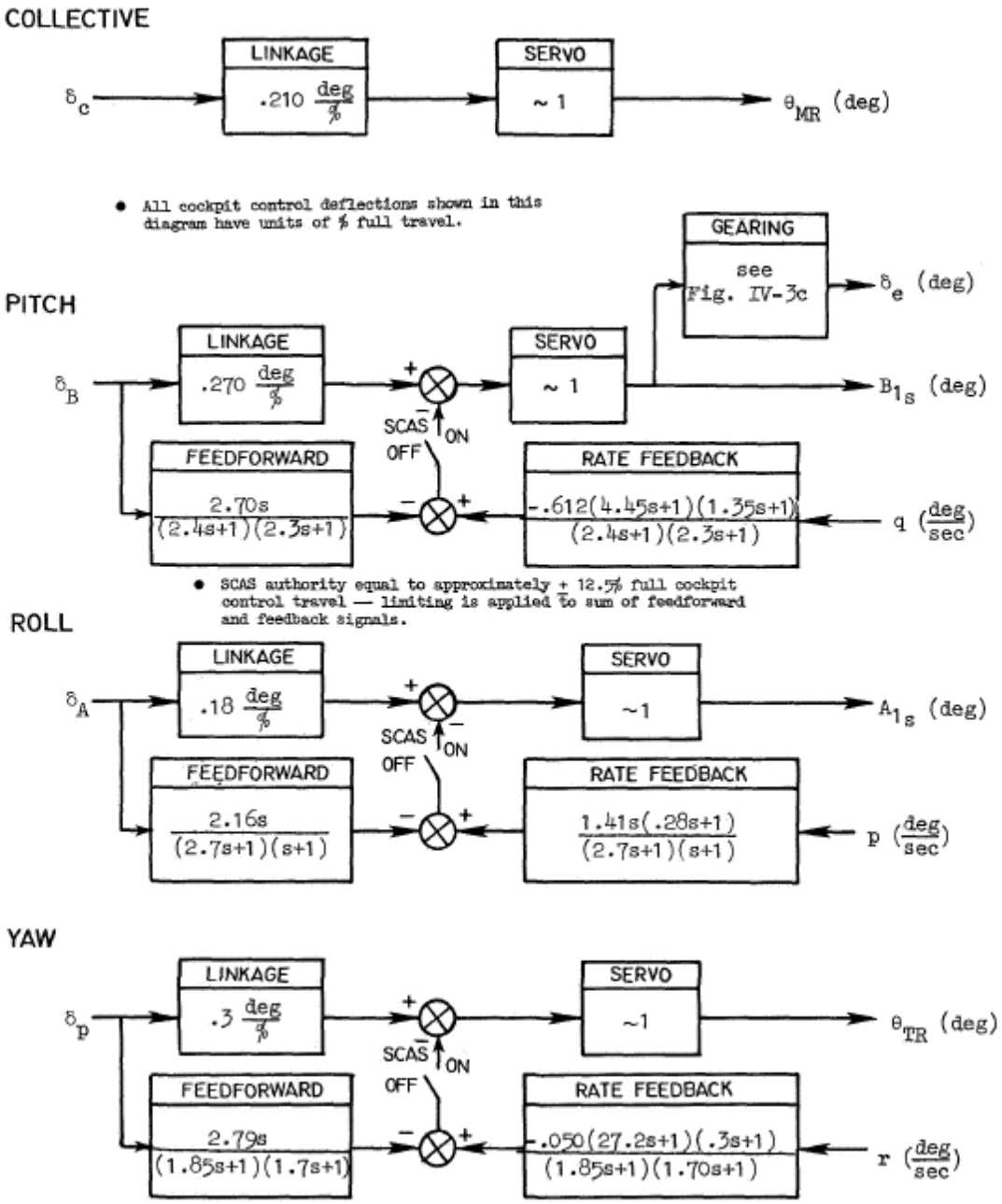

Figure A-2 AH-1G Control System Description (Control Deflections)

Table A-2 Cockpit Controller Characteristics

CONTROLLER	100% FULL TRAVEL cm (in)	FORCE GRADIENT N/cm (lb/in)
Collective, δ_c	25.4 (10.)	—
Longitudinal Cyclic, δ_B	30.48 (12.)	2.12 (1.21)
Lateral Cyclic, δ_A	30.48 (12.)	1.73 (.99)
Pedal, δ_p	16.51 (6.5)	19.6 (11.2)

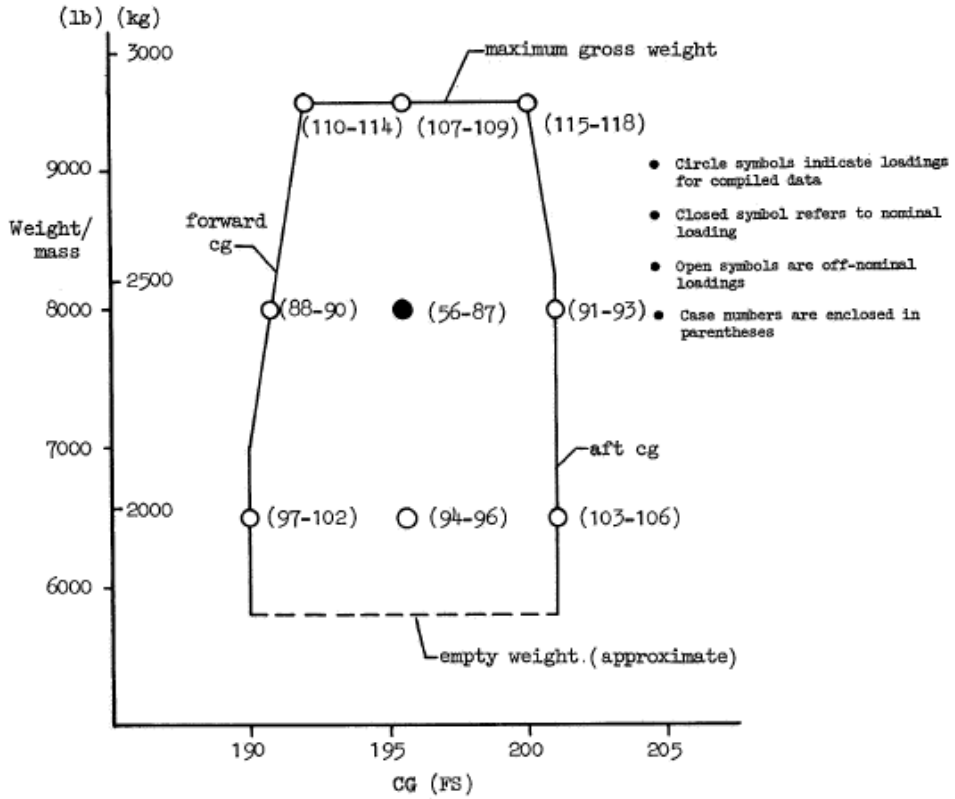

Figure A-3 Loading Envelope

Table A-3 Moments of Inertia for Complied Data

CONDITION	MASS (WEIGHT) kg (lb)	CG FS	CG WL	I_x	I_y	I_z	I_{xz}
				kg-m^2 (slug-ft^2)			
Nominal Weight	3629(8000)	190.8 to 201.0	73.0	3661(2700)	17354(12800)	14643(10800)	1288(950)
Light Weight	2948(6500)	190.0 to 201.0	78.0	2983(2200)	15863(11700)	13151(9700)	1288(950)
Heavy Weight	4309(9500)	192.0 to 200.0	68.0	4271(3150)	18032(13300)	16066(11850)	1288(950)

Table A-4 AH-1G Index of Flight Conditions for Derivatives and Transfer Function Factors

CASE	CONDITION	AIRSPEED kt	VERTICAL VELOCITY m/sec(ft/sec)	ALTITUDE m(ft)	MASS(WEIGHT) kg(lb)	cg FS	REPORT PAGE NUMBER: DERIVATIVES SI(US)	TRANSFER FUNCTIONS: SCAS OFF	TRANSFER FUNCTIONS: SCAS ON
56	Airspeed Variation	-40	Zero	Sea Level	3629(8000)	195.5	122(143)	164	
57	↓	-20	↓	↓	↓	↓		165	166
58		-10							
59		Hover					123(144)	167*	171*
60		10							
61		20						175*	179*
62		40					124(145)	183	184
63		60						185*	189*
64		80						193	194
65		100					125(146)	195	196
66		120						197	198
67	↓	140	↓					199	
68	Maximum Power Climb	Zero†	8.5(28.0)				126(147)		
69	↓	60	11.9(39.0)					200	201
70		100	10.6(34.9)						
71	Autorotation	60	-9.5(-31.1)				127(148)	202	203
72	↓	100	-11.4(-37.5)						
73	Descent	Zero†	-3.0(-10)						
74			-6.1(-20)				128(149)		
75	Climb	↓	3.0(10)						
76	↓		6.1(20)						
77		60	6.1(20)				129(150)	204	
78	↓	↓	3.0(10)						
79	Descent		-3.0(-10)						
80	↓		-6.1(-20)				130(151)		
81	Operation at Altitude	Hover	Zero	3048(10000)				205	
82	↓	60	↓	↓					
83		100					131(152)		
84	Maximum Climb at Altitude	Zero†	6.1(20)						
85	↓	60	8.5(28.0)						
86	Autorotation at Altitude	↑	-8.5(-27.8)				132(153)		
87	↓	100	-9.1(30.0)	↓		↓			
88	Fwd cg, Nominal Weight	Hover	Zero	Sea Level		190.8			
89	↓	60				↓	133(154)		
90		100							
91	Aft cg, Nominal Weight	Hover				201.0		206	
92	↓	60			↓	↓	134(155)		
93		100							
94	Light Weight	Hover			2948(6500)	195.5		207	
95	↓	60			↓	↓	135(156)	208	
96		100							
97	Fwd cg, Light Weight	Hover				190.0			
98	↑	60					136(157)		
99	...and Maximum Climb	Zero†	14.4(47.4)						
100	↑	60	14.6(48.0)					209	
101	...and Autorotation	Zero†	-15.2(-50.0)				137(158)		
102	↑	60	-8.5(-28.0)						
103	Aft cg, Light Weight	Hover	Zero			201.0			
104	↑	60	Zero				138(159)		
105	...and Maximum Climb	↓	15.5(50.9)		↓	↓			
106	...and Autorotation		-8.8(-29.0)						
107	Heavy Weight	Hover	Zero		4309(9500)	195.5	139(160)	210	
108	↓	60	↓		↓	↓		211	
109		100							
110	Fwd cg, Heavy Weight	Hover				192.0	140(161)		
111	↑	60							
112	...and Maximum Climb	Zero†	3.7(12.0)						
113	↑	60	9.6(31.4)				141(162)		
114	...and Autorotation	60	-8.1(-26.5)						
115	Aft cg, Heavy Weight	Hover	Zero			200.0			
116	↑	60	Zero				142(163)		
117	...and Maximum Climb	↓	9.8(32.2)	↓	↓	↓			
118	...and Autorotation		-8.8(-28.8)						

* Extended list of transfer function factors.
† Zero forward velocity, i.e., airspeed is equal to vertical velocity.

Table A-5 General Layout of Stability and Control Derivative Data

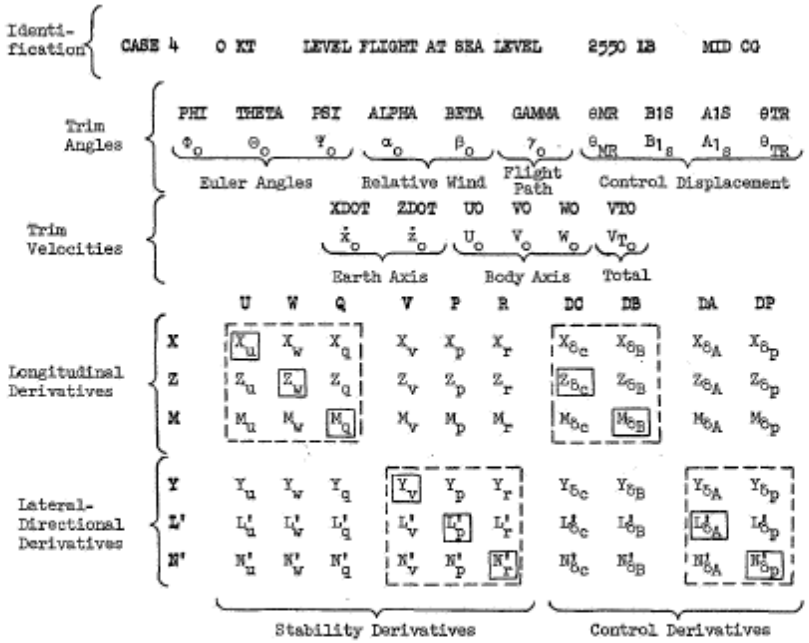

Solid boxes enclose on-diagonal stability derivatives and direct control derivatives

Dashed boxes enclose usual three degrees of freedom derivatives

$$L'_{()} = \frac{L_{()} + \frac{I_{xz}}{I_x} N_{()}}{1 - \frac{I_{xz}^2}{I_x I_z}}$$

$$N'_{()} = \frac{N_{()} + \frac{I_{xz}}{I_z} L_{()}}{1 - \frac{I_{xz}^2}{I_x I_z}}$$

Table A-6 US Units for Numerical Values of Stability and Control Derivatives

CASE 4 0 KT LEVEL FLIGHT AT SEA LEVEL 2550 LB MID CG

PHI	THETA	PSI	ALPHA	BETA	GAMMA	GMR	B1S	A1S	GTR
ϕ_o(deg)	θ_o(deg)	ψ_o(deg)	α_o(deg)	β_o(deg)	γ_o(deg)	θ_{MR}(deg)	B_{1_s}(deg)	A_{1_s}(deg)	θ_{TR}(deg)

XDOT	ZDOT	UO	VO	WO	VTO
$\dot{x}_o$(ft/sec)	$\dot{z}_o$(ft/sec)	U_o(ft/sec)	V_o(ft/sec)	W_o(ft/sec)	V_{T_o}(ft/sec)

	U	W	Q	V	P	R	DC	DB	DA	DP
X	X_u(1/sec)	X_w(1/sec)	$X_q(\frac{ft}{sec\text{-}rad})$	X_v(1/sec)	$X_p(\frac{ft}{sec\text{-}rad})$	$X_r(\frac{ft}{sec\text{-}rad})$	$X_{\delta_C}(\frac{ft}{sec^2\text{-}in})$	$X_{\delta_B}(\frac{ft}{sec^2\text{-}in})$	$X_{\delta_A}(\frac{ft}{sec^2\text{-}in})$	$X_{\delta_P}(\frac{ft}{sec^2\text{-}in})$
Z	Z_u(1/sec)	Z_w(1/sec)	$Z_q(\frac{ft}{sec\text{-}rad})$	Z_v(1/sec)	$Z_p(\frac{ft}{sec\text{-}rad})$	$Z_r(\frac{ft}{sec\text{-}rad})$	$Z_{\delta_C}(\frac{ft}{sec^2\text{-}in})$	$Z_{\delta_B}(\frac{ft}{sec^2\text{-}in})$	$Z_{\delta_A}(\frac{ft}{sec^2\text{-}in})$	$Z_{\delta_P}(\frac{ft}{sec^2\text{-}in})$
M	$M_u(\frac{rad}{ft\text{-}sec})$	$M_w(\frac{rad}{ft\text{-}sec})$	M_q(1/sec)	$M_v(\frac{rad}{ft\text{-}sec})$	M_p(1/sec)	M_r(1/sec)	$M_{\delta_C}(\frac{rad}{sec^2\text{-}in})$	$M_{\delta_B}(\frac{rad}{sec^2\text{-}in})$	$M_{\delta_A}(\frac{rad}{sec^2\text{-}in})$	$M_{\delta_P}(\frac{rad}{sec^2\text{-}in})$
Y	Y_u(1/sec)	Y_w(1/sec)	$Y_q(\frac{ft}{sec\text{-}rad})$	Y_v(1/sec)	$Y_p(\frac{ft}{sec\text{-}rad})$	$Y_r(\frac{ft}{sec\text{-}rad})$	$Y_{\delta_C}(\frac{ft}{sec^2\text{-}in})$	$Y_{\delta_B}(\frac{ft}{sec^2\text{-}in})$	$Y_{\delta_A}(\frac{ft}{sec^2\text{-}in})$	$Y_{\delta_P}(\frac{ft}{sec^2\text{-}in})$
L'	$L'_u(\frac{rad}{ft\text{-}sec})$	L'_w(1/sec)	L'_q(1/sec)	$L'_v(\frac{rad}{ft\text{-}sec})$	L'_p(1/sec)	L'_r(1/sec)	$L'_{\delta_C}(\frac{rad}{sec^2\text{-}in})$	$L'_{\delta_B}(\frac{rad}{sec^2\text{-}in})$	$L'_{\delta_A}(\frac{rad}{sec^2\text{-}in})$	$L'_{\delta_P}(\frac{rad}{sec^2\text{-}in})$
N'	$N'_u(\frac{rad}{ft\text{-}sec})$	N'_w(1/sec)	N'_q(1/sec)	$N'_v(\frac{rad}{ft\text{-}sec})$	N'_p(1/sec)	N'_r(1/sec)	$N'_{\delta_C}(\frac{rad}{sec^2\text{-}in})$	$N'_{\delta_B}(\frac{rad}{sec^2\text{-}in})$	$N'_{\delta_A}(\frac{rad}{sec^2\text{-}in})$	$N'_{\delta_P}(\frac{rad}{sec^2\text{-}in})$

Table A-7 AH-1G Stability and Control Derivatives in US Units
(in Body Fixed Reference Frame)

CASE 56 -40 KT LEVEL FLIGHT AT SEA LEVEL 8000 LB MID CG

PHI	THETA	PSI	ALPHA	BETA	GAMMA	BSR	BIS	AIS	BTR
-0.75	-2.43	0.00	177.57	-0.03	180.00	12.72	-4.46	-0.13	3.81

XDOT	ZDOT	UO	VO	WO	VTO
-67.51	0.00	-67.45	-0.04	2.87	67.51

	U	W	Q	V	P	R	DC	DB	DA	DP
X	-0.0136	-0.0434	1.6395	-0.0021	-1.5035	0.1217	-0.4800	1.1679	0.0433	0.1869
Z	0.1286	-0.6508	0.2369	-0.0093	1.0227	1.7931	-13.4701	-1.8621	-0.1004	-0.0877
M	0.0018	0.0027	-0.1329	0.0006	0.1793	-0.0082	-0.0295	-0.1541	-0.0065	-0.0269
Y	-0.0019	-0.0249	-1.5326	-0.0429	-1.8438	0.5650	-0.4874	-0.1026	0.8243	1.5756
L'	0.0019	-0.0173	-0.7887	-0.0057	-1.0348	0.0873	-0.1477	-0.0723	0.4784	0.3088
N'	0.0046	-0.0079	0.1078	0.0065	-0.0414	-0.4312	0.3508	-0.0304	0.0332	-0.8177

CASE 57 -20 KT LEVEL FLIGHT AT SEA LEVEL 8000 LB MID CG

PHI	THETA	PSI	ALPHA	BETA	GAMMA	BSR	BIS	AIS	BTR
-0.97	-2.95	0.00	177.05	-0.05	180.00	13.79	-3.99	-0.53	5.75

XDOT	ZDOT	UO	VO	WO	VTO
-33.76	0.00	-33.71	-0.03	1.74	33.76

	U	W	Q	V	P	R	DC	DB	DA	DP
X	0.0028	-0.0369	1.1267	-0.0032	-1.5259	0.1156	-0.4286	1.3493	0.1261	0.3919
Z	0.2097	-0.4833	-0.9979	-0.0246	0.5470	1.7875	-12.2503	-0.8752	-0.0759	-0.0979
M	0.0034	-0.0004	-0.1475	0.0009	0.1847	-0.0166	-0.0359	-0.1745	-0.0182	-0.0432
Y	0.0009	-0.0151	-1.5411	-0.0407	-1.3228	0.5782	-0.3639	0.0190	0.8954	1.5810
L'	0.0067	-0.0123	-0.8199	-0.0075	-0.7911	0.0787	-0.0397	-0.0055	0.5115	0.3193
N'	0.0076	-0.0059	0.3394	0.0083	-0.1375	-0.3874	0.4758	-0.0114	0.0358	-0.7695

CASE 58 -10 KT LEVEL FLIGHT AT SEA LEVEL 8000 LB MID CG

PHI	THETA	PSI	ALPHA	BETA	GAMMA	BSR	BIS	AIS	BTR
-1.07	-1.92	0.00	178.08	-0.04	180.00	14.41	-2.79	-1.08	7.34

XDOT	ZDOT	UO	VO	WO	VTO
-16.89	0.00	-16.87	-0.01	0.56	16.88

	U	W	Q	V	P	R	DC	DB	DA	DP
X	-0.0208	-0.0211	0.7565	-0.0101	-1.9146	-0.1819	-0.5291	1.1479	-0.0278	-0.0908
Z	0.1777	-0.4042	-1.1236	-0.0405	0.3318	2.0194	-12.3492	-0.2496	0.0112	0.1051
M	0.0077	-0.0037	-0.2056	0.0016	0.2236	0.0162	0.0090	-0.1397	0.0041	0.0280
Y	0.0058	-0.0141	-1.7777	-0.0877	-1.1490	0.6386	-0.4689	-0.0216	0.8492	1.4108
L'	0.0095	-0.0087	-0.9266	-0.0073	-0.7256	0.0289	-0.0536	-0.0160	0.4968	0.2807
N'	0.0068	-0.0023	0.2837	0.0122	-0.2546	-0.4296	0.5488	-0.0148	0.0346	-0.7780

Table A-8 AH-1G Stability and Control Derivatives in US Units (Continued)
(in Body Fixed Reference Frame)

CASE 59 1 KT LEVEL FLIGHT AT SEA LEVEL 8000 LB MID CG

PHI	THETA	PSI	ALPHA	BETA	GAMMA	RHO	B1S	A1S	RTR
-1.15	-0.71	0.00	-0.73	0.01	0.00	14.83	-0.76	-1.80	0.40

XDOT	ZDOT	UO	VO	WO	VTO
1.69	0.00	1.69	0.00	-0.02	1.69

	U	W	Q	V	P	R	DC	DR	DA	DP
X	-0.0165	-0.0155	0.3655	-0.0285	-1.8499	-0.1273	-0.2560	1.2425	-0.0130	-0.1653
Z	-0.1208	-0.3726	-0.0113	-0.0932	-0.1385	2.0756	-12.7606	0.1799	-0.0035	-0.0305
M	0.0005	-0.0033	-0.2345	0.0007	0.2305	0.0175	0.0076	-0.1462	0.0035	0.0322
Y	0.0173	-0.0051	-1.5941	-0.0552	-1.1026	0.7182	-0.5515	-0.1182	0.8095	1.2837
L'	0.0085	-0.0060	-1.0559	-0.0087	-0.7662	-0.0403	-0.0925	-0.0686	0.4709	0.1816
N'	-0.0012	-0.0047	-0.1161	0.0158	-0.3945	-0.5366	0.5795	-0.0095	0.0319	-0.8120

CASE 60 10 KT LEVEL FLIGHT AT SEA LEVEL 8000 LB MID CG

PHI	THETA	PSI	ALPHA	BETA	GAMMA	RHO	B1S	A1S	RTR
-1.05	-1.10	0.00	-1.10	0.02	0.00	14.82	-0.69	-2.02	7.52

XDOT	ZDOT	UO	VO	WO	VTO
16.88	0.00	16.87	0.01	-0.32	16.88

	U	W	Q	V	P	R	DC	DR	DA	DP
X	-0.0163	-0.0106	0.9706	-0.0154	-1.7470	-0.0595	-0.2890	1.3148	0.0403	-0.0044
Z	-0.2090	-0.4060	0.8210	-0.0530	-0.3136	1.9603	-12.3576	0.4270	0.0170	-0.0210
M	0.0002	-0.0026	-0.2299	0.0017	0.2141	0.0049	0.0085	-0.1607	-0.0056	0.0036
Y	0.0180	0.0002	-1.5623	-0.0562	-1.1609	0.8066	-0.3238	0.0141	0.8870	1.4888
L'	0.0068	-0.0033	-0.9165	-0.0063	-0.8109	0.0164	0.0198	0.0073	0.5144	0.3136
N'	-0.0040	-0.0044	0.0522	0.0133	-0.4245	-0.5325	0.5436	-0.0008	0.0351	-0.7733

CASE 61 20 KT LEVEL FLIGHT AT SEA LEVEL 8000 LB MID CG

PHI	THETA	PSI	ALPHA	BETA	GAMMA	RHO	B1S	A1S	RTR
-0.91	-1.59	0.00	-1.59	0.03	0.00	13.81	-0.73	-2.12	6.11

XDOT	ZDOT	UO	VO	WO	VTO
33.76	0.00	33.74	0.01	-0.93	33.76

	U	W	Q	V	P	R	DC	DR	DA	DP
X	-0.0281	-0.0198	1.2469	-0.0139	-1.7129	-0.0625	-0.4383	1.3050	0.0265	-0.0416
Z	-0.2485	-0.5022	0.8870	-0.0429	-0.4206	1.8029	-12.1662	0.8873	0.0346	-0.0232
M	0.0004	-0.0018	-0.2289	0.0014	0.2102	0.0059	0.0258	-0.1590	-0.0033	0.0106
Y	0.0142	0.0000	-1.5746	-0.0599	-1.4716	0.8115	-0.2437	0.0017	0.8630	1.3622
L'	0.0036	-0.0021	-0.8171	-0.0064	-0.9490	0.0241	0.0425	0.0061	0.5018	0.2706
N'	-0.0064	-0.0037	0.1952	0.0119	-0.5410	-0.5011	0.4781	0.0032	0.0141	-0.7121

Table A-9 AH-1G Stability and Control Derivatives in US Units (Continued)
(in Body Fixed Reference Frame)

CASE 62 40 KT LEVEL FLIGHT AT SEA LEVEL 8000 LB MID CG

PHI	THETA	PSI	ALPHA	BETA	GAMMA	θHR	B1S	A1S	θTR
-0.71	-1.81	0.00	-1.91	0.02	0.00	12.77	-0.10	-1.93	3.49

XDOT	ZDOT	U0	V0	W0	VT0
67.51	0.00	67.48	0.03	-2.13	67.51

	U	W	Q	V	P	R	DC	DB	DA	DP
X	-0.0273	-0.0263	1.5624	-0.0084	-1.6517	-0.0980	-0.5425	1.3186	0.0156	-0.0750
Z	-0.1688	-0.7094	-0.2633	-0.0315	-0.9439	1.6536	-13.2839	1.8147	0.0528	-0.0696
M	0.0017	-0.0023	-0.2805	0.0007	0.1951	0.0149	0.0304	-0.1590	-0.0023	0.0151
Y	0.0081	0.0017	-1.5067	-0.0793	-1.9277	1.0265	-0.0712	0.0378	0.8501	1.4574
L'	0.0005	-0.0014	-0.7411	-0.0060	-1.2312	0.0250	0.0989	0.0327	0.4938	0.2938
N'	-0.0061	-0.0063	0.2837	0.0128	-0.4142	-0.7310	0.3660	0.0273	0.0295	-0.7841

CASE 63 60 KT LEVEL FLIGHT AT SEA LEVEL 8000 LB MID CG

PHI	THETA	PSI	ALPHA	BETA	GAMMA	θHR	B1S	A1S	θTR
-0.69	-2.25	0.00	-2.25	0.03	0.00	12.82	0.70	-1.54	2.39

XDOT	ZDOT	U0	V0	W0	VT0
101.27	0.00	101.19	0.05	-3.98	101.27

	U	W	Q	V	P	R	DC	DB	DA	DP
X	-0.0268	-0.0286	1.7170	-0.0046	-1.6069	-0.0668	-0.6761	1.3088	0.0163	-0.0506
Z	-0.1060	-0.8377	-1.4214	-0.0245	-1.4280	1.7699	-15.0092	2.9518	0.0731	-0.0848
M	0.0019	-0.0030	-0.3244	0.0000	0.1854	0.0199	0.0287	-0.1574	-0.0029	0.0152
Y	0.0006	-0.0003	-1.4114	-0.1019	-2.0845	1.3044	-0.0597	0.0196	0.8415	1.7390
L'	-0.0031	-0.0031	-0.6703	-0.0046	-1.2781	0.0375	0.0774	0.0227	0.4875	0.3409
N'	-0.0048	-0.0087	0.3029	0.0144	-0.3518	-0.4970	0.2937	0.0342	0.0268	-0.9430

CASE 64 80 KT LEVEL FLIGHT AT SEA LEVEL 8000 LB MID CG

PHI	THETA	PSI	ALPHA	BETA	GAMMA	θHR	B1S	A1S	θTR
-0.78	-2.71	0.00	-2.71	0.04	0.00	12.55	1.77	-1.11	2.02

XDOT	ZDOT	U0	V0	W0	VT0
135.02	0.00	134.87	0.09	-6.38	135.02

	U	W	Q	V	P	R	DC	DB	DA	DP
X	-0.0296	-0.0261	1.7668	-0.0027	-1.5508	-0.0997	-0.6853	1.3064	0.0158	-0.1066
Z	-0.0731	-0.9241	-2.3562	-0.0213	-1.9784	1.7432	-16.4353	4.2224	0.0954	-0.1037
M	0.0022	-0.0042	-0.3656	-0.0008	0.1714	0.0251	0.0195	-0.1618	-0.0042	0.0238
Y	0.0022	-0.0053	-1.4209	-0.1236	-1.9680	1.5329	-0.0941	0.0627	0.9514	1.8191
L'	-0.0021	-0.0056	-0.6943	-0.0083	-1.2282	0.0451	0.0826	0.0494	0.4912	0.3369
N'	-0.0042	-0.0091	0.2947	0.0150	-0.3360	-1.0138	0.2546	0.0459	0.0232	-1.0179

Table A-10 AH-1G Stability and Control Derivatives in US Units (Continued)
(in Body Fixed Reference Frame)

CASE 65 100 KT LEVEL FLIGHT AT SEA LEVEL 8000 LB MID CG

PHI	THETA	PSI	ALPHA	BETA	GAMMA	θMR	B1S	A1S	θTR
-0.99	-3.34	0.00	-3.34	0.06	0.00	13.36	3.06	-1.29	2.03

XDOT	ZDOT	UO	VO	WO	VTO
168.78	0.00	168.49	0.17	-9.83	168.78

	U	W	Q	V	P	R	DC	DB	DA	DP
X	-0.0353	-0.0206	1.6410	-0.0022	-1.5577	-0.0754	-0.6101	1.2576	0.0048	-0.0974
Z	-0.0520	-0.9907	-3.1263	-0.0216	-2.5720	1.8685	-17.6603	5.5388	0.1214	-0.1588
M	0.0026	-0.0058	-0.3849	-0.0007	0.1739	0.0329	0.0062	-0.1688	-0.0021	0.0298
Y	0.0031	-0.0112	-1.4483	-0.1451	-1.7498	1.7320	-0.1958	0.0842	0.8395	1.9244
L'	-0.0015	-0.0081	-0.7296	-0.0025	-1.1043	0.0254	-0.0069	0.0641	0.4858	0.3537
N'	-0.0032	-0.0076	0.1597	0.0152	-0.3083	-1.1848	0.2738	0.0542	0.0263	-1.0719

CASE 66 120 KT LEVEL FLIGHT AT SEA LEVEL 8000 LB MID CG

PHI	THETA	PSI	ALPHA	BETA	GAMMA	θMR	B1S	A1S	θTR
-1.32	-4.24	0.00	-4.24	0.10	0.00	14.03	4.67	-1.52	2.49

XDOT	ZDOT	UO	VO	WO	VTO
202.54	0.00	201.98	0.35	-14.97	202.54

	U	W	Q	V	P	R	DC	DB	DA	DP
X	-0.0416	-0.0105	1.5367	-0.0011	-1.4691	-0.1026	-0.4136	1.1830	0.0009	-0.1385
Z	-0.0317	-1.0451	-3.5457	-0.0266	-3.1835	2.0681	-18.7277	6.8985	0.1534	-0.1602
M	0.0029	-0.0080	-0.4074	-0.0011	0.1566	0.0391	-0.0206	-0.1762	-0.0020	0.0450
Y	0.0048	-0.0204	-1.4747	-0.1659	-1.3656	1.9750	-0.3545	0.1576	0.8505	1.9970
L'	-0.0008	-0.0109	-0.8015	-0.0026	-0.9010	0.0414	-0.0608	0.0971	0.4933	0.3611
N'	-0.0023	-0.0028	-0.0174	0.0145	-0.3474	-1.3367	0.3666	0.0320	0.0288	-1.1193

CASE 67 140 KT LEVEL FLIGHT AT SEA LEVEL 8000 LB MID CG

PHI	THETA	PSI	ALPHA	BETA	GAMMA	θMR	B1S	A1S	θTR
-1.79	-5.54	0.00	-5.54	0.17	0.00	15.57	6.59	-2.02	3.49

XDOT	ZDOT	UO	VO	WO	VTO
236.29	0.00	235.19	0.71	-22.82	236.29

	U	W	Q	V	P	R	DC	DB	DA	DP
X	-0.0514	0.0025	1.3481	0.0001	-1.3803	-0.1495	-0.1154	1.0837	-0.0026	-0.1796
Z	-0.0204	-1.0882	-3.8267	-0.0174	-3.9656	2.3527	-19.7911	8.4228	0.1864	-0.1762
M	0.0034	-0.0108	-0.4142	-0.0017	0.1170	0.0509	-0.0621	-0.1978	-0.0033	0.0691
Y	0.0057	-0.0311	-1.5771	-0.1871	-0.8231	2.2114	-0.6064	0.2766	0.8775	2.0301
L'	0.0000	-0.0128	-0.9581	-0.0041	-0.6093	0.0347	-0.1278	0.1278	0.5051	0.3525
N'	-0.0013	0.0049	-0.2919	0.0116	-0.3738	-1.5129	0.4729	-0.0518	0.0268	-1.1471

APPENDIX B

UNGUIDED 2.75” ROCKETS

Air-launched unguided 2.75” rockets were originally developed in the late 1940s by the NOTS (Naval Ordnance Test Station). 2.75” rocket systems provide an effective attack capability against a variety of targets. They are widely used for military purposes since 1940s [25].

2.75” rockets are composed of the motor and the warhead section. Several motors and warheads are produced so far for these weapons. 2.75” rockets are identified according to the components like motor and / or warhead type which are assembled on it [25].

B.1 MK 4 Mighty Mouse, MK 40

The 2.75” FFAR (Folding-Fin Aircraft Rocket) (Figure B-1) was originally developed by the NOTS as an air-to-air weapon. The original rocket model was the MK 4, which was spin-stabilized by the fins around the nozzle. Length of the MK 4 Mighty Mouse was 1.2 m, and it weighed 8.4 kg. Maximum range was around 6 km but it is more practical to use for the targets which have 3 km range [25].

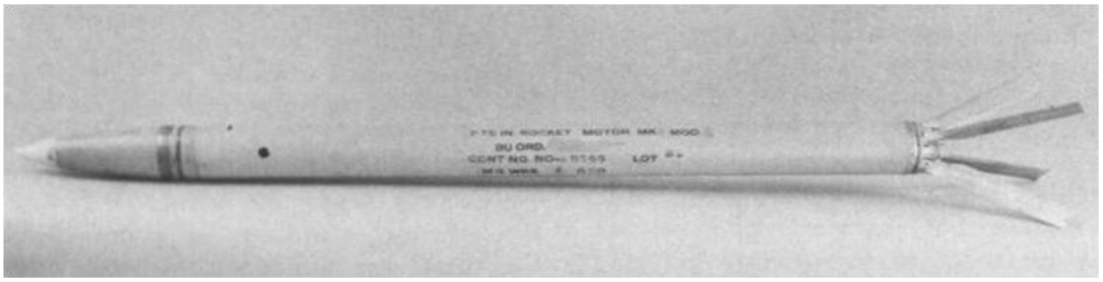

Figure B-1 MK 4 Mighty Mouse

The 2.75-inch rocket was modified later for air-to-ground use. The 2.75-inch rocket was also adopted by the U.S. Army and Marine Corps as a primary weapon for its armed helicopters. For better performance rocket motor is modified and named as MK 40 [25].

B.2 MK 66 Hydra 70

The current 2.75” rockets (Hydra 70 rocket system) (Figure B-2) which are developed by the U.S. Army for both fixed-wing aircraft and helicopters use the MK 66 rocket motors. The MK 66 motor which is longer than the MK 4/40 is produced with an improved propellant. Therefore it has higher thrust than MK 4/40 and accordingly MK 66 rockets have higher range than those of MK 4/40 rockets. In addition, with a modified fin and nozzle assembly, MK 66 rockets have higher spin rate which increases the firing accuracy [25].

Figure B-2 MK 66, Hydra 70 System

B.3 Weapon Ballistic Trajectories

Ballistics is a science that deals with the projectile motions and the conditions that affect these motions. The ballistics is divided in to three main groups. Interior ballistics analyzes the factors that affect the accuracy of the weapon before it leaves the launcher. Exterior ballistics analyzes the weapon accuracy as it moves along the trajectory and the terminal ballistics analyzes the effects of the weapon at the impact point [27].

This study focuses on the exterior ballistics. Several factors affect the exterior ballistics on weapon shooting accuracy. These factors are caused by both the helicopter and the weapon. This thesis focuses on controlling / setting these factors caused by the helicopter like aiming the helicopter (target alignment) or setting the helicopter forward velocity during target engagement.

APPENDIX C

PD CONTROLLERS GAIN SELECTION

The helicopter natural frequency range for changing forward velocities;

- 0.7 - 1.5 rad/s in pitch channel (Chapter 3 Table 2, short period mode)
- 0.8 - 1.5 rad/s in roll channel (Chapter 3 Table 2, roll mode)
- 0.5 – 1.9 rad/s in yaw channel (Chapter 3 Table 2, dutch roll mode)

The actuator bandwidth is selected as 8 rad/s. Then the inner loop design frequency is selected as 3 rad/s which is slower than the actuator dynamics. Later, the outer loop design frequency is determined. To avoid coupling between the inner and the outer loop dynamics [10], the outer loop design frequency is selected as (0.7 rad/s) sufficiently below the inner loop design frequency. The reason why the outer loop design frequency is slower than the inner loop design frequency is that the slow translational states are controlled in the outer loop whereas the fast rotational states are controlled in the inner loop.

The relationship between the inner and outer loop design frequencies and the PD controller gains are expressed by the formulations given in Equation C.1 [17];

$$R_p = \frac{\omega_o^2 \omega_i^2}{\omega_i^2 + 4\zeta_o \omega_o \zeta_i \omega_i + \omega_o^2}; \quad R_d = \frac{\omega_o \omega_i \left(\zeta_o \omega_o + \zeta_i \omega_i\right)}{\omega_i^2 + 4\zeta_o \omega_o \zeta_i \omega_i + \omega_o^2};$$

$$K_p = \omega_i^2 + 4\zeta_o \omega_o \zeta_i \omega_i + \omega_o^2; \quad K_d = 2\zeta_o \omega_o + 2\zeta_i \omega_i \tag{C.1}$$

Where, Rp, Rd, Kp and Kd are the PD controller gains for the inner loop and the outer loop and the subscripts i and o, denotes the inner and the outer loop values respectively. By these equations, the proportional and derivative controller gains are calculated as 15 and 6 for the inner loop and the corresponding gains are 0.3 and 0.4 for the outer loop. Then the simulations are performed with these values. Although the controller satisfies the system requirements with these gains, the inner and the outer loop gains are tuned to get better results. The resultant gains and the natural frequency values are given in Table C-1.

Table C-1 Controller Gains and Design Frequencies

outer loop command filter	outer loop w/o command filter	outer loop Kp and Kd values	inner loop command filter	inner loop w/o command filter	inner loop Kp and Kd values	actuator	helicopter
0.7 rad/s	2 rad/s (north channel)	0.1, 0.5 (north channel)	3 rad/s	3.2 rad/s	15, 5	8 rad/s	0.7 - 1.5 rad/s (pitch channel)
	1.9 rad/s (east channel)	0.05, 0.5 (east channel)					0.8 - 1.5 rad/s (roll channel)
	2.3 rad/s (altitude channel)	4, 2 (altitude channel)					0.5 – 1.9 rad/s (yaw channel)

APPENDIX D

MODEL ERROR TRANSFER FUNCTIONS SELECTION

At 1 knot forward velocity condition, the roll mode, the short period mode and the dutch roll mode poles are -0.8191, -0.5981 ± 0.3885i and 0.1326 ± 0.5261i respectively. Then the transfer functions are selected as;

$$\Rightarrow TF_{roll\ \ err} = \frac{s + 0.8191}{s + 0.2}$$

$$\Rightarrow TF_{short\ \ period\ \ err} = \frac{(s + 0.1326 + 0.5261i)\cdot(s + 0.1326 - 0.5261i)}{(s + 0.3 + 0.3i)\cdot(s + 0.3 - 0.3i)}$$

$$\Rightarrow TF_{dutch\ \ roll\ \ err} = \frac{(s - 0.1326 + 0.5261i)\cdot(s - 0.1326 - 0.5261i)}{(s - 0.14 + 0.6i)\cdot(s - 0.14 - 0.6i)}$$